EPA-600/3-77-110
October 1977

Ecological Research Series

MEASUREMENT OF RATE CONSTANTS OF IMPORTANCE IN SMOG

LIBRARY
U. S. ENVIRONMENTAL PROTECTION AGENCY
EDISON, N. J. 08817

Environmental Sciences Research Laboratory
Office of Research and Development
U.S. Environmental Protection Agency
Research Triangle Park, North Carolina 27711

RESEARCH REPORTING SERIES

Research reports of the Office of Research and Development, U.S. Environmental Protection Agency, have been grouped into nine series. These nine broad categories were established to facilitate further development and application of environmental technology. Elimination of traditional grouping was consciously planned to foster technology transfer and a maximum interface in related fields. The nine series are:

1. Environmental Health Effects Research
2. Environmental Protection Technology
3. Ecological Research
4. Environmental Monitoring
5. Socioeconomic Environmental Studies
6. Scientific and Technical Assessment Reports (STAR)
7. Interagency Energy-Environment Research and Development
8. "Special" Reports
9. Miscellaneous Reports

This report has been assigned to the ECOLOGICAL RESEARCH series. This series describes research on the effects of pollution on humans, plant and animal species, and materials. Problems are assessed for their long- and short-term influences. Investigations include formation, transport, and pathway studies to determine the fate of pollutants and their effects. This work provides the technical basis for setting standards to minimize undesirable changes in living organisms in the aquatic, terrestrial, and atmospheric environments.

This document is available to the public through the National Technical Information Service, Springfield, Virginia 22161.

EPA-600/3-77-110
October 1977

MEASUREMENT OF RATE CONSTANTS OF IMPORTANCE IN SMOG

by

John R. Barker, Sidney W. Benson,
G. David Mendenhall, and David M. Golden

SRI International
(formerly Stanford Research Institute)
Menlo Park, California 94025

Grant No. R802288

Project Officer

Marcia C. Dodge
Atmospheric Chemistry and Physics Division
Environmental Sciences Research Laboratory
Research Triangle Park, North Carolina 27711

ENVIRONMENTAL SCIENCES RESEARCH LABORATORY
OFFICE OF RESEARCH AND DEVELOPMENT
U.S. ENVIRONMENTAL PROTECTION AGENCY
RESEARCH TRIANGLE PARK, NORTH CAROLINA 27711

LIBRARY
U. S. ENVIRONMENTAL PROTECTION AGENCY
EDISON, N. J. 08817

DISCLAIMER

This report has been reviewed by the Chemistry and Physics Laboratory, U.S. Environmental Protection Agency, Research Triangle Park, North Carolina, and approved for publication. Approval does not signify that the contents necessarily reflect the views and policies of the U.S. Environmental Protection Agency, nor does mention of trade names or commercial products constitute endorsement or recommendation for use.

PREFACE

For some time, considerable effort has been devoted to understanding and characterizing the complex phenomenon of photochemical smog. This effort has encompassed several different areas of study so as to take full advantage of the wide range of expertise in the scientific community. The extensive experience accumulated using smog chambers to simulate smog conditions, and the results of field observation indicate that a complete understanding of smog depends on the development and validation of reliable chemical mechanisms consisting of elementary reactions.

Since the polluted atmosphere is highly complex and depends sensitively on parameters such as solar irradiance, temperature, pollutant concentration, and transport phenomena, any errors in the reaction mechanisms are likely to be magnified at the extremes of the parameter ranges. A general approach to formulating general reaction mechanisms is to include all elementary reactions thought to be important, and then test them using smog chamber simulations. Although smog chamber simulations are designed to be simplified versions of the polluted atmosphere, the gas mixtures are so complex and spurious chamber effects often are so important that the technique cannot be used to ascertain elementary rate processes and can only be used for validation purposes.

To develop a reliable chemical mechanism describing smog, elementary reaction rate constants are needed. Such rate constants preferably can be obtained by direct experimentation, but estimates can sometimes be made if sufficient experimental data on related reactions are available. Such rate constants, once obtained, are often useful, not only for

understanding smog chemistry, but also for understanding pollutant formation in combustion processes, and the like. As rate constant measurements of higher quality are performed, inaccurate rate constants are superceded and the general understanding of photochemical smog is improved.

In the absence of good elementary reaction rate studies, one must resort to estimation techniques to formulate an overall reaction scheme. Such estimation techniques draw upon data available for reactions analogous to the one of interest. If no analogous reactions have been studied, the estimated rate parameters must be considered highly uncertain. A-factors can be estimated much more reliably and readily than activation energies, but even A-factors can be in error if the true chemical nature of a reaction is misunderstood. Hence, it is desirable to observe the products of elementary reactions in order to guarantee that the chemistry is correct. Until more complete data of higher quality become available, estimation techniques, like those illustrated in this report, will be valuable adjuncts to experiments.

No satisfactory substitute for experimental determinations for elementary reaction rate constants is available, however. All estimates are subject to errors that can distort the results of computer simulations of photochemical smog. The experiments described in this report were intended to help refine estimates of unmeasured reaction rate constants.

ABSTRACT

In an effort to understand elementary reactions of importance in smog, we have carried out a three-part investigation: (1) experimental determinations of certain elementary reaction rate constants, (2) development of general techniques for estimating elementary reaction rate constants, and (3) estimation of rate parameters for many reactions important in smog.

The experimental studies determined rate constants for the following reactions:

$$CH_3CH_2CH_2ONO_2 \underset{-a}{\overset{a}{\rightleftarrows}} CH_3CH_2CH_2O + NO_2$$

$$t\text{-}BuONO \underset{-b}{\overset{b}{\rightleftarrows}} t\text{-}BuO + NO$$

$$CH_3OOCH_3 \underset{-c}{\overset{c}{\rightleftarrows}} 2CH_3O$$

$$CH_3 + CH_3OOCH_3 \overset{d}{\rightarrow} CH_3OH + CH_2OOCH_3$$

$$CH_3O + NO_2 \underset{(M)}{\overset{e}{\rightarrow}} CH_3ONO_2$$

$$CH_3O + NO_2 \overset{f}{\rightarrow} CH_2O + HONO$$

$$CH_3O + O_2 \overset{g}{\rightarrow} CH_2O + HO_2$$

Specific estimated rate constants included the following reactions:

(1) Decomposition of alkoxy radicals

(2) Isomerization of alkoxy radicals

(3) Reactions of alkoxy radicals with oxygen

(4) The reaction $HO_2 + NO_2 \overset{(M)}{\rightleftarrows} HO_2NO_2$.

CONTENTS

Preface iii
Abstract v
Figures ix
Tables x
Abbreviations and Symbols xii
Acknowledgments xiii

1. Introduction 1
2. Conclusions and Recommendations 3
3. Experimental Studies 5
   A. The Very Low-Pressure Pyrolysis (VLPP) of n-Propyl Nitrate, tert-Butyl Nitrite, and Methyl Nitrite. Rate Constants for Some Alkoxy Radical Reactions 5
      Experimental 6
      Results--n-Propyl Nitrate 8
      Results--tert-Butyl Nitrite 10
      Results--Methyl Nitrite 11
      Results--Methyl Peroxide and NO_2 11
      Discussion 12
      Thermochemistry 19

   B. The Decomposition of Dimethyl Peroxide and the Rate Constant for $CH_3O + O_2 \rightarrow CH_2O + HO_2$ . . . 20
      Experimental 23
      Results and Discussion 26
         Dimethyl Peroxide Decomposition 26
         Dimethyl Peroxide with Added NO_2 32
         Dimethyl Peroxide with Added NO_2 and O_2 . 42
      Summary 50

4. Estimation Methods 51
   A. Methods for the Estimation of Rate Parameters . . 51
      Transition State Theory 52
      A-Factors and Entropies of Activation 54
      A-Factors for Metathesis Reactions 60
      Addition Reactions 68
      Recombination Reactions Involving Atoms . . . 71
      Activation Energies 77

B. Rate Parameter Evaluation and Estimates 80
Alkoxyl Radical Decomposition Reactions . . . 81
Alkoxyl Radical Reactions with Oxygen 89
Alkoxyl Radical Isomerization Reactions . . . 92
Reaction of NO_2 with HO_2 96
Simulations of Smog Chamber Experiments . . . 102
Reactions of n-Butane 104
Reactions of Propene 111
Conclusions 113

References and Footnotes 116

Appendix A: VLPP Unimolecular Rate Theory 123

FIGURES

Number		Page
1	$nPrONO_2$ Pyrolysis	9
2	tBuONO Pyrolysis	9
3	Schematic Diagram of Apparatus	24
4	Decomposition of Initially Pure DMP	28
5	Arrhenius Plot Summarizing Data for DMP Decomposition	30
6	Decomposition of DMP with Added NO_2	34
7	Gas Chromatography Results Demonstrating Mass Balance	36
8	$-k_N^{-1}$ (dP/dt) vs. $[DMP]_0$ for Four Temperatures	38
9	Decomposition of DMP with Added NO_2 and O_2	43
10	Arrhenius Plot of Data for k_{17}	48
11	t-BuO· $\xrightarrow{M}$ Me + Acetone	83
12	EtO· $\xrightarrow{M}$ Me + CH_2O	83
13	i-PrO· $\xrightarrow{M}$ Me + MeCHO	84
14	s-BuO· $\xrightarrow{M}$ Et + MeCHO	84
15	Correlation Between Activation Energy E and Enthalpy of Reaction ΔH_R^o	86
16	Falloff Calculated by RRKM Theory as a Function of Activation Energy for the Reaction $HO_2NO_2 \rightarrow HO_2 + NO_2$	101
17	Reactions of n-Butane	105
18	(a) Simulation of Run EC-41 in Reference 90	108
	(b) Simulation of Run EC-41 as in (a)	108
19	Simulation of Run EC-41 in Reference 90	109
20	Reactions of Propene	112
21	Simulation of Run EC-121 in Reference 90	114

Appendix: VLPP Unimolecular Weight Theory 123

TABLES

Number		Page
I	Reactor Parameters	7
II	Decomposition of Dimethyl Peroxide in the Presence of Nitrogen Dioxide	13
III	Molecular Parameters Used for RRKM Calculations; Molecular Parameters for n-$PrONO_2$ and tert-BuONO	14
IV	Thermochemical Quantities	15
V	Rate Constants	15
VI	Rate Constants for Computer Calculation	31
VII	Dimethyl Peroxide Rate Constants	31
VIII	Data Summary for $MeO + O_2 \rightarrow HO_2 + CH_2O$	46
IX	Standard Entropies and Heat Capacities at 300°K of Some Structurally Similar Molecules	57
X	Standard Entropies and Heat Capacities of Some Complex but Structurally Similar Molecules	58
XI	Standard Entropies and Heat Capacities of Some Complex but Structurally Similar Molecules	58
XII	Arrhenius Parameters for Some Metathesis Reactions Involving H-Atoms	62
XIII	Arrhenius Parameters for Metathesis Reactions Involving Atoms	63
XIV	Arrhenius Parameters for Some Metathesis Reactions of Radicals	66
XV	Arrhenius Parameters for Some Addition Reactions of Atoms and Radicals to Pi Bonds	69
XVI	Experimental Values for RO· Decomposition Rates	82
XVII	Estimated RO· Decomposition Rates	87
XVIII	Estimates: RO· + O_2 Reactions	91

Number		Page
XIX	RO· Isomerization Reactions--Estimation Procedure	94
XX	Estimated RO· Isomerization Reaction Rates	95
XXI	Frequency Assignment for HO_2NO_2	98
XXII	RRKM Calculated k/k_∞ for HO_2NO_2 Decomposition	99

LIST OF ABBREVIATIONS AND SYMBOLS

BuO - Butoxy Free Radical

DMP - Dimethyl Peroxide (CH_3OOCH_3)

EtO - Ethoxy Free Radical

Me - Methyl Free Radical or Substituent Group

MeO - Methoxy Free Radical

Omega (ω) - Collision Frequency

PrO - Propoxy Free Radical

RO - Alkoxy (Alkoxyl) Free Radical

RRKM - Rice, Ramsperger, Kassell, and Marcus Theory of Unimolecular Reaction Rate

VLPP - Very Low-Pressure Pyrolysis Experimental Technique

ACKNOWLEDGMENTS

Thanks go to Karan Lewis for preparing many batches of dimethyl peroxide and to Dr. L. Batt, H. Niki, and J. G. Calvert for permission to use some of their respective results prior to publication.

SECTION 1

INTRODUCTION

To develop an explicit mechanism for photochemical smog formation, it is desirable to have experimental determinations of elementary reaction rate constants. In the absence of such experimental data, estimation techniques must be developed and utilized for estimating appropriate rate parameters. This report summarizes efforts made in both these areas.

The experimental studies reported below were conducted to elucidate the chemical reactions of alkoxyl radicals in the polluted atmosphere.[1] These radicals are present, not only in the atmosphere, but also in flames and combustion processes where they are potential chain carriers and propagators.

Alkoxy radical rates with the free radical traps, nitric oxide and nitrogen dioxide, had been reported[2a] to be about two orders of magnitude slower than for other similar reactions.[2b] An investigation was undertaken to test this unexpected result, and it is described in Section 3.A of this report.

Another reaction of particular importance is that of alkoxyl radicals with molecular oxygen. The prototype alkoxy radical $—CH_3O—$ was used to determine the rate constant in a study described in Section 3.B. This reaction is important in the oxidation of nitric oxide to form NO_2 according to the following sequence:

$$RH + OH \rightarrow R + H_2O$$

$$R + O_2 \xrightarrow{M} RO_2$$

$$RO_2 + NO \rightarrow RO + NO_2$$

$$RO + O_2 \rightarrow HO_2 + \text{carbonyl}$$

$$HO_2 + NO \rightarrow OH + NO_2$$

Other reactions of alkoxyl radicals can compete under certain circumstances, and their rates must be estimated to achieve formulation of a proper chemical mechanism. General procedures for estimating rate constants are described in Section 4.A, and specific applications are presented in the remaining sections.

Alkoxyl radicals larger than methoxy can undergo β-cleavage, and the rates for such processes were estimated on the basis of data in the literature, as described in Section 4.B. For still larger alkoxy free radicals, isomerization reactions are possible, leading to the sequential oxidation and degradation of hydrocarbons (Section 4.B). The relative rates of these competing processes are important in developing an explicit reaction mechanism, and the resulting mechanism appears to be a relatively good representation of reality.

A reaction for which virtually no data exists is $HO_2 + NO_2 \overset{M}{\rightleftarrows} HOONO_2$. The technique described in Section 4.A was used to estimate the forward and back rates of this reaction, and the sensitivity of the reaction mechanism to variations of these rates are presented in Section 4.B.

Each section of this report contains a detailed discussion of the background behind each rate, along with a thorough description of the experimental technique or estimation procedure used and a discussion of the result.

SECTION 2

CONCLUSIONS AND RECOMMENDATIONS

In the course of this work, a number of elementary reaction rate parameters have been measured :

(a) $CH_3CH_2CH_2ONO_2 \underset{-a}{\overset{a}{\rightleftarrows}} CH_3CH_2CH_2O + NO_2$

$\log k_a(sec^{-1}) = 16.5 - 40.0 \text{ kcal mole}^{-1}/2.3\ RT$

$\log k_{-a}(M^{-1}\ s^{-1}) = 9.5$

(b) $t\text{-BuONO} \underset{-b}{\overset{b}{\rightleftarrows}} t\text{-BuO} + NO$

$\log k_b\ (sec^{-1}) = 15.8 - 39.3 \text{ kcal mole}^{-1}/2.3\ RT$

$\log k_{-b}(M^{-1}\ s^{-1}) = 9.8$

(c) $CH_3OOCH_3 \underset{-c}{\overset{c}{\rightleftarrows}} 2CH_3O$

$\log k_c\ (sec^{-1}) = (15.7 \pm 0.5) - (37.1 \pm 0.9) \text{ kcal mole}^{-1}/2.3\ RT$

$\log k_{-c}(M^{-1}\ s^{-1}) = 9.7 \pm 0.5$

(d) $CH_3 + CH_3OOCH_3 \rightarrow CH_3OH + CH_2OOCH_3$

$k_d(400\ K) \approx 5 \times 10^4\ M^{-1}\ s^{-1}$

(e) $CH_3O + NO_2 \overset{M}{\rightarrow} CH_3ONO_2$

(f) $CH_3O + NO_2 \rightarrow CH_2O + HONO$

$k_f/k_e = 0.30 \pm 0.05$

If $\log k_e(M^{-1}\ s^{-1}) = 9.8 \pm 0.5$, then $\log k_f(M^{-1}\ s^{-1}) = 9.3 \pm 0.5$

(g) $CH_3O + O_2 \rightarrow CH_2O + HO_2$

$\log k_g(M^{-1}\ s^{-1}) = (8.5 \pm 1.5) - (4.0 \pm 2.8) \text{ kcal mole}^{-1}/2.3\ RT$

The rate parameters for reaction (g) are the most uncertain, and further investigations are desirable.

In addition to the experimental determination of rate constants, an effort has been made to develop general techniques for estimating unknown rate constants by using data from analogous reactions. Applications of these techniques have been quite successful, and their utility has been demonstrated for the following reactions:

(1) Decomposition of alkoxy radicals

(2) Isomerization of alkoxy radicals

(3) Reactions of alkoxy radicals with oxygen

(4) The reaction $HO_2 + NO_2 \overset{M}{\rightleftarrows} HOONO_2$

Application of the estimated rate constants to butane and propene smog chamber experiments shows fair agreement and indicates sensitive areas for further work:

(1) Experimental determination of the rate parameters for $HOONO_2$ decomposition and association.

(2) Experimental determination of the photolysis rates of aldehydes and ketones in oxygen gas.

(3) Experimental determination of the products of the reaction of olefins with OH, O, and O_3 under conditions of atmospheric interest.

Although a great effort has been expended to understand photochemical smog formation, the phenomenon is so complex that much work remains to be done. Until more experimental data become available, the estimation technique described in this report will play an important role.

SECTION 3

EXPERIMENTAL STUDIES

A. THE VERY LOW-PRESSURE PYROLYSIS (VLPP) OF n-PROPYL NITRATE, tert-BUTYL NITRITE, AND METHYL NITRITE. RATE CONSTANTS FOR SOME ALKOXY RADICAL REACTIONS

Although alkoxy radicals play a central role in the oxidative degradation of hydrocarbons, few absolute rate constants of reactions involving these radicals have been reported in the literature. The reasons for this situation include their lack of distinctive spectral features, high reactivity, and complexities introduced into most systems due to multiple pathways available for their decomposition and secondary reactions of products. This situation has recently become more acute because of the use of alkoxy rate constants in smog-modeling studies,[1] and the assignment of certain rates, e.g., that for the reaction leading to PAN, on the basis of the former.

We initially had hoped to generate methoxy radicals in a VLPP reactor and directly observe their reaction rate with oxygen. (Higher alkoxy radicals undergo β-cleavage under these conditions--see Section 4.I., this report.) A variety of precursors, including dimethyl peroxide, methyl nitrite, methyl hyponitrite, and methyl t-butyl peroxide, were decomposed between 400°K and 800°K, and with quartz, carbon, Teflon, and boric acid coated surfaces. A small signal at m/e = 31 (at low ionization voltage) was observed when methyl t-butyl peroxide was decomposed in a boric acid coated reactor, but the intensity was too low to be useful.

The rate constant for a reaction X + OR → ROX can be calculated from the rate of reverse reaction if the thermodynamic parameters are known.

This method was used by Gray, Shaw, and Thynne[2a] to derive recombination rates for $CH_3O + NO$ and $CH_3O + NO_2$. These, however, were based on rates for the reverse reactions which have been questioned.[2b]

By pyrolysis of tert-butyl nitrite and n-propyl nitrate we have derived recombination rates that are $\sim 10^2$ higher than the earlier values. Recently Batt, McCulloch, and Milne[3] in a paper on several nitrites reported results for tert-butyl nitrite pyrolysis by a separate technique that are in excellent agreement with ours.

In a separate study with a conventional static system, we determined the yield of methyl nitrate from methyl peroxide and NO_2 as a function of total pressure, in order to determine whether the reaction of methoxy radicals with NO_2 is in the high-pressure region at atmospheric pressure.

Experimental

n-Propyl nitrate (Eastman Kodak) and tert-butyl nitrite (Frinton Laboratories) were fractionally distilled on a vacuum line. The center 1/3 was stored in a large bulb wrapped in Al foil. Methyl nitrate was synthesized on 1/10 the scale reported by Delepine[4] and fractionally distilled as above. Dimethyl peroxide was synthesized by the procedure of Hanst and Calvert[5] and fractionally distilled to remove dimethyl ether (m/e 46). The gas detonated twice during handling and transfer, though at low pressures in a seasoned vessel it was stable for weeks. Methyl nitrite and methyl-d_3 nitrite were synthesized by adding 200 μl of 25% by volume H_2SO_4 in water to the requisite alcohols (1 cc) and excess $NaNO_2$ at -78^0 and distilling the product into a bulb on a vacuum line.[6] Other reagents and gases were commercial samples.

The static system for the methoxy radical-NO_2 work has been described.[7] Product analysis was accomplished by glc (F and M Model 720, thermal conductivity detector, 10 ft. x 0.25 in. column of 20% di-(2-ethyl hexyl)sebacate on 60-80 M chromasorb at 25°; detector at 100°). Seven percent of the reaction mixture was removed with each aliquot, and 42% of the aliquot was swept onto the glc column. The peak areas were related to concentrations in the reactor with appropriate factors and a linear calibration curve made from peak areas of various pressures of pure CH_3ONO_2.

The theory and practice of the VLPP technique have been described previously.[8] Essentially this involves the pyrolysis of a gas flowing through a heated reactor with three different possible apertures (1-mm, 3-mm, and 10-mm) diameters). The pressure of the gas in the reactor is very low (~ 0.1-1.0 μ), such that the flow is molecular, gas-gas collisions are few and most secondary reactions are eliminated. The characteristics of the reactor are given in Table I, and the exact VLPP unimolecular rate theory is presented in Appendix A, where it is shown that ordinary RRKM theory is adequate.

TABLE I. Reactor Parameters

Volume, $V = 130\ cm^3$; Surface Area, $A_w = 160\ cm^2$; Collision Frequency, $\omega = 4.48 \times 10^3\ (T/M)^{1/2}\ sec^{-1}$

Aperture Diameter (cm)	0.115	0.305	0.995
k_e/sec^{-1}	$0.4\ (T/M)^{1/2}$	$1.8\ (T/M)^{1/2}$	$12\ (T/M)^{1/2}$
Collision Number = Z	11,200	2,470	387

Results--n-Propyl Nitrate

Rate constants for the unimolecular disappearance were obtained for n-propyl nitrate over a 220° temperature range, and with a 100-fold variation in flow rates. The M-29 peak at 76 amu was monitored (see Figure 1).

The complete reaction is assumed to involve β-scission or isomerization:

$$\text{n-}CH_2CH_2ONO_2 \rightarrow \text{n-}CH_3CH_2CH_2O^{\bullet} + NO_2 \qquad (1)$$

$$CH_3CH_2CH_2O^{\bullet} \rightarrow CH_3CH_2{}^{\bullet} + CH_2O$$

$$\rightarrow {}^{\bullet}CH_2CH_2CH_2OH \rightarrow C_2H_4 + {}^{\bullet}CH_2OH$$

of n-propoxy and subsequent reactions, perhaps on the walls, between NO_2, formaldehyde and ethyl radicals. Due to the spectral similarity of the products we did not analyze quantitatively for them in this case, although intense signals were observed at the masses where they appear. We did show quantitatively in two runs that propionaldehyde (yield ≤ 10%) and propylene (yield ≤ 3.7%) were not significant products. This observation indicates that neither of two anti-Markovnikov reactions were occurring:

$$\text{n-}CH_3CH_2CH_2ONO_2 \rightarrow CH_3CH{=}CH_2 + HONO_2$$

$$\rightarrow CH_3CH_2CH{=}O + HONO$$

That β-scission (or isomerization followed by scission) is the predominant fate of n-propoxy can be determined from an RRKM calculation,[9] Using values of the Arrhenius parameters determined recently by Batt et al.,[3] and a value of $s = (C_p^0-4R)/R$ for the number of "effective oscillators," the values for k(β-scission) are much greater than the escape rate constant. Batt[3] et al. report $\log k \sim 16-17/\theta$. For nPrO•,[10] $C_p \sim 33$; thus, $s = 12.5$, $B = E/RT = 12$ at 700°K, and $D = \log A$, $\log \omega \sim 16 - 4 = 12$ under VLPP conditions. $k/k_\infty \sim 8 \times 10^{-8}$, and thus $k \sim 400\ sec^{-1}$, which is rapid compared to escape from the reactor. The parameters for isomerization are not as well known, but if we estimate $\log k_{isom} \sim 12-12/\theta$, this reaction followed by scission would precede escape as well.

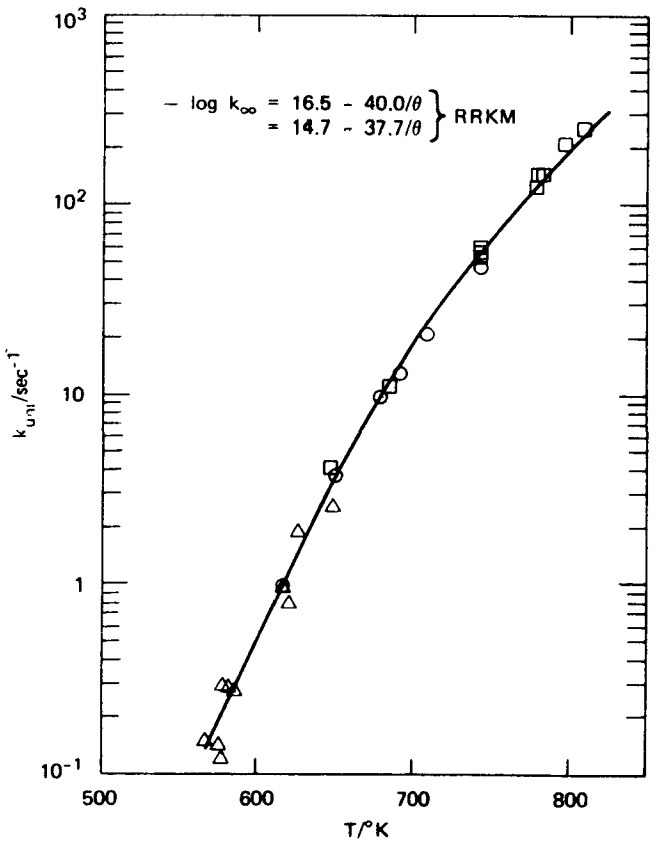

FIGURE 1. $nPrONO_2$ Pyrolysis
Δ—Z = 11,200;
○—Z = 2,470;
—Z = 387.

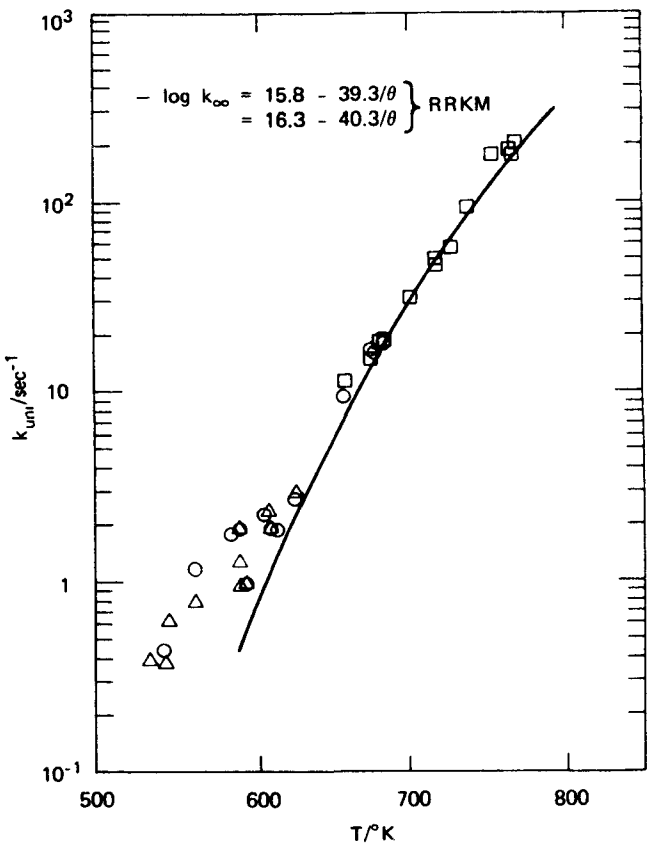

FIGURE 2. tBuONO Pyrolysis
Δ—Z = 11,200;
○—Z = 2,470;
—Z = 387.

Results--tert-Butyl Nitrite

Rate constants for the unimolecular disappearance of t-BuONO were obtained over a 240° temperature range and with a 100-fold variation in flow rates. The peak at M-15 (88 amu) was monitored.

Above 650°K the data lie on a smooth curve of the type expected in a unimolecular homogeneous process (Figure 2). Between 525 and 650°K the rates are relatively too fast and exhibit considerable scatter.

At the higher temperature we observe fragments at m/e 58, 43, and 15, corresponding to the reactions:

$$\underline{\text{tert}}\text{-BuONO} \xrightarrow{2} \underline{\text{tert}}\text{-BuO} + \text{NO} \qquad (2)$$

$$\underline{\text{tert}}\text{-BuO} \rightarrow CH_3COCH_3 + CH_3$$

At the lower temperatures no methyl radicals were observed, and the principal organic product is isobutylene:

$$\underline{\text{tert}}\text{-BuONO} \rightarrow \text{HONO} + (CH_3)_2C{=}CH_2$$

Batt and coworkers[3] have also reported this reaction. A significant signal at m/e 59 in the product spectrum was ascribed to tert-butyl alcohol, though the yield was measured as only 1.6% in one case. Under the reaction conditions, tert-butanol decomposed to give isobutylene (k_{uni} = 1.5 sec^{-1} at 672°K, Z = 20,000).

RRKM curves were accordingly fitted to the data >650°K, and the presence of small side reactions does not affect the result for the alkoxy forming reaction.

Results--Methyl Nitrite

The decomposition of methyl nitrite was studied briefly in a search for methoxy radicals. At 650°K we observed intense signals at m/e 30 and 31 with low-ionizing voltage. Either of two reactions were considered possible:

$$CH_3ONO \rightarrow CH_3O + NO$$
$$\text{m/e } 31 \quad 30$$

$$\rightarrow CH_2O + HNO$$
$$\text{m/e } 30 \quad 31$$

To resolve the question we prepared methyl-d_3 nitrite and found under these conditions product signals at m/e 30, and 32, with a smaller increase at m/e 36 (CD_3OD). A signal at m/e 34, corresponding to CD_3O, did not appear.

At 650°K methyl nitrite gave a 42% yield of methanol (Z = 200, 3 x 10^{16} molec/sec). The value of k_{uni} was 20 sec^{-1}. From Batt's[3] data, we predict $k_{\infty}^{650°K}$ = 93 sec^{-1} for the fission into RO and NO, and RRK calculations indicate k_{uni}/k_{∞} is about 10^{-5}, so we cannot be observing a homogeneous process.

Results--Methyl Peroxide and NO_2

At two temperatures, 121° and 163°K methoxy radicals, produced thermally from dimethyl peroxide, give methyl nitrate by coupling with NO_2 in the system. An alternate reaction is disproportionation:

$$CH_3OOCH_3 \longrightarrow 2CH_3O$$

$$CH_3O + NO_2 \xrightarrow{a} CH_3ONO_2$$

$$\xrightarrow{b} CH_2O + HONO$$

At the reaction temperatures NO_2 reacts further with formaldehyde. There is some scatter in the data in Table II, particularly at 163°, where the reaction was carried to greater conversion, but a trend to higher yields of CH_3ONO_2 as the total pressure rises is indicated at both temperatures. When we attempted to pressurize a mixture of peroxide and NO_2 at 163° with air, the reaction vessel was destroyed in an explosion.

Discussion

The frequencies of the molecules and activated complexes are given in Table III. These provide the input for a computer program based on the RRKM theory, which computes values of the apparent first-order rate constant as a function of pressure and temperature for various values of the critical energy (activation energy at 0°K). Frequencies in the molecule were selected to give total entropies at 300°K, in agreement with experimental data or results obtained by group additivity. The experimental rate constants (k_{uni}) over a range of temperatures and the predicted curves appear in the figures. The frequencies for the complex found in Table III were actually selected to give a model transition state which would, in turn, have a value of $\Delta S^{\ddagger}$ (i.e., A-factor) which would fit the VLPP data when the choice of critical energy was confined to a value such that the activation energy at 298°K was identical with the known value of $\Delta E(298^{\circ}K)$ for the reaction (Table IV).

The Arrhenius parameters which best describe the VLPP data are shown in Figures 1 and 2 and in Table V. These parameters combined with the known entropy change for the reaction allow the calculation of the rate constants for the reverse processes, the combination of the requisite alkoxy radicals with NO and NO_2. These rate constants are also given in Table V.

TABLE II. Decomposition of dimethyl peroxide in the presence of nitrogen dioxide.

T°C	p^o(torr)		Other	$\frac{k_a}{k_a + k_b}$	Time (min.)
	Me_2O_2	NO_2			
121	30.5	58	--	0.72	14
				0.63	30
				0.62	45
				0.67	60
121	10.0	44.5	--	0.74	40
				0.56	64
				0.81	105
121	10.5	13.0	740	0.4	30
			torr	0.96	51
			air	1.0	70
				1.1	90
121	10.0	5.0	745	0.4	30
			torr	0.7	50
			N_2	0.9	70
				0.9	90
121	10.0	5.0	745	0.3	30
			torr	0.7	50
			O_2	0.7	70
				0.7	90
				0.7	110
163	7.0	55.0		0.56	3.6
				0.64	11.6
				0.59	28
				0.55	42
				0.54	55
163	1.6	21.4		0.38	3
				0.42	6.8
				0.44	15
				0.48	25
				0.54	33
				0.42	59
163	4.8	3.2		0.41	17
				0.44	30
				0.38	101
163	13.5	188.5		0.89	3.1
				0.95	6.6
				0.76	19
				0.71	32
				0.67	42
				0.61	51

TABLE III. Molecular parameters used for RRKM calculations; molecular parameters for *n*-$PrONO_2$ and *tert*-BuONO.

	n-$PrONO_2$			tert-BuONO		
	Molecule	Complex 1	Complex 2	Molecule	Complex 1	Complex 2
Frequencies, cm^{-1} with degeneracy	3000 (7)	3000 (7)		3000 (9)	3000 (9)	
	1600 (1)	1600 (1)		1600 (1)	1600 (1)	
	1450 (4)	1450 (4)		1400(15)	1400(15)	
	1350 (4)	1350 (4)		1200 (1)	1200 (1)	
	1200 (1)	1150 (5)		1000 (3)	1000 (2)	
	1000 (2)	1000 (2)		800 (1)	800 (1)	
	1150 (4)	720 (2)		200 (3)	200 (3)	
	750 (3)			410 (5)	350 (3)	350 (2)
	350 (4)	125 (6)	260 (6)	100 (4)	100 (6)	100 (7)
	250 (3)	50 (3)				
	100 (1)					
	50 (2)					
RO–NO_x, Å	1.46	2.46	- -	1.46	3.60	- -
10^{120} $I_A I_B I_C/(gcm^2)^3$	6.07×10^7	1.30×10^8		2.93×10^7	1.53×10^8	
10^{40} $I_{red}/(gm\ cm^2)$	- -	6.10	- -	- -	1.00	- -
log $[A(300°K)/sec^{-1}]$	- -	16.5	14.7	- -	15.8	16.3

TABLE IV. Thermochemical quantities.

Species	$\Delta H^0_{f,298}$ [a]	Ref	S^0_{298} [b]	Ref.
n-$PrONO_2$	− 41.6	c	91.1	d
n-PrO	− 9.0	h,e	74.0	e
NO_2	7.9	f	57.3	f
t-BuONO	− 41.0	g	89.6	d
t-BuO	− 22.7	d	75.0	e
NO	21.6	f	50.3	f

[a] kcal/mole.
[b] cal/mole · deg.
[c] Reference (11).
[d] See "Thermochemistry" section.
[e] Reference [10].
[f] Reference [12].
[g] Reference [3].
[h] We have chosen the value of −9.0 rather than the −9·7 listed in [103] because it is more consistent with a large number of measurements of alkoxy compounds as well as with a uniform RO–H bond strength of 104.0 ± 1.0 kcal/mole.

TABLE V. Rate constants.

$$\text{n-PrONO}_2 \underset{-1}{\overset{1}{\rightleftharpoons}} \text{n-PrO} + NO_2$$

$$\text{t-BuONO} \underset{-2}{\overset{2}{\rightleftharpoons}} \text{t-BuO} + NO$$

	(1)	(2)
ΔH^0_{300}/kcal mole^{-1}	40.5	39.9
ΔS^0_{300}/cal mole^{-1} dec^{-1}	40.2	35.7
log k^+_{300}/sec^{-1} [VLPP]	16.5 − 40.0/θ	15.8 − 39.3/θ
$\log\left[\frac{A^+/\text{sec}^{-1}}{A^-/M^{-1}\ \text{sec}^{-1}}\right] = \frac{\Delta S^0 - R(1 + \ln R'T)}{2.3\ R}$	6.95	5.97
log k^-_{300}/M^{-1} sec^{-1}	9.5	9.8
log k^+_{300}/sec^{-1} [Ref. 3]		16.3 − 40.3/θ

The combination rates given in Table V are $\sim 10^2$ higher than values currently accepted. The rate for t-BuO + NO is in good agreement with the results by Batt et al.[3] Phillips and Shaw,[11] and Baker and Shaw[12] reported relative rates for recombination of NO and NO_2 with RO (R = Me, Et, t-Bu) between 1.7 and 2.7. The ratio $k_{-2}/k_{-1} = 10^{0.3} \cong 2$ is in the center of this range.

The results from the methyl peroxide-NO_2 study are in good agreement with those of Baker and Shaw[12] who obtained $k_a/(k_a + k_b) = 0.90$ at 130°C. Extrapolation of the data shows that the combination at 760 torr is in its high-pressure limit, and hence that combination of larger RO radicals with NO_2 will also be pressure independent.

The decomposition of n-propyl nitrate appears to be a uniform process at various temperatures, collision numbers, and flow rates. The rate constant reported here for $nPrONO_2$ decomposition was chosen so that the activation energy at 298°K was $E_{298} = \Delta H_{298} - 0.6$. Thus we find a best fit RRKM value of $\log k_\infty/sec^{-1} = 16.5 - 40.0/\theta$. There is a value reported in reference 2a of $\log k_\infty/sec^{-1} = 14.7 - 36.9/\theta$. If we change frequencies in the transition state to produce an A-factor of $\log A/sec^{-1} = 14.7$, we find that E = 37.7 kcal/mole (Figure 1). Thus we cannot really distinguish between these values from the VLPP data alone, but require the values of ΔH_1 from other sources, as well as the increasing evidence that the combination of alkoxy radical with NO_2 would have to be higher than the value of $\log k_{-1}/M^{-1}\ sec^{-1} = 7.7$ which would follow from the lower A-factor.

The rate constant for tBuONO decomposition was evaluated in the same way as above. The data could be equally well fitted by the parameters of reference 3 (Figure 2), and since the value of ΔH_{298} is uncertain by at least ± 1 kcal/mole, no distinction is possible.

The scattered points in the VLPP plot for tert-butyl nitrite at the low temperature end, as well as the isobutene formation in that temperature range, indicate that a surface-catalyzed process is operative that produces nitrous acid and isobutene. In an earlier study of 1- and 2-nitropropane pyrolysis[13] it was found that nitrous acid decomposed under VLPP conditions, even though it could not have occurred in a homogeneous manner. We suggest that tert-butyl nitrite decomposition is autocatalytic in the low-temperature range, in that acid produced in the β-scission is absorbed onto the walls, where it both decomposes and catalyzes elimination of more HONO. Surface effects for RONO have been described by Batt et al.[3] and the decomposition of tert-butanol in our system to give isobutene must be a catalyzed process, because the homogeneous rate is prohibitively slow. The origin of tert-butanol from tert-butyl nitrite is not clear. It could arise from H-abstraction from walls or HONO by tert-butoxy, or by a surface-catalyzed hydrolysis of the nitrite by water in equilibrium with nitrous acid.

The decomposition of methyl nitrite was not studied extensively. The NO and HNO may arise by homogeneous or multistep mechanisms; the falloff for this small molecule [0.3, assuming $\log (k_\infty/\mathrm{sec}^{-1}) = 15.6 - 41.1/\theta$],

$$\begin{aligned} CH_3ONO &\xrightarrow{r} CH_2O + HNO \\ &\xrightarrow{s} CH_3O + NO \\ CH_3O + HNO &\xrightarrow{t} CH_3OH + NO \\ CH_3O + NO &\xrightarrow{u} CH_2O + HNO \end{aligned}$$

is much less than predicted (10^{-5}), and the process is probably wall catalyzed. Methanol can arise by two mechanisms as discussed for t-BuONO above.

In a relative rate study, Wiebe et al. [20] have concluded that for the reactions:

$$CH_3O + O_2 \xrightarrow{3} CH_2O + HO_2 \quad (3)$$

$$CH_3O + NO \xrightarrow{4} CH_3ONO \quad (4)$$

$$k_3/k_4 = 5.5 \times 10^{-5} \text{ at } 25^oC$$

If we take k_4 to be the same as k_{-2} proposed in this work (i.e., $k_4 = 10^{9.8}$ M^{-1} sec^{-1}), then $k_3 = 1.7 \times 10^5$ M^{-1} sec^{-1}. Heicklen has estimated k_3 as $10^{7.6-6/\theta}$ M^{-1} sec^{-1} = $10^{3.2}$ at 25°C. The importance of measuring k_3 is underscored. Demerjian et al.[1] pointed out that a ratio of $k_3/k_5 = 4.9 \times 10^{-5}$ is compatible with CH_3ONO_2 formation in smog chamber studies:

$$CH_3O + NO_2 \xrightarrow{5} CH_3ONO_2 \quad (5)$$

If k_5 is taken as $\sim k_{-1}$ of this study (i.e., $k_5 = 10^{9.5}$ M^{-1} sec^{-1}), this would also make $k_3 \sim 10^5$ M^{-1} sec^{-1}.

Thermochemistry

Entropy of $nPrONO_2$:

The value used, 91.1 cal/mole-deg was computed from group additivity[14] by assigning the value 72.3 cal/mole-deg to CH_3ONO_2, in agreement with Stull et al.,[15] and adding twice the value of the group $\underline{C}$-$(C)_2(H)_2$ which is 9.42 cal/mole-deg [i.e., $\underline{C}$-$(C)(O)(H)_2$ = $\underline{C}$-$(C)_2(H)_2$].

Entropy of tBuONO:

The entropy of tBuONO may be calculated from group additivity if a value for the group $\underline{O}$-(C)(N=O) can be found. This, in turn, is found from the entropy of CH_3ONO whose value is in some dispute.[15] The value[16] $S^0_{298}(CH_3ONO)$ = 69.7 cal/mole-deg has been chosen. This leads to $S^0_{298}(tBuONO)$ = 90.4 cal/mole-deg.

The entropy of tBuONO can also be calculated from the entropy of 2,2-dimethylpentene-1 by correcting for the difference between CH_3ONO and butene-1. This yields a value of 88.7 cal/mole-deg, and we have chosen 89.6 cal/mole-deg as the best choice.

Heat of Formation of tBuO:

The value $\Delta H_{f,298}(tBuO)$ = 21.6 kcal/mole found in most recent references[3,10] comes from the activation energy of the decomposition of ditertiary butyl peroxide,[17] and the heat of formation of the same compound.[16] The value in Reference 18 of $\Delta H_{f,298}(t\text{-}C_4H_9O)_2$ = −81.5 kcal/mole is only correct if the heat of vaporization used therein is also correct. Two values exist[19] for ΔH_{vap}, and the second value gives $\Delta H_f(t\text{-}C_4H_9O)_2$ = −83.4 kcal/mole which yields $\Delta H_f(tBuO)$ = −22.7 kcal/mole.

B. THE DECOMPOSITION OF DIMETHYL PEROXIDE AND THE RATE CONSTANT FOR $CH_3O + O_2 \rightarrow CH_2O + HO_2$

The methoxy radical (MeO) is a ubiquitous species present in the atmosphere as well as in flames and combustion processes where it is potentially active as a chain-carrier and propagator. A reaction of particular importance is that of methoxy radicals with molecular oxygen. In the polluted troposphere that reaction plays an important role in the oxidation of nitric oxide according to the following sequence of reactions:[21]

$$\begin{aligned} CH_4 + OH &\rightarrow CH_3 + H_2O \\ CH_3 + O_2 &\xrightarrow{M} CH_3O_2 \\ CH_3O_2 + NO &\rightarrow CH_3O + NO_2 \\ CH_3O + O_2 &\rightarrow HO_2 + CH_2O \qquad (17) \\ HO_2 + NO &\rightarrow OH + NO_2 \\ &\text{etc.} \end{aligned}$$

Not included in this sequence are two reactions which can compete with reaction (17) under certain circumstances:

$$CH_3O + NO \xrightarrow{M} CH_3ONO \qquad (14a)$$

$$CH_3O + NO_2 \xrightarrow{M} CH_3ONO_2 \qquad (12a)$$

It is desirable that absolute rate constants for reactions (17), (14a), and (12a) be obtained by direct observation. Unfortunately, the detection of MeO is difficult, necessitating the use of indirect techniques which can give the rate constants with as little attendant uncertainty as possible. Since relative measurements are necessary it is advantageous

to choose either reaction (14a) or (12a) as the reference reaction, since these reactions are also of importance in the troposphere.

The reverse of reaction (14a) was the subject of a recent and thorough study by Batt and coworkers[3] who obtained Arrhenius parameters for the unimolecular decomposition of methyl nitrite. Using the experimental parameters and the equilibrium constant for the reaction, they then deduced the absolute rate constant for the forward direction of reaction (14a).

Reaction (12a) has been studied by a number of investigators[20,11,12] who have obtained rate constant ratios k_{12a}/k_{14a} Although the experimental values do not agree exactly, the net uncertainty in log k_{12a} is only about ± 0.3. This point will be discussed in more detail later.

The rate constant for reaction (17) has never been measured directly, and the rate constant ratio k_{17}/k_{14a} has been obtained only at room temperature.[20] For our study, we decided to measure the ratio k_{17}/k_{14a} as a function of temperature in order to obtain the Arrhenius parameters for the reaction. We chose reaction (12a) because NO_2 is stable in an oxygen atmosphere, and because the activation energy of reaction (12a) is about zero.[2b] Since there can also be uncertainties due to an assumed mechanism, we have made a considerable effort to understand the reaction system as thoroughly as possible in order to reduce consequent uncertainties in the resulting rate constant.

Dimethyl peroxide (DMP) was chosen as the precursor for producing MeO since it decomposes cleanly and at relatively low temperatures and it has been well studied before.[22,23,5] To understand the chemistry as thoroughly as possible, numerous experiments and analyses were carried out in three stages: decomposition of pure DMP, decomposition of DMP in the presence of NO_2, and decomposition of DMP in the presence

of added NO_2 and O_2. The results we have obtained are entirely consistent with those from earlier studies of DMP decomposition, and differ only slightly from earlier investigations of DMP decomposing in the presence of added NO_2.[2a,11,12] As a result, we feel that the value we obtain for k_{17} is relatively free of errors arising from an erroneous reaction mechanism.

In the next section, the experimental techniques are described, followed by a section on Results and Discussion that is divided into three parts: 1) Pure DMP, 2) DMP + NO_2, and 3) DMP + NO_2 + O_2.

Experimental

A schematic diagram of the experimental apparatus is shown in Figure 3. The apparatus was changed from one configuration to another, depending on the information needed. Thus, pressure measurements were always made, but gas chromatography was carried out only for some experiments with DMP + NO_2, and *in situ* spectrophotometric observations of NO_2 were made principally in the experiments with DMP + NO_2 + O_2.

The experimental apparatus consisted of a reaction vessel surrounded by an oven whose temperature was regulated to within ± 0.2°C by a ProportioNull temperature regulator. The reaction vessel was connected to a Validyne (Model 7D) pressure transducer so that the pressure of the reaction mixture could be recorded continuously on a strip-chart recorder. Also connected to this reaction vessel was an F & M (Model 720) gas chromatograph fitted with a 10 ft. by 0.25 in. column of 20% di-(2 ethyl hexyl)sebacate on 60-80 mesh chromasorb at 40°C for product analysis. A standard vacuum line was used for mixture preparation and gas handling.

For all experiments except for the *in situ* spectrophotometric runs, the reaction vessel, RV, consisted of a double-walled pyrex vessel of about 200 cc. The outer jacket of RV could be used as the reference side of the pressure tranducer to reduce the effect of minor temperature fluctuations, but this procedure was not really necessary and the gas-filled outer jacket simply served to eliminate "hot spots" on the inner walls. The temperature of RV was measured by either a copper-constantan or Chromel-Alumel thermocouple.

For the *in situ* measurement of NO_2, a conventional quartz cell (~ 500 cc) fitted with windows and an optical path of ~ 15 cm was employed.

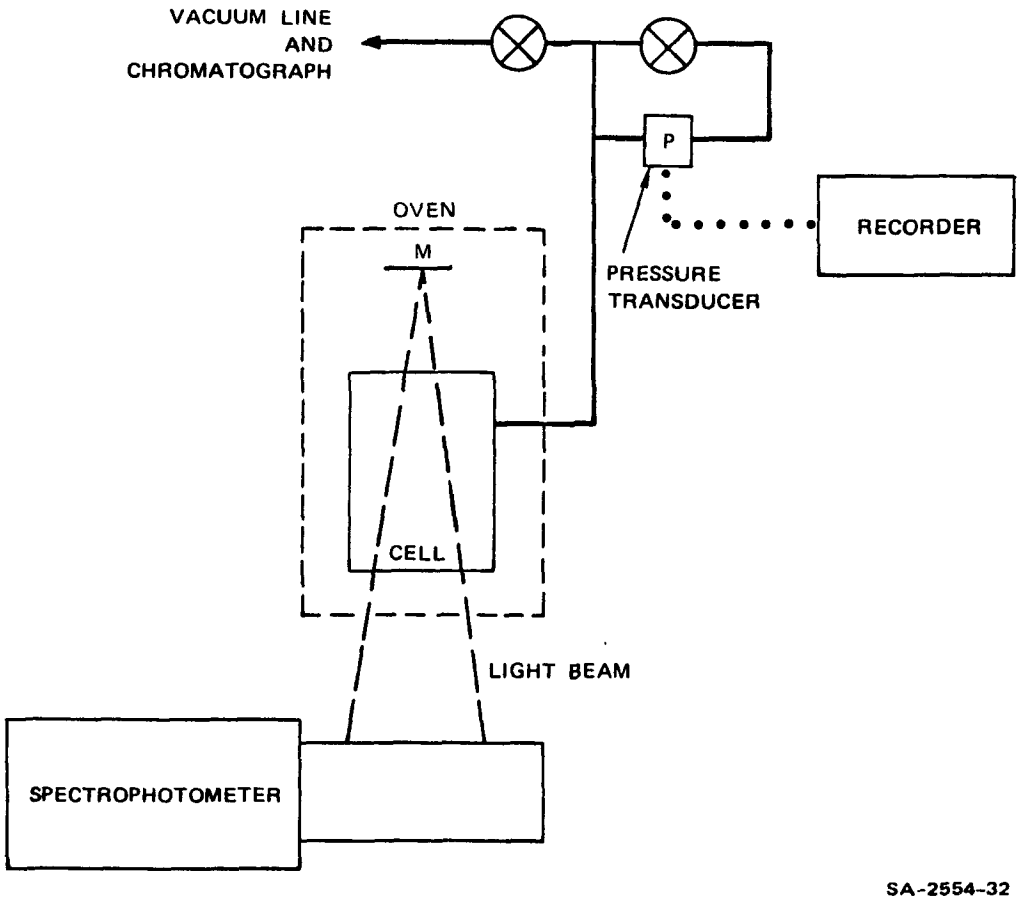

FIGURE 3 SCHEMATIC DIAGRAM OF APPARATUS

A special oven, incorporating a window and a mirror, was used to house the cell,[24] and a Cary 15 spectrophotometer was employed to continuously monitor the absorbance (at 4200 Å) due to NO_2.

Dimethyl peroxide was prepared according to Hanst and Calvert.[5] (One explosion occurred during preparation of DMP when the concentrated base was added too rapidly to the hydrogen peroxide-dimethyl sulfate mixture.) The DMP was conveniently purified by passage through a trap cooled to $-78^{o}C$. This procedure gave DMP with only a trace (< 1% by gas chromatography) of a single unknown impurity. Occasionally, CH_3ONO was present in the apparatus after many runs had been performed. It was found that the vapor pressure of DMP at $-78^{o}C$ (~ 2 torr) was a useful indicator of higher-volatility impurities.

Nitrogen dioxide was obtained from Matheson Gas products, Inc. and purified by bulb-to-bulb distillation. Oxygen gas was also obtained from Matheson.

Results and Discussion

In the next sections, we will discuss our results in the light of other work on dimethyl peroxide decomposition. Since our primary objective was to evaluate rate constant k_{18}, we have attempted to make a self-consistent interpretation of our data, even though our interpretation differs in small ways from those in the literature. In some cases, the differences disappear when further considerations are made, but in others, we feel that our results are the most consistent.

Dimethyl Peroxide Decomposition:

The decomposition of DMP has been studied by three different groups. Takezaki and Takeuchi[23] (TT) pyrolyzed DMP in the presence of excess methanol, which acted as a radical trap, and found that $\log k_6/s^{-1} = 15.61 - (36.9 \pm 1.1)/\theta$ ($\theta = 2.3$ RT in kcal/mole).

$$\text{MeOOMe} \rightarrow 2\ \text{MeO} \tag{6}$$

In a related study,[25] Takezaki and coworkers concluded that the activation energy for reaction (7) is $E_7 \lesssim 5.8$ kcal/mole.

$$\text{MeO} + \text{MeOOMe} \rightarrow \text{MeOH} + \text{MeOOCH}_2 \tag{7a}$$

$$\text{MeOOCH}_2 \rightarrow \text{MeO} + \text{CH}_2\text{O} \tag{7b}$$

Since the pre-exponential factor for many methoxy radical reactions is $\log [A/M^{-1}\ s^{-1}] \approx 8.5$,[2a] reaction (7) is expected to lead to a chain reaction, if no radical trap is present.

Hanst and Calvert[5] (HC) studied the decomposition of DMP without a radical trap. They found that the stoichiometry was given by

$$2\ DMP \rightarrow 3\ MeOH + CO, \qquad (A)$$

and reported $\log k_6/s^{-1} = 15.2 - (35.3 \pm 2.5)/\theta$, giving a rate constant about three times larger than that reported by TT. The larger rate constant is consistent with a contribution from a chain reaction, but HC concluded that there was no chain contribution. On the contrary, our results (see below) explain the discrepancy as due to a chain reaction.

In a recent study, Batt and McCulloch[22] (BM) studied the decomposition of DMP using isobutane as a radical trap. They found $\log k_6/s^{-1} = (15.5 \pm 0.5) - (37.0 \pm 0.2)/\theta$; in close agreement with the value reported by TT. They also found that DMP is a "clean" thermal source of MeO and wall reactions are not important.

Our own experiments are best described in terms of a mechanism consisting of reactions (6) and (7) followed by a series of termination reactions:

$$MeO + MeO \rightarrow MeOH + CH_2O \qquad (8)$$

$$MeO + CH_2O \rightarrow CHO + MeOH \qquad (9)$$

$$MeO + CHO \rightarrow MeOH + CO \qquad (10)$$

$$CHO + CHO \rightarrow CH_2O + CO \qquad (11)$$

This mechanism is consistent with the stoichiometry found by HC and is consistent with our results, as well.

In our experiments, we added pure DMP to the reaction vessel and simply observed the pressure as a function of time as shown in Figure 4

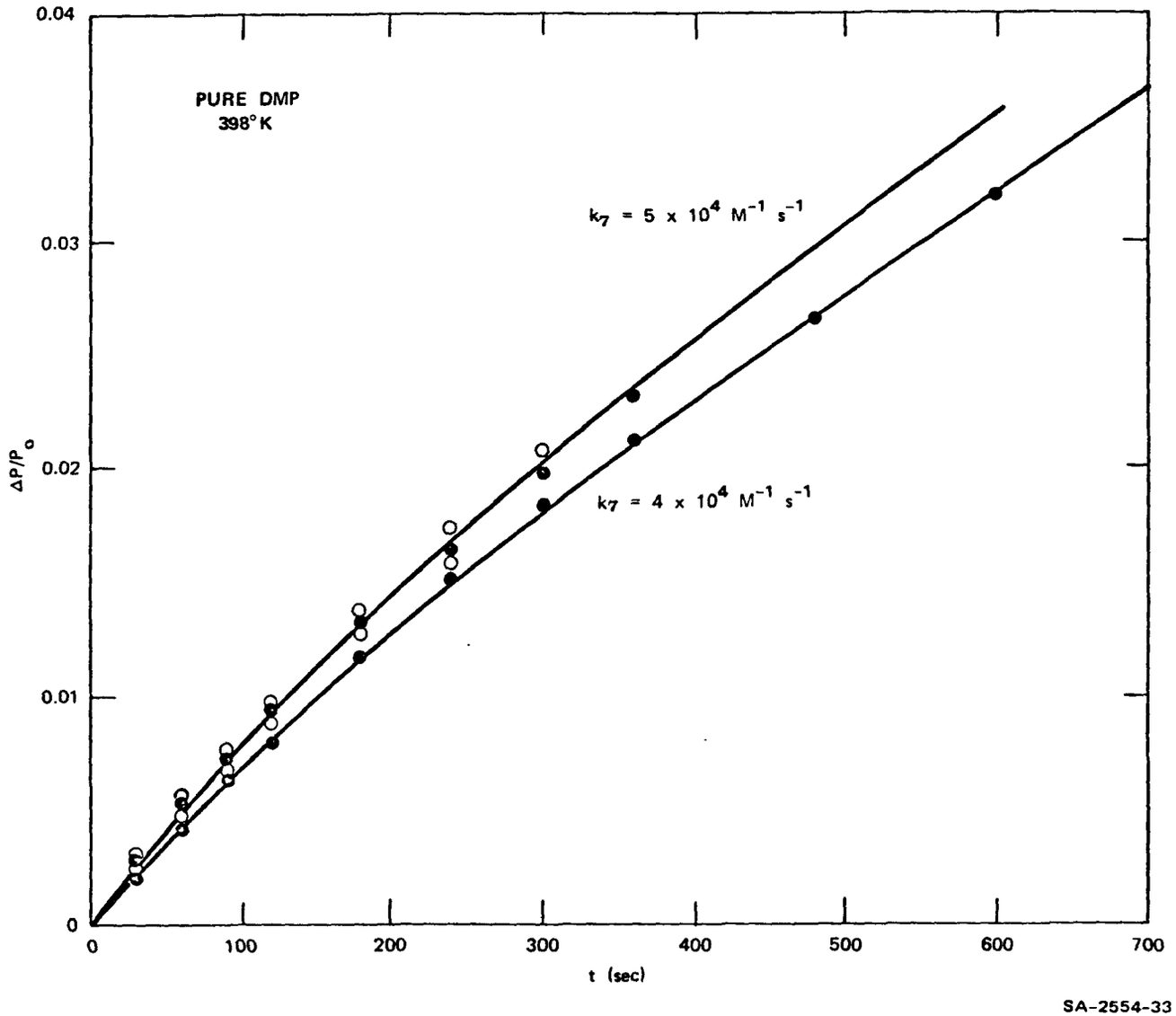

FIGURE 4 DECOMPOSITION OF INITIALLY PURE DMP. Data points from four representative experiments (18.4 torr < $[DMP]_o$ < 55.3 torr) are compared to computer simulations for two assumed values of k_7.

for four runs. Typically, the rate of pressure increase, dP/dt, is greater initially, and gradually decreases to a constant value as the experiment progresses. In general terms, this is due to the chain reaction being gradually inhibited by one or more of the reaction products, i.e., formaldehyde. Since the rate of reaction (9) is much greater than that of reaction (7), the MeO preferentially attacks the formaldehyde to produce the relatively inactive CHO radicals, thus partially quenching the chain.

We carried out a series of runs at different temperatures and obtained data similar to that presented in Figure 4. From the data, we deduced $k_{obs} \equiv P_{DMP}^{-1}$ (dP/dt) at run times greater than about 180 seconds, when the rates approach a constant value. Despite some scatter in the results, we found our data (Figure 5) to be very well fitted by the expression obtained by HC: $\log k = 15.2 - 35.3/\theta$. This good agreement confirms the consistency between pressure measurements and the spectrophotometric measurements of HC.

To test the proposed mechanism in detail, numerical calculations were performed using the Gear computer program for integrating coupled sets of stiff differential equations.[26] Reasonable estimates for the rate constants were made (Table VI) for all reactions except for k_7, which was used as an adjustable parameter. We experienced no difficulty in fitting the experimental results, which indicates that the proposed mechanism is consistent with the data. The particular rate constants we chose may be somewhat in error, thus the rate constant k_7 can also be slightly in error. Nonetheless, the best fits were obtained for $k_7 \approx 5 \times 10^4\ M^{-1}\ s^{-1}$, which can be compared to that for similar reactions.

Typical A-factors for methoxy radical reactions are about $10^{8.5 \pm 0.5}$ $M^{-1}\ s^{-1}$, giving an activation energy $E_7 = 7 \pm 1$ Kcal mole^{-1}, in good agreement with the $E_7 \leq 5.8$ Kcal mole^{-1} deduced in Reference 25. These values

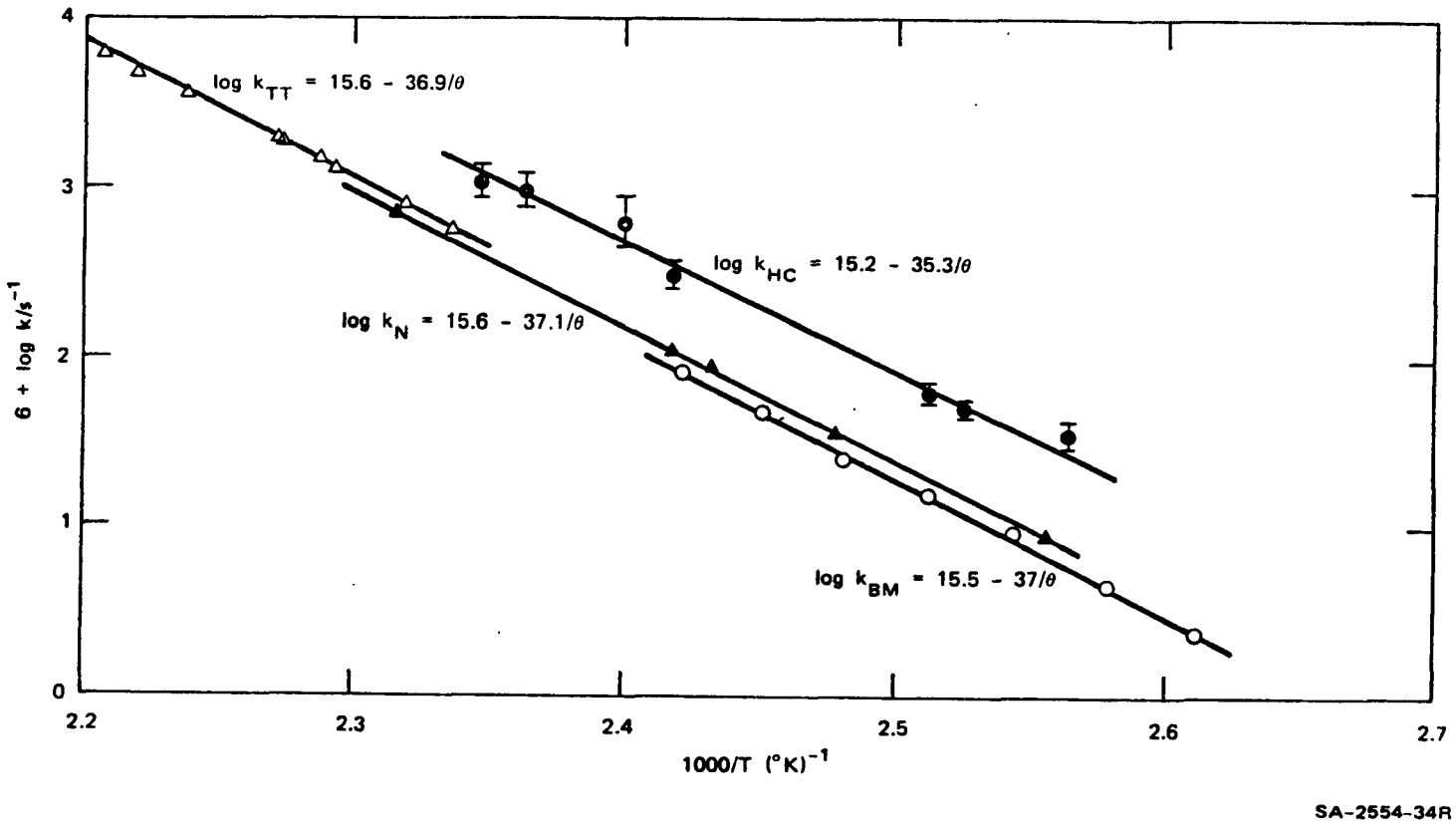

FIGURE 5 ARRHENIUS PLOT SUMMARIZING DATA FOR DMP DECOMPOSITION.

○ k_{BM} from ref [7];

△ k_{TT} from ref [8];

● data from this work and k_{HC} from ref [9];

▲ k_N this work (see text for definition of k_N).

Table VI. Rate constants for computer calculation.

	Reaction	log k[a]	Ref
6	$MeOOMe \rightarrow 2\ MeO$	$15.7 - 37.1/\theta$	This Work
7	$MeO + DMP \rightarrow MeO + CH_2O + CH_3OH$	Adjusted	--
8	$MeO + MeO \rightarrow MeOH + CH_2O$	10	(b)
9	$MeO + CH_2O \rightarrow MeOH + CHO$	$8 - 3/\theta$	10
10	$MeO + CHO \rightarrow MeOH + CO$	10	(b)
11	$CHO + CHO \rightarrow CH_2O + CO$	10	(b)
12a	$MeO + NO_2 \xrightarrow{M} MeONO_2$	9.8	See Text
12b	$MeO + NO_2 \rightarrow HONO + CH_2O$	9.3	This Work
13	$HONO \xrightarrow{wall} \frac{1}{2} NO + \frac{1}{2} NO_2 + \frac{1}{2} H_2O$	0.05	28, (b)
14a	$MeO + NO \xrightarrow{M} MeONO$	10.1	3
15	$MeO + NO \rightarrow HNO + CH_2O$	9.4	3, 20
16	$NO_2 + CHO \rightarrow HONO + CO$	9	(b)

[a] Units are as follows: unimolecular: sec^{-1}; bimolecular: $M^{-1} \cdot sec^{-1}$; wall reaction: sec^{-1}; activation energies: kcal/mol.

[b] Many of these rate constants are estimates, since the computer calculations are only meant to be used as a test of the steady-state assumptions and not a definitive simulation of the mechanism.

Table VII. Dimethyl peroxide rate constants.[a]

T (°K)	k_N (s^{-1})[b]	k_6 (s^{-1})[c]
391	8.99 (−6)[d]	1.06 (−5)[d]
404	3.52 (−5)	4.15 (−5)
411	8.90 (−5)	1.05 (−4)
414	1.06 (−4)	1.25 (−4)
432	7.39 (−4)	8.72 (−4)

$$\log (k_N / s^{-1}) = (15.6 \pm 0.5)^e - (37.1 \pm 0.9)^e/\theta$$
$$\log (k_1 / s^{-1}) = (15.7 \pm 0.5)^e - (37.1 \pm 0.9)^e/\theta$$

[a] Uncertainties are estimated to be ±10%.

[b] See text for definition of k_N.

[c] $k_6 = 1.18\ k_N$.

[d] Notation: $1.00(-5) = 1.00 \times 10^{-5}$.

[e] Uncertainties are one standard deviation.

may be compared to log $k_7 = 9.3 - 10/\theta$ estimated by O'Neal and Richardson,[27] which is about a factor of seven too low at 400°K. Thus, we have reproduced the results of HC and can explain them in terms of a reasonable chain mechanism.

Dimethyl Peroxide with Added NO_2:

Nitrogen dioxide is an effective radical trap and effectively quenches the chain reaction in the pyrolysis of DMP. As long as sufficient NO_2 is present, the mechanism for DMP decomposition consists of reaction (6) followed by

$$MeO + NO_2 \xrightarrow{M} MeONO_2 \qquad (12a)$$

$$\rightarrow HONO + CH_2O \qquad (12b)$$

$$HONO \rightarrow \frac{1}{2} NO + \frac{1}{2} NO_2 + \frac{1}{2} H_2O \qquad (13)$$

$$MeO + NO \xrightarrow{M} MeONO \qquad (14a)$$

$$\rightarrow CH_2O + HNO \qquad (14b)$$

$$HNO + NO_2 \rightarrow HONO + NO \qquad (15)$$

$$MeO + CH_2O \rightarrow CHO + MeOH \qquad (9)$$

$$NO_2 + CHO \rightarrow HONO + CO \qquad (16)$$

This reaction mechanism is similar to those suggested by other authors.[3,4,5] Reaction (13) has been inferred to be wall-catalyzed and to have rate constant $k_{13} \approx 0.01\ sec^{-1}$ at room temperature;[28] at 400°K it may well be somewhat faster. Rate constants for all of these reactions are presented in Table VII. It should be pointed out that the following

reactions have been omitted, even though they may be important when the NO_2 concentration is very low:

$$MeO + CH_3OH \rightarrow MeOH + CH_2OH$$

$$MeO + CH_3ONO_2 \rightarrow MeOH + CH_2ONO_2$$

$$MeO + CH_3ONO \rightarrow MeOH + CH_2ONO$$

These reactions have been neglected since their rates are unknown, but they are expected to be unimportant unless the NO_2 concentration falls to a very low value.

When the NO_2 has been consumed, the termination reactions mentioned earlier as well as those listed above become important. Note that if $k_{12b} \ll k_{12a}$ the stoichiometry for the reaction would be

$$DMP + 2\ NO_2 \rightarrow 2\ MeONO_2 \qquad \text{(B)}$$

and a pressure <u>decrease</u> results. When all of the NO_2 has been consumed, the stoichiometry reverts to equation (A) and a pressure <u>increase</u> results. Thus the "titration endpoint" for NO_2 consumption is signaled by the change in sign of dP/dt at time τ as shown in Figure 6. Using this simple picture, a rate constant k_N can be defined:

$$k_N = -\frac{1}{\tau} \ln \left[\frac{2\,[DMP]_0}{2\,[DMP]_0 - [NO_2]_0} \right] \qquad \text{(C)}$$

This equation was written assuming stoichiometry equation (B) and assuming all of the NO_2 has been consumed at time τ.

Typical experimental data for a single run are shown in Figure 6. These data qualitatively resemble the simple picture described in the preceding paragraph. The total pressure steadily decreases until nearly

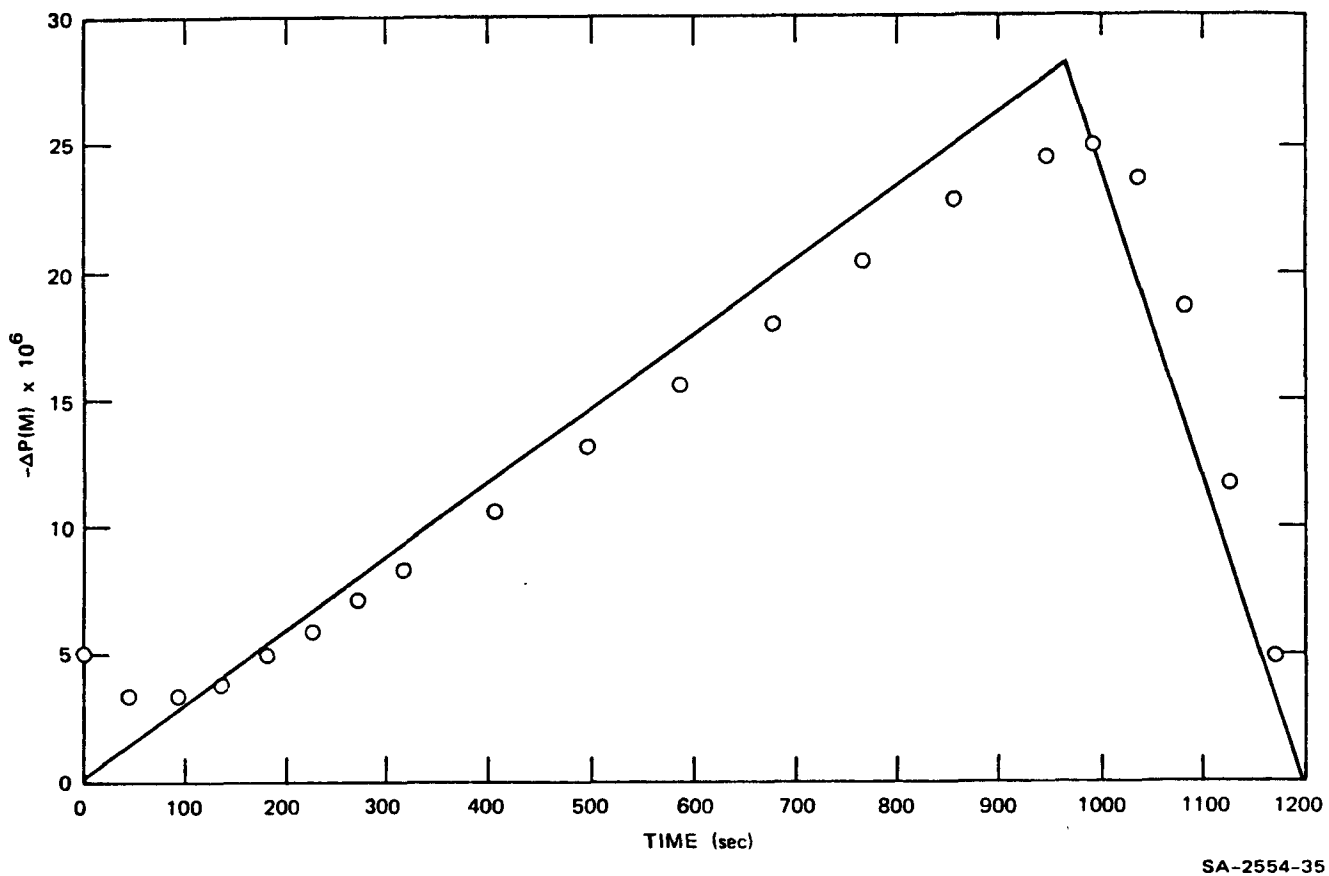

FIGURE 6 DECOMPOSITION OF DMP WITH ADDED NO_2. Comparison of experimental data ($-\Delta P$ in molar units) to computer simulation (see text for rate constants); $[DMP]_o = 9.92 \times 10^{-4}$ M, $[NO_2]_o = 1.30 \times 10^{-4}$ M, 410^oK.

all of the NO_2 has been consumed and then starts to increase. In most runs, the titration endpoint at τ is very sharp and easily recognized. Typical uncertainties in τ are of the order of a few seconds.

Gas chromatographic analyses for MeONO and $MeONO_2$ and spectrophotometric analyses for NO_2 were carried out to test the proposed mechanism for consistency. The gas chromatography was slightly hampered by the tendency of the DMP and $MeONO_2$ to decompose suddenly at the chromatograph inlet. On several occasions, the DMP decomposed completely during gas chromatography. The experimental data are presented in Figure 7. The co-ordinates are reduced variables: the ordinate is the ratio of the component concentration to the concentration of NO_2 initially present, and the abscissa is the reduced time, t/τ. Despite the experimental scatter, virtually all of the original NO_2 shows up later as $MeONO_2$ and MeONO. Only small quantities of MeONO were observed ($\sim$0.1 - 0.3 times $[MeONO_2]$), but the reproducibility was poor and that detected may have been due to residual amounts in the inlet lines. In any event, the observed products are consistent with the proposed mechanism. Note that $[NO_2]_\tau/[NO_2]_0 \approx 0.06$ for this series of runs; for another series of runs, $[NO_2]_\tau/[NO_2]_0 = 0.08 \pm 0.03$. The relative constancy of this value may be due to the competition of reaction (k_{12a}) for MeO <u>vs</u> reactions of MeO with products such as those due to the reactions listed above that were omitted from the mechanism.

According to the simple stoichiometry equation (B), one NO_2 molecule is consumed for each MeO radical generated. In actual fact, however, k_{12b} is <u>not</u> greatly smaller than k_{12a}, and more than one methoxy radical is necessary to consume each NO_2, implying $k_N > k_6$ by some amount due to the effects of k_{12b}. Moreover, in the simple picture, it was assumed that $[NO_2]_\tau = 0$, an assumption not borne out by the data. Thus, less NO_2 has been consumed by time τ than was assumed, implying that $k_N < k_6$ Since these effects tend to cancel, $k_N \approx k_6$ to a first approximation

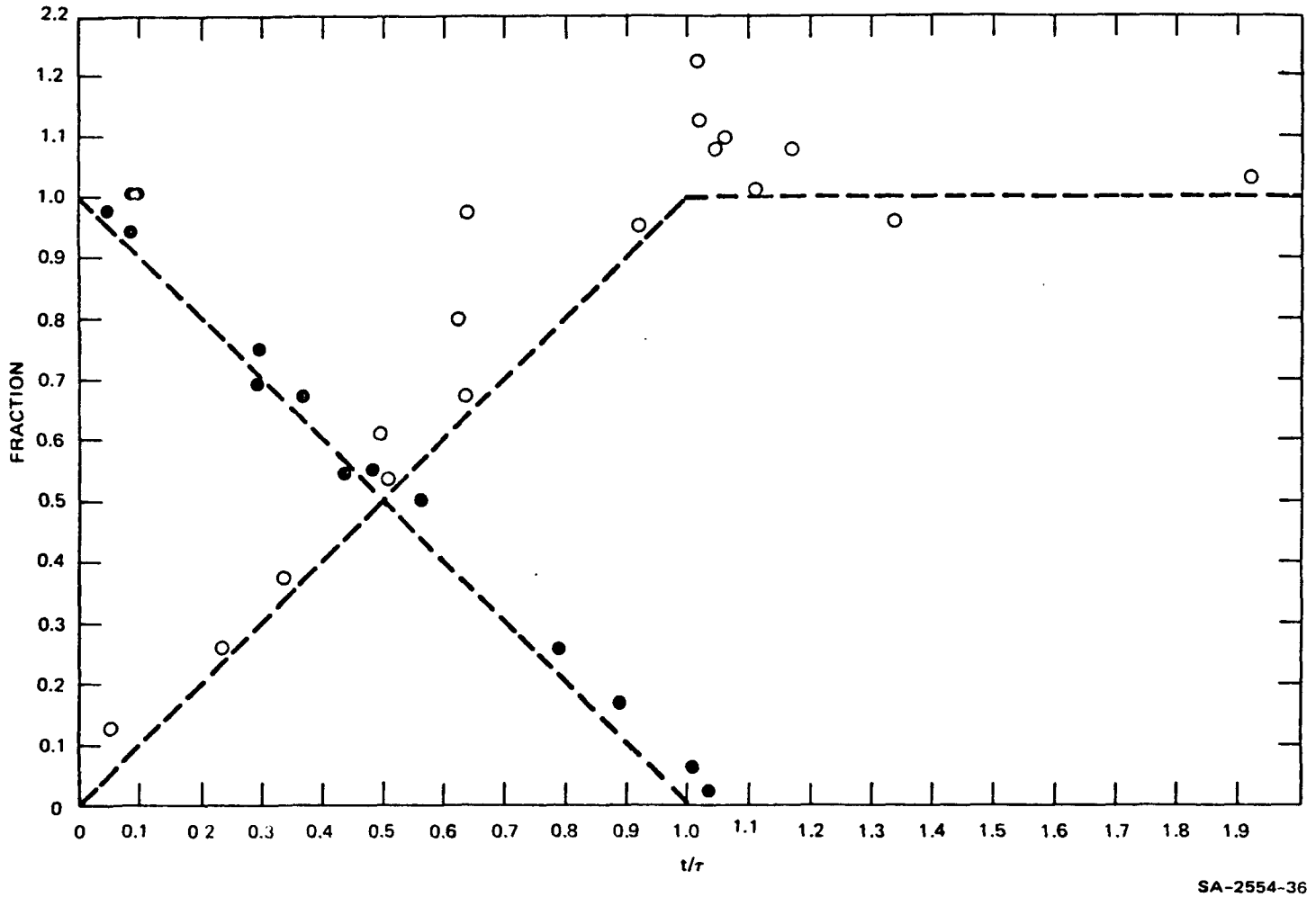

FIGURE 7 GAS CHROMATOGRAPHY RESULTS DEMONSTRATING MASS BALANCE.
● $[NO_2]/[NO_2]_o$;
○ $\{[CH_3ONO_2] + [CH_3ONO]\}/[NO_2]_o$.

(below, we find $k_N = 0.85\ k_1$). The data are presented in Table VI, and log k_N is plotted vs. $1/T$ in Figure 5, along with data from the literature. A more quantitative estimate of k_6 can be obtained if the effects of k_{12b} are taken into account.

The most obvious effect due to k_{12b} is that the relative slope $[DMP]^{-1}(dP/dt)$ is not equal to unity (Figure 8), but is ~ 0.4. This demonstrates qualitatively that (12b) is an important reaction. Baker and Shaw[12] made measurements on the DMP + NO_2 reaction system and came to the conclusion that $k_{12b}/k_{12a} = 0.1$. This value, however, is not consistent with our results.

We analyzed our data by carrying out a pseudo-steady state calculation, assuming that the following species are in steady-state: MeO, HONO, NO, and HNO. The formaldehyde was assumed to be immune from attack in the early and intermediate stages of the reaction. Using these assumptions, the rate of pressure change can be written

$$\frac{dP}{dt} = -k\ [DMP]\ \frac{k_{12a} - 3X\,k_{12b}}{k_{12a} + 3X\,k_{12b}} \qquad \text{(D)}$$

where $X = k_{14a}/(2k_{14a} - k_{14b})$. The ratio k_{14b}/k_{14a} has been measured recently by two different groups to be 0.17[29] and 0.18 ± 0.02.[3] Using $k_{14b}/k_{14c} = 0.18$ gives $X = 0.55$.

A series of <u>in situ</u> spectrophotometric runs was performed to determine $[NO_2]_T$ and it was found that $[NO_2]_T = (0.08 \pm 0.03)\ [NO_2]_0$. This finding, along with the steady-state analysis allowed us to write k_N in terms of k_6

$$k_N = \frac{C_s}{0.92}\ k_6 \qquad \text{(E)}$$

where C_s is a ratio of rate constants that depends on the assumed steady-state conditions. Using this result and the expression for (dP/dt), the

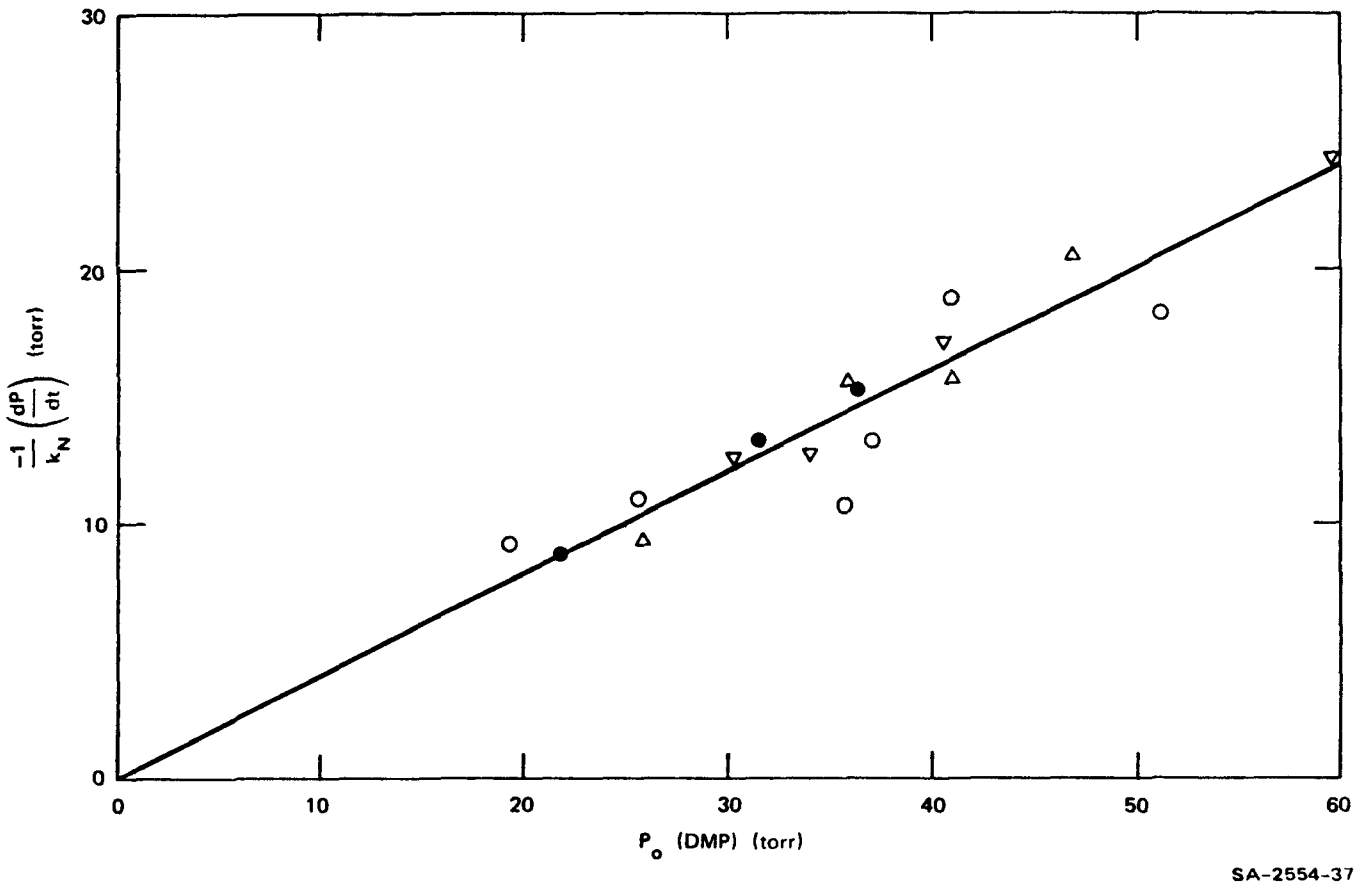

FIGURE 8 $-k_N^{-1}$ (dP/dt) vs. $[DMP]_o$ FOR FOUR TEMPERATURES.

● 391°K;
○ 403.5°K;
△ 413.5°K;
▽ 432°K.

following expression can be written:

$$- \frac{dP}{dt} \frac{1}{k_N} = [DMP] \frac{(0.92)}{C_s} \frac{k_{12a} - k_{12b}}{k_{12a} + k_{12b}} \qquad (F)$$

At early and intermediate times, $[DMP] \cong [DMP]_0$ and a plot of $-(dP/dt)/k_N$ vs. $[DMP]_0$ is expected to give a straight line. The experimental data obtained at five different temperatures are plotted this way in Figure 8 and the resulting straight line has a slope of 0.40 ± 0.05. With an appropriate value of C_s, the ratio k_{12b}/k_{12a} can be determined.

For the evaluation of C_s, three different sets of assumptions were made:

1) Initial conditions: nothing except MeO is in steady-state and no products have accumulated. This is unlikely to be the case except for a very short period after an experiment is begun.

2) Intermediate conditions: MeO, HONO, NO, and HNO are in steady-state and formaldehyde is immune from attack. This is a more likely case, since NO_2 greatly suppresses the MeO concentration and thereby prevents its attack on CH_2O. The rate of NO_2 attack on CH_2O is very slow at these temperatures.[30]

3) Final conditions: MeO, HONO, NO, HNO, CH_2O, and CHO are all at steady-state. This may be the case near the titration point, but the respective concentrations might not be the same as those calculated by the steady-state expressions.

The values of the constant C_s for these three cases are, respectively:

$$C_1 = 1.0 \qquad \text{(G)}$$

$$C_2 = \frac{k_{12a} + k_{12b}\ X}{k_{12a} + 3k_{12b}\ X} \qquad \text{(H)}$$

$$C_3 = \left[\frac{k_{12a} + 3k_{12b}X}{k_{12a} + 5k_{12b}X}\right], \left[\frac{k_{14a}}{2k_{14a} - k_{14b}}\right] = 0.55 \qquad \text{(I)}$$

The corresponding values of k_{12b}/k_{12a} are 0.26, 0.30, and 0.29, respectively. Since condition 1 is felt to be unlikely, we find that $k_{12b}/k_{12a} = 0.30 \pm 0.05$.

The result that $k_{12b}/k_{12a} = 0.30 \pm 0.05$ may be compared to the value 0.1 obtained by Baker and Shaw.[12] Those authors depended on the assumption that the attack of NO_2 on CH_2O was very fast compared to the time scale of their experiments (~ 3 hrs) carried out at 403°K. Literature values for the rate constant,[30] however, coupled with the pressures of NO_2 used by Baker and Shaw give lifetimes for CH_2O decomposition on the order of ~ 1.4 to ~ 2.8 hrs. Thus, for some of their runs, a substantial amount of CH_2O may have remained unreacted, possibly leading them to underestimate the ratio k_{12b}/k_{12a}. Thus, their results may represent a lower limit to the actual ratio and are compatible with the ratio obtained above.

Using $k_{12b}/k_{12a} = 0.3$ in equation (H) and in equation (E), the expression for k_6 becomes

$$k_6 = 1.18\ k_N \qquad \text{(J)}$$

A properly weighted least squares analysis of the data gives log $k_N/s^{-1} = (15.6 \pm 0.5) - (37.1 \pm 0.9)/\theta$; thus log $k_6/s^{-1} = (15.7 \pm 0.5) - (37.1 \pm 0.9)/\theta$, in good agreement with values obtained by TT and BM. At 420°K, this rate constant is about 1.6 times that obtained by Batt and McCulloch[22] and about 1.1 times that obtained by Takezaki and Takeuchi.[23]

One possible source of discrepancies among these three sets of data is thermal heating of the gas in the reaction vessel due to the exothermicity of the reaction itself.[31] Batt and McCulloch took special care to avoid generating thermal gradients by using low pressures of DMP ($\sim$ 0.5 – 5 torr) and high pressures of isobutane ($\sim$ 700 torr). In the present experiments and in those carried out by TT, considerably higher pressures of DMP were employed ($\sim$ 10-50 torr and 23 torr, respectively) and thermal gradients generated by the reaction could contribute to the rate. In fact, shifts of only $2^{o}K$ can account for all discrepancies between the present results and those of TT and BM. In light of these considerations, we feel that the data of BM are probably the best obtained so far for DMP decomposition.

Aside from slight differences in A-factors, the present data and those of TT agree well with those obtained by BM; the activation energies are 37.1 ± 0.9, 36.8 ± 1.1, and 37.0 ± 0.2 Kcal $mole^{-1}$, respectively. The consistency of these results strongly supports the methoxy radical heat of formation deduced by BM (ΔH_f^o (MeO) = 3.8 ± 0.2 Kcal $mole^{-1}$), and further supports their conclusion[3] that values for the dissociation energy D(RO – H) derived from ICR work and electron detachment[32] are consistently lower by $\sim$ 2 Kcal $mole^{-1}$.

To test the proposed mechanism and the rate constants deduced on the basis of the pseudo steady state assumption, a calculation was carried out using the Gear computer program[26] to do the time-integration of the coupled differential equations. The rate constants used are presented in Table VII, and the results of the calculation are presented in Figure 6 along with data from one experiment. The calculated results seem to be in good agreement with the experiment, essentially confirming the analysis. The computer calculation shows that the

pseudo-steady-state concentration of MeO is attained very quickly; that of HONO comes near the middle of the run, and those of NO, HNO, and CH_2O are attained only near $t/\tau = 1$. Thus, the "intermediate conditions" assumed earlier are probably the closest to actual fact, but the other sets of assumptions are not much in error.

Dimethyl Peroxide with Added NO_2 and O_2:

The experiments with DMP + NO_2 + O_2 were carried out by placing DMP – NO_2 mixtures in the reaction vessel, then adding ~700 torr of O_2. The reaction was followed in situ by spectrophotometric observation of NO_2 and by measuring the total pressure as a function of time. Data from a typical experiment is shown in Figure 9. The initial disturbance due to gas mixing soon subsides and smooth curves of pressure and $[NO_2]$ are obtained. In all runs, the pressure curves were noticeably more "rounded" and the amounts of NO_2 remaining at time τ were larger than when O_2 was not present.

Only two more reactions need be added to the mechanism when O_2 is added to NO_2 – DMP mixtures:

$$MeO + O_2 \rightarrow HO_2 + CH_2O \qquad (17)$$

$$HO_2 + NO_2 \rightarrow HONO + O_2 \qquad (18)$$

Reaction (17) is the reaction we have been trying to measure. Other termination steps are not important as long as NO_2 is present.

An "intermediate" steady-state treatment can be defined in which pseudo-steady-states are assumed for MeO, HONO, NO, HNO, and HO_2;

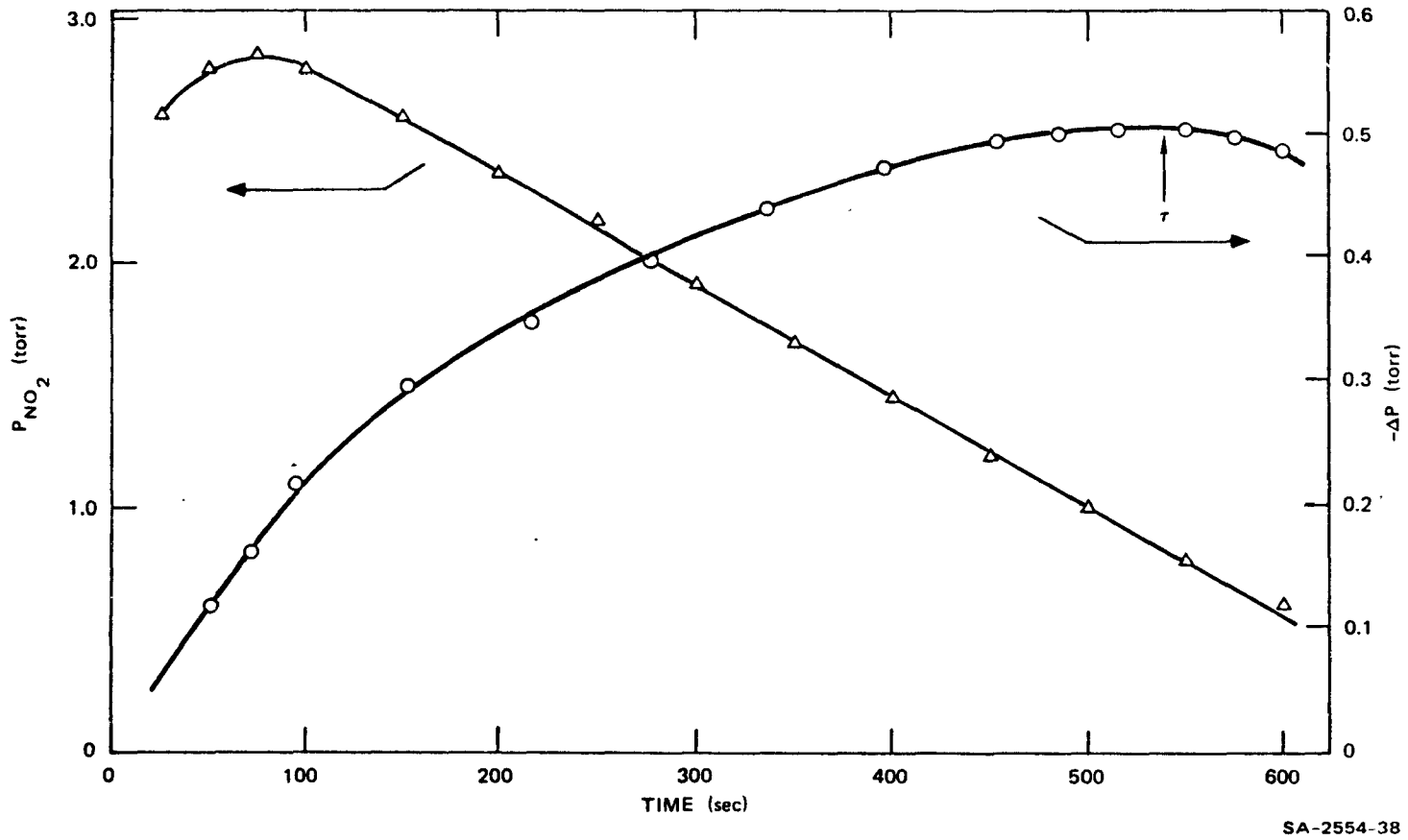

FIGURE 9 DECOMPOSITION OF DMP WITH ADDED NO_2 AND O_2. $[DMP]_0$ = 13.8 torr; $[NO_2]_0$ = 3.15 torr; $[O_2]_0$ = 685 torr, 420°K.

formaldehyde is again assumed to be immune to attack. The rate of pressure change can be written

$$\frac{dP}{dt} = k_6 [DMP] \left\{ 1 - \frac{2\, k_{12a}[NO_2]}{k_{12a}[NO_2] + 3 \left\{ k_{12b}[NO_2] + k_{17} [O_2] \right\} X} \right\} \quad (K)$$

where $X = \frac{k_{14a}}{2k_{14a} - k_{14b}} = 0.55$, just as before. At the titration point τ, $(dP/dt)_\tau = 0$ and equation (K) can be rearranged to give

$$k_{17} = \left\{ \frac{2}{3} - \frac{1}{3} \frac{k_{14b}}{k_{14a}} - \frac{k_{12b}}{k_{12a}} \right\} k_{12a} \frac{[NO_2]_\tau}{[O_2]} . \quad (L)$$

This expression is sensitive to the ratio k_{12b}/k_{12a}, justifying the care taken earlier to determine that quantity.

The expression for k_{17} consists of three parts: 1) a stoichiometry factor (in curly brackets), 2) rate constant k_{12a} and 3) experimental values for the ratio $[NO_2]_\tau/[O_2]$. The results obtained for the ratio $[NO_2]_\tau/[O_2]$ at several temperatures are presented in Table VII. These ratios are subject to experimental uncertainties of about ± 15%, as noted in the table. The stoichiometry factor depends on the ratios k_{14b}/k_{14a} (= 0.18 ± 0.02)[3] and k_{12b}/k_{12a} (= 0.30 ± 0.05) and is not subject to a large uncertainty, barring gross errors in the reaction mechanism:

$$\left\{ \frac{2}{3} - \frac{1}{3} \frac{k_{14b}}{k_{14a}} - \frac{k_{12b}}{k_{12a}} \right\} = 0.31 \pm 0.05 \quad (M)$$

Rate constant k_{12a}, on the other hand, suffers from a larger uncertainty.

Three indirect determinations of k_{12a} are reported in the literature. Baker and Shaw[12] measured the ratio $k_{14a}/k_{12a} = 2.7$ at 403°K and Phillips and Shaw[11] obtained $k_{14a}/k_{12b} = 1.8$ at 363°K. However, Baker and Shaw

felt that their data was better since the pressure of NO_2 was more constant in their experiments. Wiebe, et al.[20] measured $k_{14}/k_{12a} = 1.3$ at room temperature, leading to $k_{14a}/k_{12a} = 1.1$. It is possible that this ratio exhibits a temperature dependence, but that is not expected to be the case.[6] A likely explanation is that unrecognized systematic errors influenced the experimental determinations. On the basis of these data, a fair estimate seems to be $k_{14a}/k_{12a} = 2 \pm 1$.

As mentioned earlier, Batt and coworkers[3] measured the reverse of reaction (14a) and on the basis of their data and thermochemical calculations they concluded that $\log \left(k_{14a} / M^{-1}\ s^{-1}\right) = 10.1 \pm 0.4$ at 300°K; at temperatures near 400°K, the rate constant should be about the same. Combining their result with the ratio $k_{14a}/k_{12a} = 2 \pm 1$, we find that $\log \left(k_{12a}/M^{-1}\ s^{-1}\right) = 9.8 \pm 0.5$, where the quoted uncertainty has been derived by a propagation of errors analysis. Thus, the uncertainty associated with k_{12a} is far greater than that due to stoichiometry or that due to random experimental errors in the ratio $[NO_2]_T/[O_2]$.

The experimental values for $[NO_2]_T/[O_2]$ are presented in Table VIII. A properly weighted least squares analysis of this data gives $\log \left\{[NO_2]_T/[O_2]\right\} = -(0.82 \pm 1.46) - (4.0 \pm 2.8)/\theta$. When this value is combined with the stoichiometry factor, we obtain the expression $\log \left[k_{17}/k_{12a}\right] = -(1.33 \pm 1.46) - \frac{(4.0 \pm 2.8)}{\theta}$. The rate constant ratio itself is not subject to as much uncertainty as the individual arrhenius parameters. Combining the value $\log \left(k_{12a}/M^{-1}\ s^{-1}\right) = 9.8 \pm 0.5$ with the expression for $\log \left(k_{17}/k_{12a}\right)$, the final result is $\log \left(k_{17}/M^{-1}\ s^{-1}\right) = (8.5 \pm 1.5) - \frac{(4.0 \pm 2.8)}{\theta}$.

The large uncertainty in the Arrhenius parameters mainly reflects the relatively small temperature range of our experiments; the parameters themselves appear to be fairly reasonable. Our results are

Table VIII

DATA SUMMARY FOR $MeO + O_2 \rightarrow HO_2 + CH_2O$

T, °K	$10^3 \times [NO_2]_T/[O_2]$[a]	$10^{-6} \times k_{17}$ (M^{-1} s^{-1})
396	0.71 ± 0.10	1.4 ± 0.2
409	1.34 ± 0.11	2.6 ± 0.2
420	1.26 ± 0.10	2.5 ± 0.2
442	1.52 ± 0.19	3.0 ± 0.4

$$\log k_{17} / M^{-1} s^{-1} = (8.5 \pm 1.5)^b - (4.0 \pm 2.8)^b/\theta$$

[a] Experimental uncertainties quoted are average error.

[b] Uncertainties quoted are one standard deviation.

presented in Figure 10, along with a result (described below) obtained by Wiebe et al.[20] as well as a line corresponding to $\log k_{17} = 8.5 - 4/\theta$. The extrapolated line clearly agrees well with the results of Wiebe et al. at room temperature.

Wiebe et al. deduced $k_{17}/k_{14a} = (5.5 \pm 1.1) \times 10^{-5}$ at 300°K. Using $k_{14a} = 10^{10.1 \pm 0.4}\ M^{-1}\ s^{-1}$ due to Batt and coworkers[3], $\log \left(k_{17}/M^{-1}\ s^{-1}\right) = 5.84 \pm 0.4$ at 300°K. The authors estimated the uncertainty to be ± 20%, but did not explain how they made the estimate. Their reaction mechanism included about twenty reactions, and it is possible that unknown systematic errors have affected their results. Despite the chances for error in our own data and in theirs, the results appear to be remarkably consistent with one another, as well as with recent estimates[33] for the rate constant.

A number of other values for k_{17} have been reported in the literature. Most of these, however, were obtained by using "third generation" methoxy radicals and a complex reaction mechanism. An example of the production of "third generation" methoxy radicals is described by the sequence of reactions:

$$\text{Precursor} + \left\{\begin{matrix}\text{heat}\\ \text{or}\\ \text{light}\end{matrix}\right\} \rightarrow CH_3 \qquad (19)$$

$$CH_3 + O_2 + M \rightarrow CH_3O_2 + M \qquad (20)$$

$$2\ CH_3O_2 \rightarrow 2\ CH_3O + O_2 \qquad (21)$$

Heicklen and Johnston[34] and (later) Shortridge and Heicklen[35] used the reaction sequence given above to obtain values for the ratio $k_{17}/k_8^{1/2}$ equal to 0.020 $M^{-1/2}\ s^{-1/2}$ and 0.021 $M^{-1/2}\ s^{-1/2}$, respectively, at 300°K. Choosing $k_8 \approx 10^{10}\ M^{-1}\ s^{-1}$ leads to the low values of k_{17} which Heicklen used to estimate[36] the arrhenius parameters for the reaction. More recent estimates[33] gave a much faster rate.

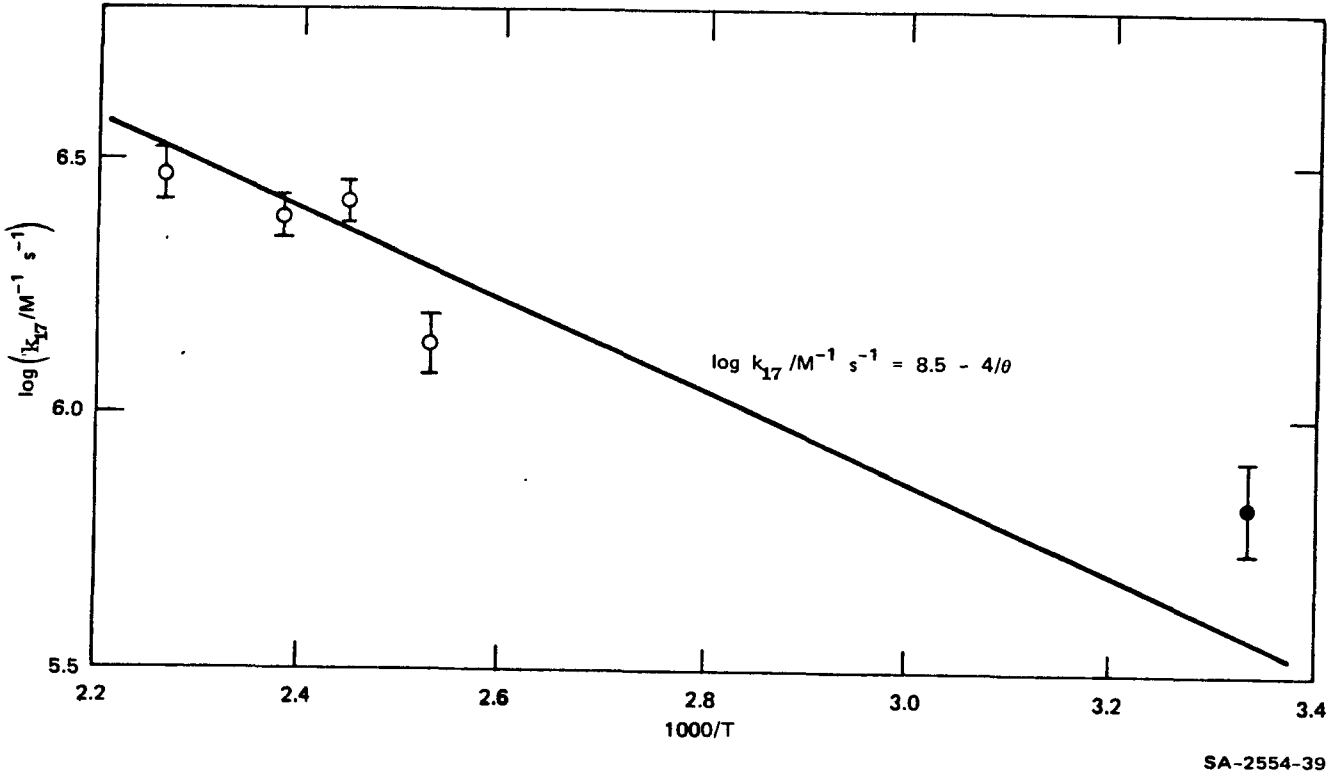

FIGURE 10 ARRHENIUS PLOT OF DATA FOR k_{17}.

● from ref 20, see text for details.

○ this work.

In a similar study at 373°K, Alcock and Mile[37] found k_{17} = $1.2 \times 10^6\ M^{-1}\ s^{-1}$, in good agreement with our results. Their data analysis consisted of a computer simulation of the reaction mechanism, and they found it necessary to include the reaction

$$CH_3O_2 + CH_3O_2 \rightarrow CH_3OH + CH_2O + O_2 \qquad (22)$$

where $k_{22} \approx k_{21}$. Recent data obtained by Bayes et al.[38] indicate that reaction (23) should be considered along with reaction (20),

$$CH_3 + O_2 \rightarrow CH_2O + OH \qquad (23)$$

complicating the picture still further since other evidence[8] indicates that reaction (23) is unimportant. A possible alternative to reaction (22) that would also give stable products and a lower MeO yield is:

$$2\ CH_3O_2 \rightarrow CH_3OOCH_3^{*} + O_2 \qquad (24)$$

$$CH_3OOCH_3^{*} \xrightarrow{M} CH_3OOCH_3 \qquad (25)$$

$$\rightarrow 2\ MeO \qquad (26)$$

Reaction (24) is about 43.5 Kcal $mole^{-1}$[39] exothermic and D(MeO–OMe) is about 37.6 Kcal $mole^{-1}$,[22] making reaction (26) possible. The way the reactions are now written, the yield of MeO will be pressure-dependent. An alternative would be to assume that the O_2 carries away much of the excess energy, leaving mostly stabilized DMP behind and giving an even lower yield of MeO.

In a recent paper, Heicklen and coworkers[40] reported the results of a study on the photo-oxidation of $CD_3N_2CD_3$. They concluded that reactions (21), (22), and (24) occur 43%, 50%, and 7% of the time, respectively, in good agreement with the relative rate constants deduced

by Alcock and Mile,[37] They also concluded that $k_{17} = (0.5 - 1.25) \times 10^4$ M^{-1} s^{-1} at 300 K, a value that is somewhat higher than those obtained earlier,[34,35] and is not inconsistent with our results. On the other hand, the use of "third generation" radicals necessitates very complex data analysis and much additional work is needed if such methods are used to obtain unambiguous methoxy radical rate constants.

Summary

The present study has demonstrated that the decomposition of dimethyl peroxide is now well understood. The value obtained for $k_6 = 10^{(15.7 \pm 0.5) - (37.1 \pm 0.9/\theta)}$ is consistent with those obtained by Takezaki and Takeuchi[23] and by Batt and McCulloch.[22] Due to the extra care taken by Batt and McCulloch to eliminate the possibility of thermal gradients, their determination of the A-factor of k_1 is probably the most reliable. The data obtained by Hanst and Calvert[5] are explained by invoking a chain reaction mechanism, and $k_7 \approx 5 \times 10^4$ M^{-1} s^{-1} was obtained near 400°K.

By adding NO_2 to the decomposing DMP, a value of the disproportionation/recombination ratio for MeO + NO_2 was obtained; $k_{12b}/k_{12a} = 0.30 \pm 0.05$.

The reaction of MeO with O_2 was measured relative to the reaction of MeO + NO_2, yielding $\log [k_{17}/M^{-1}s^{-1}] = (8.5 \pm 1.5) - (4.0 \pm 2.8)/\theta$, where most of the uncertainty in the Arrhenius parameters is due to the limited temperature range used. The Arrhenius parameters are quite reasonable and compare well with recent estimates; however, further work is needed to reduce the uncertainties.

SECTION 4

ESTIMATION METHODS

A. METHODS FOR THE ESTIMATION OF RATE PARAMETERS

The thrust in modern science and technology has been increasingly to analyze complex systems at a molecular level. To the impatient engineer, much of this may appear to be a narcissistic infatuation with unimportant detail. For the working scientist, however, who has lived with these complexities for some time, the exhaustive examination of just this detail is his only guarantee that he has really understood the phenomena involved. More important, it is the only reliable path he has available to him for making any continuing progress in analyzing, diagnosing and hopefully controlling the systems under study.

Almost all of the technical problems facing our society today (and how many are not technological) share in common this molecular complexity. It is strikingly evident in the subject of our current symposium, the kinetics of atmospheric processes involved in pollution. Although possibly half-a-dozen elementary reactions involving O_2, O_3, NO, NO_2, and O atoms dominate the diurnal chemistry of the troposphere and stratosphere, the secondary reactions which can affect the stationary concentration of some of these species may run into the tens, and if we include "pollutants", into the hundreds. The sheer volume of kinetic information required to analyze these systems has put a large premium on theoretical and semi-empirical methods for obtaining rate data. In principle, one would prefer to have direct experimental measurements of the important reactions under the prevailing atmospheric conditions of temperature, pressure, and composition. Practically, this is not always attainable. Some reactions involving excited atoms or free radicals are just not

measurable by current techniques. Others can only be measured in temperature or pressure regimes very far from atmospheric (tropo- or strato-) and need to be extrapolated with, in some cases, great uncertainty.

It is the purpose of the present report to examine the techniques which have been used to generate rate data from theoretical or empirical considerations and to attempt to place some quantitative measures on their reliability. The reactions to be considered will be elementary gas-phase reactions and the emphasis will be on the ones significant in atmospheric chemistry. For these reasons the bulk of our attention will be given to biomolecular processes.

Transition State Theory

There is at present only one kinetic model with any broad claims to generality which can be used quantitatively to describe elementary, chemical rate processes. This is the model incorporated into what has become known as Transition State Theory.

Transition State Theory rests on a number of independent assumptions. The first of these is that any elementary chemical reaction can be described in statistical mechanical terms by the passage through phase space of a complex aggregate, containing the reactant species across an energy maximum on the potential energy surface describing the complex. The second and most important assumption is that the reaction complex in the neighborhood of this maximum (i.e., the transition state) can be considered to be in thermodynamic equilibrium with the reactant species. This gives rise to the familiar kinetic scheme for an elementary reaction of any order:

$$A + B + C + \cdots \underset{}{\overset{K^{\ddagger\prime}}{\rightleftharpoons}} [A\cdots B\cdots C\cdots]^{\ddagger} \xrightarrow{\nu^{\ddagger}} \text{products}$$

with an overall rate constant $k^{\ddagger}$ described by:

$$\text{Rate} = k^{\ddagger}(A)(B)(C) = -\frac{d(A)}{dt} = \nu^{\ddagger}(A\cdots B\cdots C\cdots)^{\ddagger}$$

$$= \nu^{\ddagger}K^{\ddagger\prime}(A)(B)(C) \qquad (27)$$

or

$$k^{\ddagger} = \nu^{\ddagger}K^{\ddagger\prime} \qquad (28)$$

where $K^{\ddagger\prime}$ is the equilibrium constant for formation of transition state complex (TS) from reactants, and $\nu^{\ddagger}$ is the probability per unit time (first-order rate constant) for decomposition of TS into products.

Making use of the extremum properties of the potential energy surface and the approximation that $h\nu^{\ddagger} \leq kT$ we can factor $K^{\ddagger\prime}$ into a product of a partition function for the reaction coordinate (i.e., passage across the maximum), $kT/h\nu^{\ddagger}$ and a remainder $K^{\ddagger}$. Hence the well known result, independent of $\nu^{\ddagger}$:

$$k^{\ddagger} = \left(\frac{kT}{h}\right)K^{\ddagger} \qquad (29)$$

or in thermodynamic language:

$$k^{\ddagger} = \left[\left(\frac{kT}{h}\right)\right]e^{-\Delta H^{\ddagger}/RT} \qquad (30)$$

There is no evidence that indicates that the approximation $h\nu^{\ddagger} < kT$ is a source of appreciable error. It would require a very compact potential energy surface with a very thin (< 0.3 Å) activation energy barrier to invalidate this approximation and no a priori calculations have so far indicated the existence of such surfaces.

If we confine our discussion to thermodynamic language, Transition State Theory is a two-parameter theory, the two parameters being $\Delta S^{\ddagger}$ and $\Delta H^{\ddagger}$. The situation is actually more complex than this since both of these

are temperature dependent. Because of this latter, it is not easy to relate $k^{\ddagger}$ to the more familiar Arrhenius form, $k = A \exp(-E/RT)$, except in a limited temperature range ($T = T_m \pm \Delta T$). The relation is:[41]

$$E = \Delta H_m^{\ddagger} + RT_m \tag{31}$$

$$A = \left(\frac{ekT_m}{h}\right) e^{\Delta S_m^{\ddagger}/R} \tag{32}$$

where T_m is the center of the temperature range chosen, and $\Delta H_m^{\ddagger}$ and $\Delta S_m^{\ddagger}$ are calculated at T_m. Remember that $\Delta H^{\ddagger}$ and $\Delta S^{\ddagger}$, if calculated statistically, must be calculated with the "reaction coordinate" ($\nu^{\ddagger}$) contribution to the TS omitted. Its contribution has already been counted in the (kT/h) term.

To make use of equations (31) or (32) requires either a total knowledge of the potential energy surface for the reaction or an empirical knowledge of the surface in the neighborhood of the transition state (i.e., the barrier). The former alternative is probably not viable for the near future, and so we must have recourse to the latter. To have empirical knowledge of the potential energy surface in the neighborhood of the TS implies that we have reliable rate data (E and A) for one or more of a related class of reactions from which we can extract experimental values of $\Delta H^{\ddagger}$ and $\Delta S^{\ddagger}$. This has proven a very fruitful approach and is the one we shall now explore.

A-factors and Entropies of Activation

Equation (32) relates directly the Arrhenius A-factor to the entropy of activation, $\Delta S^{\ddagger}$. Since this latter is the difference between the entropies of reactants and transition state, and the former can be determined directly, equation (32) gives us a method for relating A-factors to

the entropy of the transition state $S^{\ddagger}$. This by itself might not be too useful a relation were it not for the circumstance that the molar entropy of a gas-phase species is relatively insensitive to its structure. If we examine the contributions to the entropy of a gas-phase species from the different external and internal degrees of freedom, we find the following:[43]

$$S^0 \cong S^0_{trans} + S^0_{rot} + S^0_{vib} + S^0_{elec} \tag{33}$$

$$S^0_{trans} = 37.0 + \frac{3}{2} R\ln\left(\frac{M}{40}\right) + \frac{3}{2} R\ln(T/298) + R\ln(n) \tag{34}$$

$$S^0_{rot}\,[\text{linear molecule}] = 6.9 + R\ln(I/\sigma) + R\ln(T/298)$$

$$S_{rot}\,[\text{non-linear molecule}] = 11.5 + R\ln\left[(ABC)^{1/2}/\sigma\right] + \frac{3}{2} R\ln(T/298)$$

$$S^0_{rot}\,[\text{1-dimensional rotor}] = 4.6 + R\ln(I^{1/2}/\sigma) + \frac{1}{2} R\ln(T/298) \tag{35}$$

where M = molecular weight in atomic mass units (AMU), I = moment of inertia about the center of gravity, ABC = product of moments of inertia (AMU-Ang^2), σ = total symmetry number, and n is the number of optical isomers.

The vibrational entropy consists of contributions from each of the internal vibrations. Each of these is usually small compared to the contributions from translation and rotation, and generally only the bending motions involving atoms heavier than H or D are significant in the range 200-400^{0}K. The only significant (i.e., > 0.5 e.u.) contributions from internal modes arise from hindered internal rotations. These can be in the range of 2 to 5 gibbs/mole per rotor, and hence are comparable to the contributions from external rotations.

Electronic contributions generally take the form of $R\ln g_e$, where g_e, the electronic partition function, is usually the electronic degeneracy of the ground state. For free radicals this usually reduces to a contribution of $R\ln 2 = 1.4$ gibbs/mole from their spin degeneracy. In exceptional cases of atoms, such as O, and odd radicals such as NO and O_2, the electronic partition function is more complex and changes significantly with temperature in the range of atmospheric interest 200-300°K.

High frequencies ($\nu \geq 800$ cm^{-1}) contribute less than 0.2 gibbs/mole to S^0 at 300°K. We can thus make gross errors in guessing them (± 20%) without incurring a significant error in S^0. A frequency of 400 cm^{-1} will have an entropy of 1.0 e.u. at 300°K and a 10% error in its value will introduce an uncertainty of ± 0.1 e.u. in S^0. This doubles at 200 cm^{-1} and triples at 100 cm^{-1}, but only torsional motions have frequencies in this range. We thus observe that in estimating $S^{0\ddagger}$ the chief structural features of interest are the moments of inertia and barriers to internal rotation.

The moments of inertia can be guessed from simple empirical rules involving bond lengths and angles[39] and even errors of ± 10% in the latter will introduce uncertainties in S^0 of only ± 0.2 e.u. At low temperatures it is the uncertainty in barriers to internal rotation which constitute our chief source of error.

The relative intensity of molar entropy to precise structural details and to the number of H-atoms in a species is illustrated in the following Tables IX, X, and XI, which compare the molar entropies and heat capacities at 300°K of some structurally similar species.[43]

Table IX. Standard entropies and heat capacities at 300°K of some structurally similar molecules.[a]

	Molecule	C^o_{p300}	$S^o_{300(int)}$ [b]	σ	S^o_{300}
A	H_2O	8.0	46.5	2	45.1
	NH_3	8.5	48.2	3	46.0
	CH_4	8.5	49.3	12	44.5
	BH_3	8.7	48.4	6	44.9
B	CH_3CH_3	12.7	60.6	18	54.9
	NH_2NH_2	12.2	58.5	2	57.1
	HOOH	10.3	58.0	2	56.6
	CH_3NH_2	11.9	59.9	3	57.7
	CH_3OH	10.5	59.5	3	57.3
	BH_3BH_3	13.9	58.5	4	55.7

[a]Units of C_p and S are gibbs/mol.
[b]S^o_{300} (intrinsic) = S^o_{300} + Rln σ.

Table X. Standard entropies and heat capacities of some complex, but structurally similar, molecules.

	Molecule	C^o_{p300}	$S^o_{300}(int)$ [a]	σ	S^o_{300}
A	$CH_3CH_2CH_3$	17.7	70.3	18	64.6
	CH_3OCH_3	15.8	70.4	18	63.7
	CH_3CH_2OH	15.7	69.7	3	67.5
	CH_3NHCH_3	16.6	69.8	9	65.4
	$CH_3CH_2NH_2$	17.6	69.9	3	67.7
	CH_3NHNH_2	17.0	68.8	3	66.6
B	CHF_3	12.2	64.2	3	62.0
	BF_3	12.1	64.3	6	60.7
	NF_3	12.8	64.5	3	62.3
	COF_2	11.3	63.3	2	61.9
	FNO_2	11.9	63.6	2	62.2
	N_2F_2 (cis)	11.9	63.4	2	62.0
	$CH_2{=}CF_2$	14.2	64.8	2	63.4

[a] $S^o_{intrinsic} = S^o + R\ln\sigma$; units are gibbs/mol for C^o_p and S^o.

Table XI. Standard entropies and heat capacities of some complex, but structurally similar, molecules.

	Molecule	C^o_{p300}	$S^o_{300}(int)$ [a]	σ	S^o_{300}
A	$COCl_2$	13.8	69.2	2	67.8
	$CH_2{=}CCl_2$	16.1	69.7	2	68.3
	$CHCl{=}CHCl$ (cis)	15.6	70.8	2	69.4
B	C_6H_6 (benzene)	19.7	69.2	12	64.3
	C_5NH_6 (pyridine)	18.8	69.1	2	67.7
	$B_3N_3H_6$(borozole)	22.0	72.1	6	68.5
	$B_3O_3H_3$(boroxine)	21.0	71.6	6	68.0

[a] $S^o_{intrinsic} = S^o + R\ln\sigma$; units are gibbs/mol for C^o_p and S^o.

For convenience, the intrinsic entropies (corrected for symmetries) are compared, as well as the absolute entropies. We note that in any of the five series of molecules compared, we would make an error less than $\pm$ 1.0 e.u. in choosing the average in the group to represent any one of them. We could do about the same for C_p and improve the latter by making a correction of about 0.4 e.u. for the contributions of H atoms. This becomes a reliable method[10] ($\pm$ 1.0 e.u.) for assigning C_p° and S° to free radicals and ions. Extensions of these methods have been made with about the same success to cyclic and polycyclic compounds.[44]

In applying these methods for estimating entropy to transition states, we proceed by selecting an initial structure which would seem reasonable in terms of the overall structural changes in the reaction. We then calculate a value of $\Delta S^{\ddagger}$ and an A-factor (eq. 32) and compare it with the experimental data. It generally turns out that once we have "calibrated" our intuition, there is not too much latitude in varying the initial structure if the agreement is not good.

The largest range in $S^{\ddagger}$ occurs between what has been designated a "tight" and a "loose" transition state. A tight transition state is one in which the bond lengths and bond angles are within 0.3 Å and 20°, respectively, of the values which describe stable structures. Loose transition states which appear to occur in simple bond fission reactions only, are characterized by unusually long bonds between nascent free radical centers. These can be as much as 2.5 to 3 times the ground bond distance. The best documented example is the transition state for $CH_3 \cdots CH_3$ recombination in which the C...C distance is at least 3.8 Å, and possibly 4.5 Å, long in comparison to a normal C-C single bond distance of 1.54 Å.

A-Factors for Metathesis Reactions

Bimolecular reactions can be divided into three categories:

(1) Energy transfer processes

(2) Metathesis reactions (atom transfer)

(3) Addition reactions

Each of these is characterized by a "strong" collision between two discrete species and can from this point of view be looked upon as a type of addition reaction. We distinguish the true addition reaction from the others by using it to characterize those exothermic reactions in which the adduct is more stable than the reactants, for example, the recombination of radicals and addition of atoms to double bonds.

The formation of the transition state in a bimolecular event can be looked upon as involving the net transformation of translational and rotational degrees of freedom of reactants into vibrational and torsional degrees of the complex TS. Because of the relative magnitudes of the entropies associated with these degrees of freedom, $\Delta S^{\ddagger}$ for the process is always negative. It is more negative for heavy species than for light and becomes increasingly more negative with increasing complexity of the colliding species.

In the reaction of a light atom, such as H or D, with a large polyatomic molecule, the TS complex has about the same intrinsic entropy as the molecule, and hence $-\Delta S^{\ddagger} \sim S^{o}(H)$ corrected for spin and symmetry. $S^{o}_{298}(H) = 27.4$ gibbs/mole (e.u.) or 21.0 e.u. (mole/liter standard state). Correcting for spin, $R\ln 2 = 1.4$ e.u., and adding R for the change in $\Delta n = -1$ (bimolecular event), we find $\Delta S^{\ddagger}_{c} \sim -17.6$ e.u. per atom attacked. Since $ekT/h = 10^{13.25}$ sec^{-1} at $300^{o}K$, this would lead to a minimum A-factor

for metathesis by H-atoms of $10^{9.5}$ l/mole-sec per atom attacked. For attack on C_2H_6, which has six equivalent H-atoms, we would raise this by a factor of 6 to $10^{10.3}$. Observed A-factors could be a power of 10 higher than these values if the TS complex had a structure in which the H•••X•••R bonds were bent and possessed a torsional mode with low or zero internal barrier-to-rotation of the H atom.

The observed values for H-atom metatheses, some of which are shown in Table XII, are in excellent agreement with these conclusions. Moreover, the values are sufficiently above the lower limits to suggest that the TS complexes have an H-atom which is not co-linear with the H-R bond being attacked. The attack of H-atoms on E_2 and I_2 have A-factors even more than a power of ten higher than the minimum values, and only a very nonlinear TS can account for these high A-factors. This may, in fact, be typical of H-atom attacks on all group V, VI, and VII elements and thus the inverse reactions as well. A simple rule of thumb for H-atom metatheses is that their A-factors are $10^{10.5\pm0.5}$ l/mole-sec.

It would be extremely difficult to defend, on structural grounds, A-factors (per atom) for metathesis by H-atoms which were less than the minimum values calculated. Hundreds of reported rate constants [45,46,47] support these conclusions and reported A-factors which fall below these limits must be looked upon as suspect.

When we consider atoms heavier than H or D, the analysis is not so simple. While these heavier atoms have larger translational entropies, their TS complexes in compensation will also have increased translational and rotational entropies and the net result is not expected to be much different than for H-atoms. Table XIII shows rate parameters for heavy atom metathesis, and we note that again an average value of $10^{10.5\pm0.5}$ l/mole-sec will bracket most of the results.

Table XII. Arrhenius Parameters for Some Metathesis Reactions Involving H-Atoms.

Ref.	Reaction	T_m (°K)	log A (M^{-1} sec^{-1})	E (kcal/mole)
1a	$H + D_2 \rightarrow HD + D$	900	10.6	8.0
b		(177-477)	10.7	9.4
2	$H + HOH \rightarrow H_2 + OH$	(300-2500)	10.9	20.5
3	$H + F_2 \rightarrow HF + F$	(300-560)	11.1	2.4
4a	$H + HCl \rightarrow H_2 + Cl$	(200-500)	10.4	3.5
b		(500-700)	10.4	4.2
5	$H + CH_4 \rightarrow H_2 + CH_3$	(300-600)	11.1	11.9
6	$H + C_2H_6 \rightarrow H_2 + C_2H_5$	(300-1100)	11.1	9.7
7	$H + I_2 \rightarrow HI + I$	(400-465)	11.6	0
8	$H + N_2O \rightarrow HO + N_2$	(450-1487)	10.7 ± 0.4	13 ± 1.5

1a. G. Boato, et al., J. Chem. Phys., 24, 783 (1956).
b. A. A. Westenberg and N. de Haas, Ibid. 47, 1393 (1967).

2. D. L. Baulch, et al., Evaluated Data for High Temperature Reactions, Vol. I., Butterworth, London (1972).

3. R. G. Albright, A. F. Dedonov, G. K. Lavrovskaya, I. I. Morozov, and V. L. Talrose, J. Chem. Phys., 50, 3632 (1969).

4a. A. A. Westenberg and N. deHaas, J. Chem. Phys., 48, 4405 (1968).

b. S. W. Benson, F. R. Cruickshank, and R. Shaw, Int. J. Chem.Kinetics, 1, 29 (1969)

5. R. R. Baldwin, D. E. Hopkins, A. C. Norris, and R. W. Walker, Combustion and Flame, 15, 33 (1970).

6. R. R. Baldwin and A. J. Melvin, J. Chem. Soc., 1785 (1964).

7. J. H. Sullivan, J. Chem. Phys., 30, 1292 (1959).

8. G. Dixon-Lewis, Sutton and Williams, J. Chem. Soc., 5724 (1965).

Table XIII. Arrhenius Parameters for Metathesis Reactions Involving Atoms

Ref.	Reaction	T_m (°K)	log A (M^{-1} sec^{-1})	E (kcal/mole)
1	$O + NO_2 \rightarrow O_2 + NO$	300	10.0	0.
2	$O + OH \rightarrow O_2 + H$	300	10.3	0
1	$O + O_3 \rightarrow 2O_2$	(220-1000)	10.08	4.6
1	$O + C_2H_6 \rightarrow OH + C_2H_5$	(300-650)	10.4	6.4
3	$Cl + C_2H_6 \rightarrow HCl + C_2H_5$	300	10.6	0
4	$Br + C_2H_6 \rightarrow HBr + C_2H_5$	(490-590)	11.0	14.0
5,6	$I + CH_4 \rightarrow HI + CH_3$	560	11.7	33.5
5,6	$I + CH_3I \rightarrow I_2 + CH_3$	580	11.4	20.5
7,	$I + CF_3I \rightarrow I_2 + CF_3$	(350-550)	10.9	17.8
8a		370-450	9.6	16.0
1	$N + NO \rightarrow N_2 + O$	(300-5000)	10.2	0
1	$N + O_2 \rightarrow NO + O$	300	9.3	6.3
9	$S + OCS \rightarrow S_2 + CO$	300	9.0	3.6

1. D. Garvin and R. F. Hampson, Editors "Chemical Kinetics Data Survey," VII, NBSIR 74-430, Washington, D.C. (1974).

2. D. L. Baulch, D. D. Drysdale, D. G. Horne, and A. C. Lloyd, Evaluated Data for High Temperature Reactions. I., Buttersworth, London (1972).

3. D. D. Davis, W. Braun, and A. M. Bass, Int. J. Chem. Kinetics, 2, 101 (1970).

4. K. D. King, D. M. Golden, and S. W. Benson, Trans. Faraday Soc., 66, 2794 (1970).

5. D. M. Golden, R. Walsh, and S. W. Benson, J. Amer. Chem. Soc., 87, 4053 (1965).

6. M. C. Flowers and S. W. Benson, J. Chem. Phys., 38, 882 (1963).

7. Amphlett and E. Whittle, Trans. Faraday Soc., 63, 2695 (1967).

8. (a) Lawrence, Trans. Faraday Soc., 63, 1155 (1967).

9. R. B. Klemm and D. D. Davis, J. Phys. Chem., 28, 1138 (1974).

The reaction of $N + O_2 \rightarrow NO + O$ has a sufficiently low A-factor to warrant further inspection. If we assume it has a tight transition state $(N\text{-}O\text{-}O)^{\ddagger}$, we can approximate the entropy of the latter by either the value of NO_2 if it is nonlinear or N_2O if it is linear. Starting with the former and correcting for symmetry and spin (TS must be doublet), we find $\Delta S_c^{\ddagger} > -20.5$ which leads to $A > 10^{9.2}$ l/mole-sec, in excellent agreement with the data. A linear TS (NNO model) would yield a minimum A of about $10^{8.4}$ l/mole-sec from which we can conclude that if the observed A-factor is correct, then the TS must be bent.

The last result makes the much larger A-factor for $N + NO \rightarrow N_2 + O$ of some interest. The TS complex must be a triplet and a minimum A-factor for a tight linear transition state is $10^{8.0}$ l/mole-sec, while a bent transition state has $A \geq 10^{9.0}$ l/mole-sec. The observed value of $10^{10.2}$ l/mole-sec suggests that in actual fact we must have the equivalent of a very loose TS, equivalent to those effective in radical recombination. This would be reasonable if the N···NO interaction were attractive up to distances of about 3.2 Å on the triplet surface.

The other low A-factor reported in Table XII is for the reaction $S + SCO \rightarrow S_2 + CO$. If we model the TS using $S^0_{int}(COCl_2) = 69.2$ e.u. and correct for spin (triplet), we find $A \geq 10^{9.8}$ l/mole-sec. There is no plausible structure for the TS that could account for an A-factor as small as $10^{9.0}$ l/mole-sec.

The very important atmospheric reactions $O + NO_2 \rightarrow NO + O_2$ and $O + O_3 \rightarrow 2O_2$ are structurally very similar. If we assume common non-planar transition states for both, or planar ones with low rotation barriers, we can simulate TS by FNO_2 (Table X) with corrections for spin and internal free rotation. On this basis we estimate $A(O + O) \geq 10^{9.9}$ l/mole-sec and $A(O + NO_2) \geq 10^{9.8}$ l/mole-sec, in excellent agreement with the data.

We observe in Table XIII a peculiarity unique to I atoms; that is, their abstraction reactions have unusually high A-factors, much higher in fact than we would calculate from minimum A-factors. For the reaction I + CH, in fact, we estimate $A \geq 10^{9.8}$ l/mole-sec at 300°K in contrast to the observed $10^{11.7}$ l/mole-sec (based on CH_3I as a model for TS). This suggests an extremely loose complex since even a nonlinear TS would still have an A-factor only 10-fold higher.

A postulate of Hammond[48] proposes that for very exothermic reactions having low activation energies the TS complex resembles reactants. This is, in fact, the case for the reverse of the I-atom reactions, i.e., for CH_3 + HI and for $CH_3 + I_2$ with $E_{act} = 1 \pm 1$ and 0 kcal/mole, respectively.

Applied to the I + CH_4 reaction, this suggests that the TS looks like a very weakly coupled $CH_3 \cdots HI$ with the C···H···I axis bent. If we assume that in this complex the CH_3 is freely rotating about the C···H bond (3.6 e.u.), has two rocking modes about this bond of about 350 cm^{-1} each (2.4 e.u.) and the C···H···I bend is about 200 cm^{-1} (2.2 e.u.), we can account for an A-factor of about $10^{11.5}$ l/mole-sec in reasonable agreement with the results. A similarly loose model can account for the $I + CH_3I \rightarrow I_2 + CH_3$ A-factor.

A-factors for some metatheses by diatomic and polyatomic radicals are shown in Table XIV. Although the table covers a range of radicals and atoms varying considerably in structure, the A-factors lie mainly in the range $10^{8.5 \pm 0.5}$ l/mole-sec. Despite this, there are some curious inconsistencies.

We can, for example, calculate a minimum A-factor for the reaction of HO + CH_4 based on using $S^0(CH_3OH)$ as a model for TS. We add 1.4 e.u. for spin and 2.8 e.u. for the increased moment of inertia to find

Table XIV. Arrhenius Parameters for Some Metathesis Reactions of Radicals.

Ref.	Reaction		log A (M^{-1} sec^{-1})	E (kcal/mole)
1	$HO + CH_4 \rightarrow HOH + CH_3$	(300-500)	9.5	3.8
1a		770	10.3 (10.9)[c]	4.9 (6.6)[c]
1	$HO + C_2H_6 \rightarrow HOH + C_2H_5$	(300-500)	10.1	2.5
1a		770	10.9	3.5
1	$HO + CO \rightarrow H + CO_2$	(300-500)	8.1	0.2
1b			8.5	0.6
2	$HO + O_3 \rightarrow HO_2 + O_2$	(220-450)	8.8	1.9
3	$HO_2 + O_3 \rightarrow HO + 2O_2$	(225-298)	7.8	2.5
3,4	$HO_2 + NO \rightarrow HO + NO_2$	300	>9.2 (10.3)[d]	0(?)(1.4)[d]
5	$CH_3 + C_2H_6 \rightarrow CH_4 + C_2H_5$	420	8.5	10.8
6	$CH_3 + CH_3COCH_3 \rightarrow CH_4 + CH_2COCH_3$	(400-500)	8.6	9.7
6	$CH_3 + CCl_4 \rightarrow CH_3Cl + CCl_3$	400	10.4	13
6a			8.6	9.1
7	$CF_3 + C_2H_6 \rightarrow CF_3H + C_2H_5$	(320-450)	8.0	6.5
6	$CF_3 + CCl_4 \rightarrow CF_3Cl + CCl_3$	(400-560)	8.8	9.3
		(360-510)	9.6	10.4
6	$C_2H_5 + n\text{-}C_7H_{16} \rightarrow C_2H_6 + n\text{-}C_7H_{15}$	450	8.7	10.6
6	$n\text{-}C_3F_7$ + acetone $\rightarrow C_3F_7H$ + acetonyl	(300-600)	8.8	7.2

1. N. R. Greiner, J. Chem. Phys., 51, 5049 (1969).
   (a) R. R. Baker, R. R. Baldwin, and R. W. Walker, Trans Faraday Soc., 66, 2812 (1970).
   (b) W. E. Wilson, Jr., J. Phys. Chem., Ref. Data 1, 535 (1972).
   (c) S. Gordon and W. A. Mulac, Int. J. Chem. Kinetics, Symp. 1, 289 (1975).
   (d) W. Hack and K. Hoyerman, this symposium.

2. J. G. Anderson and F. Kaufman, Chem. Phys. Lett., 19, 483 (1973).

3. Table XIII, ref. 5.

4. Activation energy not determined, estimated on the basis of radical recombination.

5. A. F. Trotman-Dickenson and E.W.R. Steacie, J. Chem. Phys., 19, 329 (1951).

6. Reference 45; (a) J. Currie, H. Sidebottom, and J. Tedder, Int. J. Chem. Kinetics 6, 481 (1974).

7. Reference 46.

$A \geq 10^{9.3}$ l/mole-sec. A similar analysis for C_2H_6 + OH gives $A \geq 10^{9.0}$ l/mole-sec. A nonlinear complex would have A-factors about a power of 10 higher for both. The value of 10^{10} l/mole-sec would seem to be reasonable for C_2H_6, and this would suggest that the higher of the two values listed, $10^{10.3}$, might be a better choice for CH_4 + OH.

The very important reaction CO + HO has a TS which can be modeled by HONO. This yields $A \geq 10^{8.6}$ l/mole-sec, suggesting that both listed A-factors are probably on the low side. All reasonable models for the HO + O_3 reaction yield A-factors in excess of $10^{9.3}$ l/mole-sec, about three-fold higher than the reported value. The A-factor for HO_2 + O_3 is in much worse agreement. The TS entropy would have to be 78.1 e.u. at 300°K to account for the anomalously low A-factor of $10^{7.8}$. The estimate for TS is about 84 e.u., suggesting $A \geq 10^{9.0}$ l/mole-sec.

The CH_3 metathesis reaction from C_2H_6 can be modeled using C_3H_8 for TS.[39] This leads to $A \geq 10^{8.0}$ l/mole-sec. Correcting for a larger moment of inertia increases this to $10^{8.3}$ and a further correction for a lower CH_3 rotation barrier of 1.5 kcal/mole instead of 3.0 increases it further to $10^{8.5}$. If we assumed either a nonlinear C·H·C structure in TS or two weakened CH_3·H·C rocking modes, this would increase to $10^{9.0}$ l/mole-sec. The bulk of A-factors for CH_3 abstraction[45-47] suggests that the TS structures are probably nearly co-linear.

The A-factor listed in Table XIV for CH_3 + CCl_4 is at least a factor of $10^{1.8}$ higher than can be accounted for in terms of any reasonable TS structure. The new value presented by Tedder et al. agrees quite well with TS estimates.

Addition Reactions

Addition reactions in which atoms or radicals attach themselves to unsaturated systems usually involve small activation energies and hence can be considered to pass through tight transition states, not unlike those for metathesis reactions. This is more or less in agreement with the much sparser data for these reactions, some of which are tabulated in Table XV. It should be observed that these are much more difficult reactions to measure experimentally since the products are not themselves stable and go on to react further. They are usually not observed directly, and their rates are often inferred from the rate of disappearance of reactants with the aid of some assumptions on chain lengths and secondary reactions. In addition, the adducts are energetically excited, and their stabilization will require subsequent deactivating collisions. In consequence, many of these reactions show a rate dependence on total pressure which may or may not be properly accounted for in the published data.

With these cautions made, we note that for $H + C_2H_4$ the simplest model for a tight transition state give $A \geq 10^{10.1}$ l/mole-sec, in excellent agreement with the data. For $O + C_2H_4$ we estimate $A \geq 10^{9.0}$ l/mole-sec. This is probably in reasonable concurrence with the data for which the reported values are uncertain by a factor of 3. For $Cl + C_2H_4$, a tight transition state, using $CH_2{=}CHCl$ as a model, leads to $A \geq 10^{9.1}$ l/mole-sec, very much lower than the reported $10^{10.6}$. Only a loose transition state characteristic of radical recombinations can account for such a large A-factor. The zero activation energy is in agreement with such a structure and can be rationalized in terms of a charge transfer attraction. The ionization potential of C_2H_4 is 10.5 e.u.[49] while the electron affinity of Cl is 3.6 e.u.[49] The difference of 6.9 e.u. is made up by coulombic attraction at distances of 2.1 Å, which is about 0.3 Å larger than the C-Cl covalent bond.[50]

Table XV. Arrhenius Parameters for Some Addition Reactions of Atoms and Radicals to Pi Bonds.

Ref	Reactants	$T_m(^oK)$	log A (ℓ/mole-sec)	E (kcal/mole)
1	$H + C_2H_4$	(296-540)	10.4	2.0
1	$O + C_2H_4$	(223-613)	9.9	1.6
2			9.5	1.1
1	$Cl + C_2H_4$	310	10.6	0
3,2	$OH + C_2H_4$	(210-460)	9.7	0.2
4	$OH + C_3H_6$	300	9.5	0 (?)
5	$O + C_2H_2$	300	[9.8](?)	[2.8](?)
6	$CH_3 + C_2H_4$	400	8.5	7.7
6	$C_2H_5 + C_2H_4$	400	8.3	7.5

1. V. N. Kondratiev, "Rate Constants of Gas Phase Reactions," Reference Book, Trans. by L. J. Holtschlag, Ed. by R. M. Fristrom, NSRDS, U.S. Government Printing Office, Washington, D.C. (1972).

2. Table XIII, ref. 1.

3. I.W.M. Smith and R. Zellner, J. Chem. Soc., Far. Trans. II, 69, 1617 (1973).

4. J. Bradley, et al., Ibid., 1889 (1973).

5. F. Stuhl and H. Niki, J. Chem. Phys., 55, 3954 (1971). Authors did not measure A and E, but reported only $k_{300} = 10^{7.9}$ ℓ/mole-sec; A and E are our choices.

6. J. A. Kerr and M. J. Parsonage, Evaluated Kinetic Data on Gas Phase Addition Reactions, Buttersworth, London (1972).

Thus, unless there is some large van der Waals' repulsion between Cl and C_2H_4, one could expect that their interaction would correspond closely to that of a recombination curve. In fact, it is expected that halogens (atoms and molecules) will form attractive Pi-bond complexes at van der Waals' distances.

One would expect all of the halogen atoms to show a similar facility in adding to Pi systems. The case of the OH radical is, from this aspect, very interesting. Its electron affinity of about 1.8 e.u. is not enough to form an ion pair with C_2H_4 except at smaller distances of the order of about 1.7 Å.[50] This is again about 0.3 Å larger than the C-O single bond distance, and hence would constitute tight complex for which we would calculate a minimum A-factor (based on $CH_2{=}CHOH$) of about $10^{8.5}$ l/mole-sec. The reported values, though uncertain, are about a power of ten or more higher, suggesting again a loose transition state characteristic of radical recombinations. A very loose transition state with two rocking modes of HO relative to C_2H_4 of about 200 cm^{-1} and a weak O···C-C bending mode of about 200 cm^{-1} would raise this value to $10^{9.6}$ l/mole-sec in good agreement.

Collision Theory which is a zero order limit of Transition State Theory will give a similar A-factor for OH + C_2H_4 collisions if the collision (i.e., impact) diameter is taken as 1.8 Å, and it is assumed that 1/3 of the surface surrounding the C_2H_4 does not permit a proper collision because of steric repulsion of the H-atoms and an additional factor of 1/2 is used to correct for the geometry of the OH approach, i.e., the H of OH should be pointing away from the C_2H_4.

The reactions of O atoms with acetylene gives, for a tight complex, $A \geq 10^{9.8}$ l/mole-sec, suggesting that the observed rate constant (the authors did not measure A and E), which is $10^{7.9}$ l/mole-sec at 300°K, must have at

least 2.8 kcal/mole of activation energy or else is too low because of pressure effects. For $O + C_2H_4$ a tight complex has $A \geq 10^{9.0}$ l/mole-sec, in reasonable agreement with the data. Note that in this reaction and in that of $O + C_2H_2$ the reaction must be mechanistically complex since the initial adduct is a triplet biradical which must eventually be transformed into a singlet species.

The addition of alkyl radicals to olefins has activation energies sufficiently high that we model the TS by tight complexes. For $CH_3 + C_2H_4$ propylene (C_3H_6) is a good model and yields $A \geq 10^{7.7}$ l/mole-sec. Corrections for a lower barrier, a slightly larger moment of inertia and a lower C-C-C bending frequency raises this to $10^{8.4}$, in excellent agreement with the reported values.

Recombination Reactions Involving Atoms

The recombination of free radicals is an exothermic process which produces an excited species that will redissociate into the initial fragments unless stabilized by a de-exciting collision. For large radicals, such as ethyl, with many internal degrees of freedom, into which the recombination energy can be partitioned, the lifetime of the energized adduct is sufficiently long and energy transfer is sufficiently efficient so that at pressures of 1-10 torr deactivation is almost always faster than redissociation. Consequently, in this pressure range, radical recombination of large radicals is bimolecular and independent of total pressure. With small species, such as atoms, the reverse is true, and recombination appears to be a third-order process.[51] It can be looked upon as a succession of bimolecular events:

$$A + B \overset{1}{\rightleftarrows} AB^*$$
$$AB^* + M \overset{2}{\rightleftarrows} AB + M$$

When A is an atom and B is a diatomic molecule, the lifetime of AB^* is so short that AB^* can be considered to be in virtual equilibrium with A and B.

In that case ($k_{-1} \gg k_2$), the overall rate can be written as:

$$-\frac{d(A)}{dt} = k_2(AB)^*(M)$$

$$= k_2K_1(A)(B)(M) \qquad (36)$$

and the third-order, recombination rate constant k_r is:

$$k_r = k_2K_1^* \qquad (37)$$

Since k_2 is the rate constant for an energy transfer process, we can write it as a product λk_z, where k_z is a simple hard-sphere collision frequency and λ is the probability of deactivation of AB^* on collision. For highly energized species possessing many quanta of energy, λ is expected to be in the range 0.2 to 1.0,[52] while $k_z \sim 10^{11.3}$ l/mole-sec.

The pseudo-equilibrium constant K^* can be looked upon in two different ways. If the recombination energy of AB is readily partitioned among its internal degrees of freedom, then on the average there will be equal numbers of quanta in each mode. If the modes are comparable in frequency and there are n of them, each will have about 1/n<u>th</u> the recombination energy, and the molecule is not expected to look very different from the normal unexcited molecule. In that case we can write K^* as:[53]

$$R\ln K^* = -\Delta S^o_{AB} + \Delta S^*_{AB} \qquad (38)$$

where ΔS^o_{AB} is the standard entropy change in forming ground state AB from A + B, and ΔS^*_{AB} is the extra entropy that results from the high energy content of AB. ΔS^*_{AB} may be evaluated as $R\ln\rho^*$, where ρ^* is the number of ways of distributing the energy of recombination E^* among the n internal

degrees of freedom of AB. If the geometric mean frequency of the active degrees of freedom of AB^* is ν_m, then a reasonable approximation to ρ^* is:

$$\rho^* \approx \frac{1}{(n-1)!} \left(\frac{E^*}{h\nu_m}\right)^{n-1} \tag{39}$$

If we apply this to the recombination of $O + NO \rightarrow NO_2$, we find:

$$\begin{aligned}
\Delta S^0_{NO} &= -31.5 \text{ e.u. (atmospheric-standard state)} \\
&= -25.1 \text{ e.u. (M/liter-standard state)} \\
\nu_m &\approx 1200 \text{ cm}^{-1} \\
E^*_{300K} &\simeq E^0 + \frac{3}{2} RT = 73 \text{ kcal} \\
\rho^* &\sim 530/2 = 265 = 10^{2\cdot 4}
\end{aligned}$$

and

$$k_r = \lambda k_z (10^{-5})(10^{2\cdot 4}) = \lambda (10^{-2\cdot 6}) k_z \tag{40}$$

If we set k_z equal to $10^{11\cdot 4}$ l/mole-sec and employ a maximum value of 1 for λ, this yields $k_r = 10^{8\cdot 8}$ l/mole-sec as compared to the measured value of $10^{10\cdot 3}$ l/mole-sec.[54] The discrepancy of a factor of 30 cannot be reconciled with any anharmonicity assignment or reasonably distorted structure for NO_2^*. The inclusion of excited electronic states simply does not help since their lifetime would be significantly less than that of the ground state due to their lower kinetic energy content E^* (eq. 39). We may thus conclude that the $(ONO)^\ddagger$ that leads to recombination cannot be a simple structural variant of the ground state NO_2.

Another way to examine this anomaly is to consider a trajectory of O + NO with impact parameter in the range ~ 3.0 Å. The rate constant $k_1(NO_2^*)$ for such collisions is 1.3×10^{11} l/mole-sec. The average relative collision

velocity v_r is 7.5×10^4 cm/sec (300°K). If we make the arbitrary, but reasonable, assumption that the range Δ of potential interaction between NO and O extends over 1 Å (1×10^{-8} cm) and that the average relative radial velocity during this portion of the collision is 1/2 the initial velocity, then the duration of the collision is:

$$\tau_c \cong \frac{2\Delta}{1/2\ v_r} = \frac{4\Delta}{v_r} = 5.3 \times 10^{-13} \text{ seconds}$$

The first-order rate constant k_{-1} for the breakup of this collision complex of NO_2^* may be taken as $1/\tau_c$, and hence we can write:

$$K^*_{NO_2} = \frac{k_1(NO_2^*)}{k_{-1}(NO_2^*)} = k_1(NO_2^*)\ \tau_c(NO_2^*)$$

$$= 7 \times 10^{-2} \text{ l/mole}$$

This value of K^* is a factor of 28 larger than the value of $10^{-2.6}$ computed for the tight collision complex and yields an excellent value for k_r when combined with a strong collision deactivation (λ=1). We are thus forced to conclude that the TS complex for O + NO recombination is loose, just as it is for all other radical recombinations. While this is not in agreement with some shock tube results[55] obtained recently, it is the only way to explain the results of Pitts, Sharp, and Chan[56] on the threshold wavelengths for NO_2 photolysis. The usual rule of a loose transition state complex for $(O{=}N\cdots O)^{\ddagger}$ would have an N···O distance of about 3.0 Å. At an N···O distance of 1.8 Å, the ion-pair curve[50] would have zero energy if we neglect ion-dipole interactions and polarization. It is likely, however, that polarization effects will stabilize the ion-pair curve out to even larger distances, and this type of interaction[57] could account for the relative ease of formation of the loose complex. Such a loose complex could

also account for the much discussed anomaly in the fluorescence lifetime of electronically[58] excited NO_2.

In further support of this "loose" model of the NO + O recombination is the atom exchange data for the exchange reactions:[57,59]

$$O^{18} + NO^{16} \rightleftarrows (O^{18}...NO^{16})^{\ddagger} \rightleftarrows {}^{18}NO + O^{16}$$

It was found that the rate of complex formation which is just twice the observed exchange rate is $19^{9.3}$ l/mole-sec at 300°K. This is about ten times slower than the rate of formation of the loose "collision" complex of NO_2^* we have just considered, but it corresponds very closely to the rate of formation of a semi-tight NO_2 transition state in which the bending mode at 760 cm^{-1} is replaced by a restricted (~ 60°) 1-dimensional rotation.[43] Such a semi-tight structure is required if the two O-atoms are to become equivalent, which is needed to allow the exchange. A loose TS with large moments of inertia will have a centrifugal barrier which will prevent the two O-atoms from becoming equivalent.

Additional evidence comes from the findings obtained by Hippler et al.[60] where a limiting bimolecular rate constant for $O + NO \rightarrow NO_2$ in high pressures of inert gases (1000 atm) is 1.8×10^{10} l/mole-sec. This now coincides with the rate of formation of a genuine loose TS for NO_2^* and suggests that at these very high pressures, every complex is quenched ($\tau_{collision} \leq 10^{-12.5}$ sec), even rotationaly hot NO_2^*.

The high ionization potential of O_2 (12.06 e.v.)[49] will permit ion-pair formation only at distances of about 1.3 Å, which is practically the normal covalent (1.28 Å) bond length in O_3. Thus, no loose transition state can be formed.

Again, supporting data comes both from $O^{18} + O_2$ exchange measurements[57,59] where the rate of complex formation is $10^{9.0}$ l/mole-sec, only a factor of two less than that found for NO_2 and presumably corresponding to the rate of formation of a semi-tight transition state. The difference in rates corresponds very closely to the differences in ΔS^0. Further support is provided by the data of Hippler et al.,[60] who find for the limiting bimolecular rate constant $k(O + O_2) \sim 10^{9.2}$, only slightly greater than the rate of formation of the semi-tight transition state, and indicating that no loose transition state is possible for O_3.

One would expect that halogen atoms with their large electron affinities would similarly form loose ion-pair complexes with NO and this is indeed compatible with the termolecular rate constants observed for the recombination of Cl + NO,[59] all in the range of $10^{10.5\pm0.1}$ l/mole-sec. In distinct and pardoxical contrast is the low recombination rate constant observed for $O + O_2 + M \rightarrow O_3 + M$[54] of about $10^{8.2}$ l^2/mole^2-sec at 300°K. This is clearly incompatible with a loose transition state complex and can instead be interpreted in terms of a tight transition state complex. Using the same analysis as for NO, we find:

$$\Delta S^0(O_3) = -30.4 \text{ e.u. (atmospheres)}$$
$$= -24.0 \text{ e.u. (moles/liter)}$$
$$\nu_M \approx 930 \text{ cm}^{-1}$$
$$E^*_{300K} \simeq 26.5 \text{ kcal}$$
$$\rho^* \sim 10^{1.7}$$

and $k_r(O_3) = \lambda k_z(10^{-4.8})(10^{1.7}) = \lambda(10^{-3.1})k_z$. If $\lambda = 1$ and $k_z = 10^{11.4}$ l/mole-sec, then $k_r = 10^{8.3}$ l^2/mole^2-sec, in excellent agreement with the observed data.

Activation Energies

The only activation energies which can be said to be reasonably well understood are those for simple bond fission reactions. The bulk of the data on these reactions support the loose transition state model for bond rupture,[26] and the activation energies are simply equal to the bond dissociation energy $(DH)^0$-RT. Hence the reverse recombination reactions have zero activation energies (for standard state, of mole/liter). This loose transition state, originally proposed by Gorin, is compatible with a potential function which extends out to form 2.5 to 3 times the covalent bond radius.

The activation energies for bimolecular processes do not fall into such a simple pattern. If we restrict our attention to what has been called the intrinsic activation energy of a reversible reaction, i.e., the activation energy in the exothermic direction, they are generally low, in the range 0-15 kcal/mole. This is true both for atom metathesis reactions and for addition reactions. Perhaps 80 percent of measured, intrinsic E_{act} fall in the range 8 ± 3 kcal/mole, while over 90 percent are in the range 8 ± 5 kcal/mole. A few fall conspicuously outside of this range, and within homologous series of reactions there are occasionally some curious deviations from general trends.

A number of semi-empirical efforts at treating metathesis reactions, such as the bond energy-bond order model[61,62] (BEBO) have succeeded in estimating $E_{intrinsic}$ to ± 2 kcal/mole. More recently, Alfassi and Benson[63] have demonstrated that $E_{intrinsic}$ can be represented by simple formulas of the form:

$$E = 13.0 - 3.3\ I \qquad (41)$$

or

$$E = X_A + X_C \qquad (42)$$

or

$$E = F_A \cdot F_C \qquad (43)$$

where $E_{intrinsic}$ is in kcal/mole, I is the sum of the electron affinities of the entering (A) and leaving (C) radicals (or atoms) in the metathesis reaction:

$$A + BC \rightleftarrows (A \cdots B \cdots C)^{\ddagger} \rightleftarrows A{-}B + C + \text{energy}$$

In relation (42), X_A and X_C are constants, characteristic of the radicals A and C, respectively, and turn out to correlate with their ionization potentials. F_A and F_C are similar group constants.

All three relations are capable of estimating E_{act} for broad categories of reactions to an average of $\pm$ 1 kcal and a maximum deviation of about 2.6 kcal/mole.

In a few cases larger deviations can be explained on the basis of dipole-dipole repulsion (CF_3 + HX). In the abstraction of halogen atoms (B = halogen), there must be a strong influence of the migrating atom B on the activation energy, but this is neglected in the correlation. The data currently available are not sufficient to further examine this point.

We have already noted that addition reactions of atoms or radicals to Pi bonds are especially sensitive to the ionization potentials and activation energies of the reacting pair. This is strikingly parallel to the empirical finding for metathetical reactions and suggests that the ability to form donor-acceptor (ion-pair) complexes plays an important role in determining the crossing of the two potential energy surfaces represented by reactants and products.

There are a few examples of exceptionally high activation energies in exothermic metathesis reactions which are worthy of further examination.

Two examples are: $CO + O_2 \rightarrow CO_2 + O$ ($E_{act} \simeq 47$ kcal) and $CO + NO_2 \rightarrow CO_2 + NO$ ($E_{act} \cong 25$ kcal) which are exothermic by some 8 and 46 kcal, respectively.

If we examine the intermediates formed in each case, we find that they are very endothermic biradicals, such that the intrinsic activation energy is in each case only 8-10 kcal/mole above the endothermicity of the addition.[64] If we neglect such exceptional cases, then we find that the intrinsic activation energies for exothermic addition reactions fall into the same range as for metathesis reactions, namely 8 ± 5 kcal/mole. Data on these activation energies is not abundant, and so empirical analyses have been made in an effort to correlate them with simple bonding properties.

B. RATE PARAMETER EVALUATION AND ESTIMATES

Extensive efforts are under way throughout the world to accurately model atmospheric chemistry. Whether the efforts are directed toward modeling tropospheric or stratospheric phenomena, there is a need to evaluate existing rate constant data and to estimate unknown rate parameters in a way that is consistent with current knowledge for similar reactions. We are developing an explicit reaction mechanism to explain data obtained in smog chambers and we are constantly faced with the fact that too few accurate rate data for elementary reactions are available.

Since the kinetic data on particular families of reactions ranges from "excellent and extensive" to "nonexistent," a variety of methods must be used for evaluation and/or estimation. As a general guiding principle, it has been found that best results are obtained when reactions are treated as "families" rather than as individuals, because only rarely are enough data available for an individual reaction to make a meaningful evaluation.

A second guiding principle often overlooked is that an estimate or evaluation is not useful unless accompanied by a fair assessment of its probable accuracy. Since A-factor and activation energy combine to give a single rate constant, we have adopted the method of propagation of errors to estimate the uncertainty in rate constants, based on the probable uncertainties associated with A-factor and activation energy. This estimate of uncertainty is very useful since it is a quantitative measure indicating over what range an estimated rate constant can be varied legitimately.

Alkoxyl Radical Decomposition Reactions

The decomposition reactions of alkoxyl radicals provide a good example of a family of reactions for which an adequate number of accurate studies have been made. Most of the studies have been made on t-butoxyl radicals, but several other radicals have been studied as well. All the studies were determinations of relative rate constants and so we returned to the original data and recomputed it on the basis of current values for the reference reaction rate constants.

Three different reference reactions have been used:

$$R_1\overset{O^{\bullet}}{C}R_2R_3 + NO \xrightarrow{M} R_1\overset{ONO}{C}R_2R_3 \qquad (44)$$

$$R_1\overset{O^{\bullet}}{C}R_2R_3 + (CH_3)_3CH \rightarrow R_1\overset{OH}{C}R_2R_3 + (CH_3)_3\dot{C} \qquad (45)$$

$$R_1\overset{O^{\bullet}}{C}HR_3 + NO \rightarrow R_1\overset{O}{\overset{\|}{C}}R_2 + HNO \qquad (46)$$

Values chosen for k_{44} were those obtained by Batt et al.,[65] and are in good agreement with those obtained by Golden et al.[33]; the value of k_{45} chosen was that determined by Berces and Trotman-Dickenson[66]; the values chosen for k_{46} were derived from disproportionation/combination ratios and values of k_{44}.[34,65] Other reported data were not used because their reference reaction rates are not sufficiently well known.

The recalculated data are presented in Figures 11 through 14, and the corresponding Arrhenius parameters are presented in Table XVI. The data

Table XVI

EXPERIMENTAL VALUES FOR RO· DECOMPOSITION RATES[a]

Radical	log A	log E	ΔS_R^o	log A_r	log A_{est}	E′	Ref.
EtO·	13.7	22.1	33.4	8.2	13.7	22.1	67
i-PrO·	16.1	20.6	37.8	8.2	14.6	17.4	68,69
s-BuO·	16.4 14.9	18.0 15.3	37.7	8.0	14.4	13.9 14.2	70 65d
t-BuO·	15.1	16.2	41.2	8.0	15.2	16.3	71-74

[a]Units: E in kcal/mole; A_r in M^{-1} s^{-1}; A in s^{-1}.

for t-BuO· are the most extensive (Figure 11), covering nearly four orders of magnitude. The individual sets of experimental data taken independently show a rather wide range of Arrhenius parameters and appear to be inconsistent, but taken together, the actual data give a reasonably good straight line with parameters, $\log k/s^{-1} = 15.1 - 16.2/\theta$. Given the entropy change of the reaction, $\Delta S_R^o = 41.2$ Gibbs/mole, the A-factor for the reverse reaction is $A_r = 10^{7.9}$ M^{-1} s^{-1}, a value very close to that for the reaction of methyl radicals with isobutene (log A = 8.0).[75] This suggests a self-consistent method for evaluating and codifying the limited data available for the other alkoxyl radical reactions: choose an A-factor for the reverse reaction and find the corresponding activation energy. If this unified scheme is used, the alkoxyl decompositions can be considered together as a class, rather than individually.

The decomposition of an alkoxyl radical is the reverse of the addition of an alkyl radical to the carbon atom of a carbonyl group, which is analogous

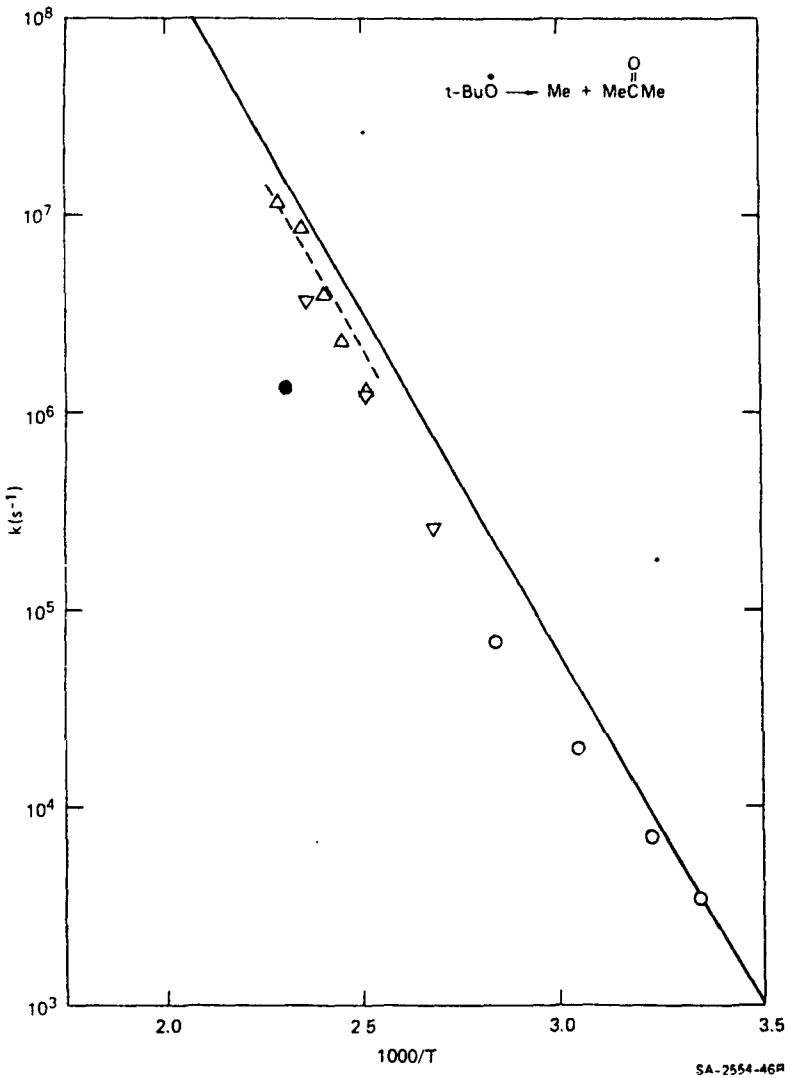

FIGURE 11 t-BuO· $\xrightarrow{M}$ Me + Acetone

▽, Ref. 71; ●, Ref. 72; △, Ref. 73; ○, Ref. 74; dashed line, Ref. 65(c); solid line given by log $k(s^{-1}) = 15.2 - 15.9/\theta$.

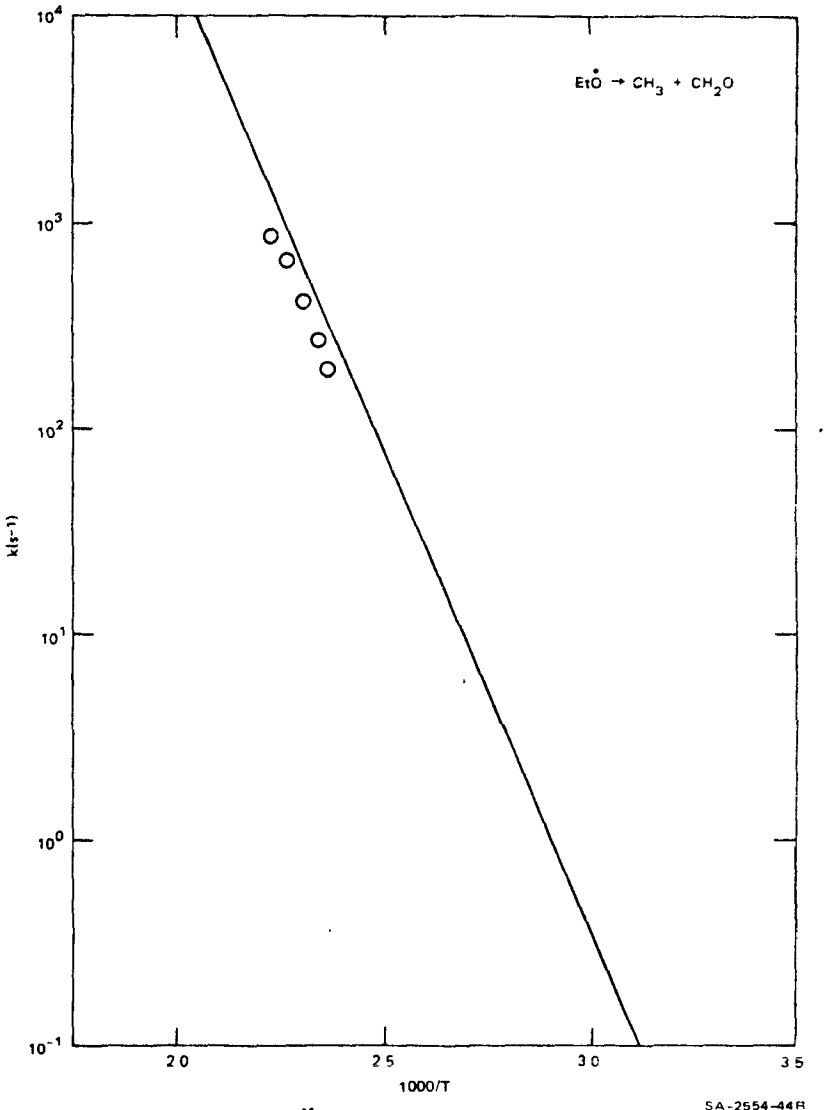

FIGURE 12 EtO· $\xrightarrow{M}$ Me + CHO

○, Ref. 67, line given by log $k(s^{-1}) = 13.7 - 21.6/\theta$

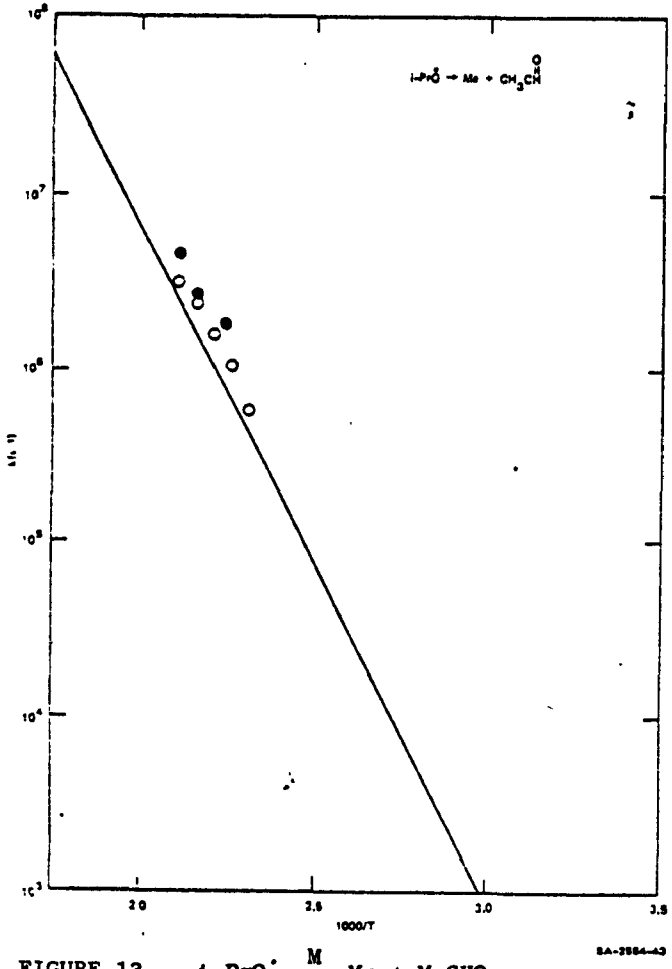

FIGURE 13 i-PrO$^{\cdot}$ $\xrightarrow{M}$ Me + MeCHO

●, Ref. 68; ○, Ref. 69; line given by log k(s^{-1}) = 14.6 − 17.8/θ.

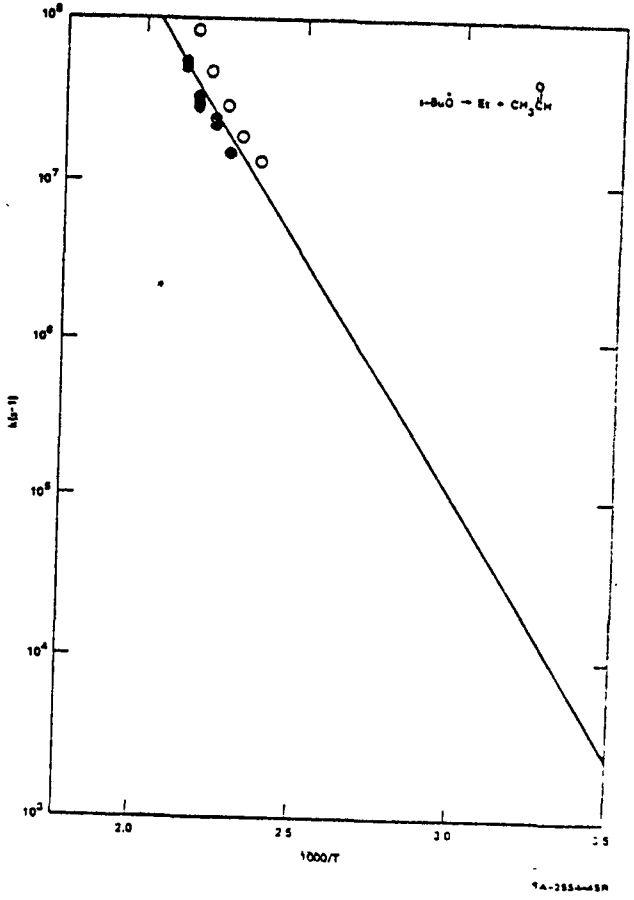

FIGURE 14 s-BuO$^{\cdot}$ $\xrightarrow{M}$ Et + MeCHO

○, Ref. 70; ●, Ref. 65d; line given by log k(s^{-1}) = 14.4 − 14.6/θ.

to alkyl radicals adding to the 2-position of a primary olefin. Since data are only available for alkyl radicals adding to the 1-position of primary olefins, the assumption was made that the A-factors for addition to both ends of an olefin double bond are the same and only the activation energies differ. Thus, A-factors for analogous alkyl radical plus olefin reactions were chosen from the tables of Kerr and Parsonage,[75] corrected for any difference in reaction path degeneracy, and applied to the alkoxyl reactions.

Assumed A-factors for the reverse reaction, A_r, are summarized along with ΔS_R, log A_{est}, and corresponding activation energies E in Table XVI. A plot of E vs ΔH_R^o is presented in Figure 15 and gives a good straight line:

$$E = 12.8 + 0.71\ \Delta H_R^o \qquad \Delta H_R^o > 0 \qquad (47)$$

$$= 12.8 \qquad \Delta H_R^o \leq 0$$

This equation predicts activation energies with an uncertainty of about ± 0.5 kcal/mole. It predicts that the reverse reaction has an activation energy given by:

$$E_r = E - \Delta H_R^o + RT = 13.6 - 0.29\ \Delta H_R^o \qquad (48)$$

Although these equations apply to ~ 400 K where most of the experiments were carried out, the estimated activation energies will be negligibly different at ~ 300 K.

Estimated decomposition rate constants for a number of alkoxyl radicals at 300 K and atmospheric pressure are presented in Table XVII. Fall-off corrections were obtained by use of the Emanuel RRK Integral Tables.[76,77] For the experimental data available, the estimated rates are accurate to about a factor of two, as demonstrated by comparing estimated and observed rate constants (Figures 11-14). The differences apparent between the estimated

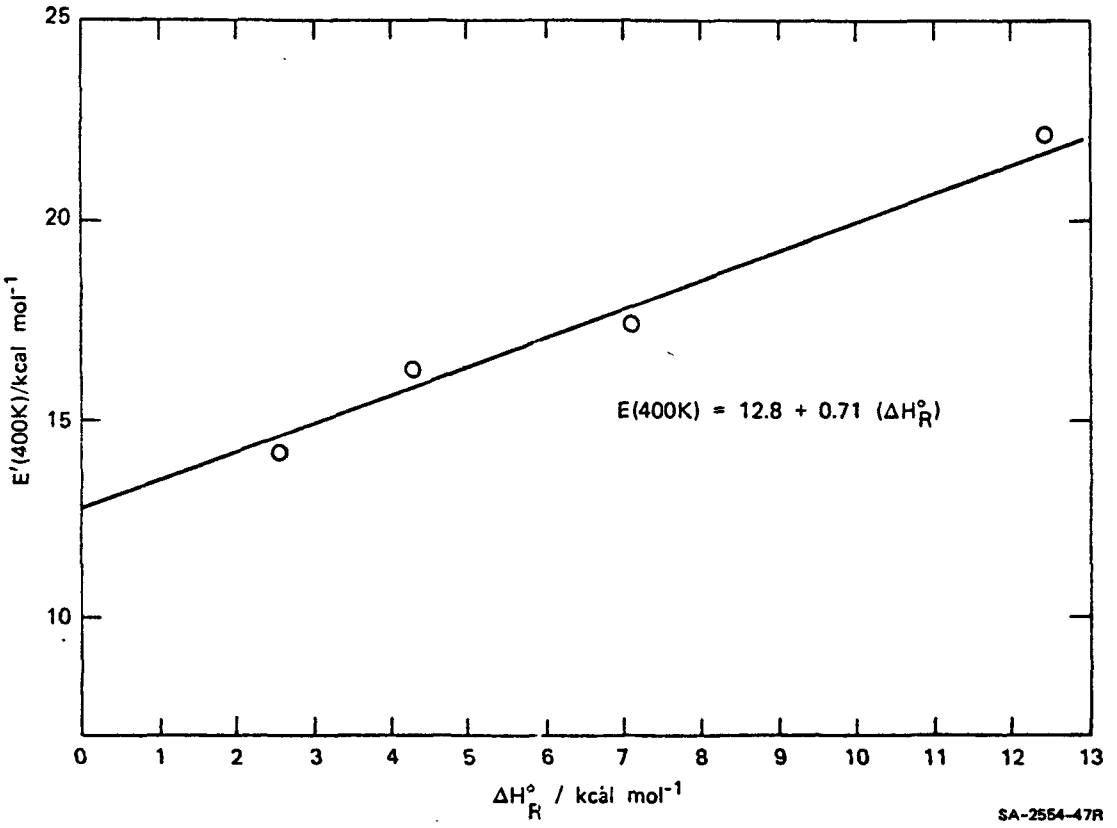

FIGURE 15 Correlation Between Activation Energy E and Enthalpy of Reaction ΔH^{o}_{R}

Table XVII

ESTIMATED RO· DECOMPOSITION RATES

Radical [a]	ΔH_R^o	ΔS_R^o	log A_r [b]	log $A(s^{-1})$	E_{est} [c]	k/k_∞ [d]	$k(min^{-1})$ [f]
C-CO·	12.4	33.4	8.2	13.7	21.6	0.003	2.1×10^{-3}
CC-CO·	9.4	35.0	8.0	13.8	19.5	0.6	1.7×10^{1}
C(O·)-CC	7.1	37.8	8.2	14.6	17.8	0.5	1.6×10^{2}
CCC-CO·	8.9	36.3	7.5	13.6	19.1	0.8	2.9×10^{1}
CC(O·)-CC	2.6	37.7	8.0	14.4	14.6	0.7	2.9×10^{5}
C-C(C)-CO·	4.3	41.2	8.0	15.2	15.9	0.5	1.5×10^{5}
HOC(O·)-CC	6.8 (3.5)[e]	38.0	8.0	14.5	17.6 (15.3)[e]	0.8	2.8×10^{3} (2.2×10^{5})[e]
HOCCC-CO·	8.7	36.6	7.1	13.3	19.0	1	2.1×10^{2}
HOCCC-C(O·)OH	-9.7	39.2	7.1	13.8	12.8	1	2.1×10^{6}
$(HO)_2CCC$-C(O·)OH	-9.6	39.2	6.8	13.5	12.8	1	1.0×10^{6}
$(HO)_2CCC$-C(O·)$(OH)_2$	-30.9	37.7	6.8	13.2	12.8	1	5.2×10^{5}
$(HO)_3CCC$-C(O·)$(OH)_2$	-24.5	37.7	6.5	12.9	12.8	1	2.6×10^{5}
HOC(C)-CO·	11.4 (8.2)[e]	37.7	7.5	13.9	20.9 (18.6)[e]	0.9	3.6×10^{0} (2.2×10^{2})[e]
CC(O)-CC(O·)	-5.1	40.3	7.5	14.5	12.8	0.8	8.2×10^{6}

[a] Notation: HOC(O·)-CC represents $HOCH_2\dot{C}(O)CH_3 \rightarrow HO\dot{C}H_2 + HC(O)CH_3$, etc.

[b] A-factor for analogous alkyl radical + alkene association reaction.

[c] E_{est} 12.8 + 0.71 ΔH_R^o (kcal/mole).

[d] Fall-off estimated from RRK Tables for 1 atm, 300°K.

[e] Based on Group Additivity,[82] not on experimental ΔH_f^o for propane-1,2-diol.[83]

[f] Rate constants for 300 K and 1 atm. air.

and experimental rate constants are due to the ± 0.5 kcal/mole uncertainty in estimating the reaction activation energy and round-off errors on the A-factors.

Estimates made when no experimental data are available can be appraised by using the propagation of errors equation. Since A-factor and activation energy are usually estimated independently, the uncertainty in log k can be written

$$\sigma^2_{\log k} = \sigma^2_{\log A} + \sigma^2_E/\theta^2 \qquad (49)$$

where $\sigma_{\log k}$, $\sigma_{\log A}$, and σ_E are standard deviations in log k, log A, and activation energy, respectively, and $\theta = 2.303$ RT. Since log A is probably uncertain by ± 0.5, and the activation energy is uncertain by about ± 1 kcal/mole, the value for $\sigma_{\log k} \approx 0.88$ at 300 K, and k is uncertain by about a factor of eight. This represents a relatively favorable case for estimations, since an adequate amount of kinetic data is available, and it is fairly consistent. For the reactions discussed below, very little data is available, and the reliability of the estimates is much lower.

Alkoxyl Radical Reactions with Oxygen

The only reliable Arrhenius parameters[78] known for this class of reactions are:

$$CH_3O + O_2 \rightarrow CH_3O + HO_2 \qquad \log k/M^{-1}\ s^{-1} = 8.5 - 4.0/\theta \qquad (50)$$

Rates for other members of this class can only be estimated after making assumptions regarding variations in A-factors and activation energies. The concomitant uncertainties in estimating rate constants will be relatively large since little is known about such variations.

The A-factors for this group of reactions are expected to be similar to that for methoxy radicals, aside from the reaction path degeneracy (n) factor; therefore, log A can be estimated as follows:

$$\log A_{est}/M^{-1}\ s^{-1} = 8.0 + \log n \qquad (51)$$

Estimates for activation energy variations are rather problematical, especially when E_a is low. Two alternative methods can be used:

(1) Assume E_a is constant for the entire homologous series

(2) Assume that an empirical relationship that holds for other radical reactions applies to this series as well.

A simple empirical relationship[79] that gives E_a with an uncertainty of about ± 3 kcal mol^{-1} for exothermic H, OH, and CH_3 reactions is given by equation (52):

$$E_a = 11.5 + 0.25\ (\Delta H_R) \quad , \qquad (52)$$

where ΔH_R is the enthalpy of reaction. For reaction (50), equation (52) predicts E_a = 5 kcal mol^{-1}, about 1 kcal mol^{-1} too high. Equation (52) has two parameters and can be modified in two different ways to give the proper E_a for reaction (44):

$$E_a = 10.5 + 0.25\ (\Delta H_R) \tag{53}$$

$$E_a = 11.5 + 0.29\ (\Delta H_R) \tag{54}$$

Rate constants for a number of alkoxyl radical reactions were estimated by the three methods and are presented in Table XVIII. Considering the large uncertainty associated with equation (45) and the low activation energies, the estimates in column III of the table are highly uncertain and may well be upper limits to the correct rate constants. Similarly, rate constants in column I of the table may be near the lower limits.

The overall uncertainties for this family of reactions may be estimated as before. Log A is probably uncertain by ± 0.5 and the activation energy is probably uncertain by an average of ± 1.5 kcal/mole. Thus, $\sigma_{\log k} \approx 1.2$, and the estimated rate constant is uncertain by about a factor of 16. If the activation energy is uncertain by an average of ~ ± 2.5 kcal/mole, the estimated rate constant is uncertain by a factor of ~ 80.

Table XVIII

ESTIMATES: $RO^{\bullet} + O_2$ REACTIONS[a]

Reaction	$\log (A)_{est}$	I $E_a = 4.0$	II $E_a = 10.6 + 0.25 \times (\Delta H_R^o)$	III $E_a = 11.5 + 0.29 \times (\Delta H_R^o)$
		k (min^{-1})	k (min^{-1})	k (min^{-1})
$CH_3O + O_2$	8.5	2.0×10^5	2.0×10^5	2.0×10^5
$EtO + O_2$	8.3	1.3×10^5	8.2×10^5	1.3×10^6
$n\text{-}PrO + O_2$	8.3	1.3×10^5	8.2×10^5	1.3×10^6
$i\text{-}PrO + O_2$	8.0	6.7×10^4	1.5×10^6	3.7×10^6
$n\text{-}BuO + O_2$	8.3	1.3×10^5	3.5×10^5	5.8×10^5
$s\text{-}BuO + O_2$	8.0	6.7×10^4	1.1×10^6	2.2×10^6

[a]Effective first-order rate constants at 300 K in air (2.1×10^5 ppm O_2).

Alkoxyl Radical Isomerization Reactions

The importance of alkoxyl radical isomerization reactions has been inferred from smog chamber data,[80] as well as from more qualitative considerations.[81] The estimation of the isomerization rates is relatively straightforward, but the estimates are somewhat uncertain, as discussed below.

A-factors for 5-membered ring (5R) and 6-membered ring (6R) isomerizations were estimated to be $10^{11.2}$ s^{-1} and $10^{10.9}$ s^{-1} (per H-atom), respectively. The estimate for the 5R transition state was made by noting that in tying up the methyl and ethyl internal rotations, the change in entropy is about −6.6 Gibbs/mole; subtracting another 0.3 Gibbs/mole for the reaction coordinate, we obtain log A_{5R} = 11.7 for three abstractable H-atoms. Thus, for each abstractable H-atom, log A_{5R} (per-H) = 11.2.

For the 6R transition state, a model transition state was used. For the decomposition of ethyl vinyl ether (EVE), log A = 11.4 at 700°K. If log A is about the same at 300°K and S^0(EVE) = 82.6 Gibbs/mole,[82] then the entropy of the transition state is 74.3 Gibbs/mole. In comparing the EVE transition state and that of n-butoxyl radical, EVE has some double bond character, and that of n-butoxyl will be looser by about 0.6 Gibbs/mole. n-Butoxyl has one more hydrogen atom, worth about 0.2 Gibbs/mole, and has spin, contributing 1.4 Gibbs/mole. Adding all of these corrections, gives $S^{0\ddagger}$ = 76.5 and log A = 11.4 for three abstractable H-atoms; thus log A_{6R}(per H) = 10.9. The uncertainties in these estimates are probably ± 4 Gibbs/mole and log A is uncertain by ± 1.

Activation energies may be estimated from the activation energies for H-abstraction by alkoxyl radicals[2a] by adding a "strain" energy of 0.5 kcal/mole for 6R reactions and 5.9 kcal/mole for 5R reactions.[82] These activation energies are rather uncertain, probably ± 2 kcal/mole. The combination of the two sources of error by the propagation of errors formula gives an estimated uncertainty in log k of ± 1.8 at room temperature. Thus, the rates are estimated to be uncertain by about a factor of 60.

The method for estimating these rates is summarized in Table XIX, and estimated rates for several alkoxyl radicals are presented in Table XX. All reactions are assumed to be at the high-pressure limit.

Table XIX

RO$^{\cdot}$ ISOMERIZATION REACTIONS--ESTIMATION PROCEDURE

E = E (abstraction) + E (strain)

Hydrogen Abstracted	E (abstraction), kcal/mole
RCH_2-H	7.2
RCH(OH)-H	6.0
R_1R_2CH-H	4.1
$R_1R_2R_3C$-H	4.1
$RC(OH)_2$-H	4.1[a]

Strain Energy	
5-membered ring	5.9 kcal/mole
6-membered ring	0.5 kcal/mole

A-Factor (per abstractable H)	
5-membered ring	$A = 10^{11.2}\ s^{-1}$
6-membered ring	$A = 10^{10.9}\ s^{-1}$

[a]Estimated.

Table XX

ESTIMATED RO$^{\bullet}$ ISOMERIZATION REACTION RATES

Reaction[a]	log A(s^{-1})	E(kcal/mole)	k(min^{-1})
$\overset{\bullet}{O}CCCC \rightarrow HOCCC\overset{\bullet}{C}$	11.4	7.7	3.7×10^{7}
$\overset{\bullet}{O}\!\!\vdots\!\!CCCC \rightarrow \overset{OH}{\vert}CCCC\bullet$	11.7	13.1	8.6×10^{3}
$HOCCCC\overset{\bullet}{O} \rightarrow HO\overset{\bullet}{C}CCCOH$	11.2	6.5	1.9×10^{8}
$HO\overset{O^{\bullet}}{\vert}CCCCOH \rightarrow (HO)_2CCC\overset{\bullet}{C}OH$	11.2	6.5	1.9×10^{8}
$(HO)_2CCC\overset{O^{\bullet}}{\vert}COH \rightarrow (HO)_2\overset{\bullet}{C}CCC(OH)_2$	10.9	4.6	2.2×10^{9}
$(HO)_2\overset{\bullet O}{\vert}CCCC(OH)_2 \rightarrow (HO)_3CCC\overset{\bullet}{C}(OH)_2$	10.9	4.6	2.2×10^{9}
$CC\overset{OH}{\vert}CCO\bullet \rightarrow \overset{\bullet}{C}C\overset{OH}{\vert}CCOH$	11.4	7.7	3.0×10^{8}

[a]Notation: $CC\overset{OH}{\vert}CCO\bullet \rightarrow \overset{\bullet}{C}C\overset{OH}{\vert}CCOH$ represents $CH_3C\overset{OH}{\vert}HCH_2CH_2O\bullet \rightarrow \overset{\bullet}{C}H_2C\overset{OH}{\vert}HCH_2CH_2OH$

Reaction of NO_2 with HO_2

These species have long been thought to react via a radical disproportionation to give HONO and O_2:

$$HO_2 + NO_2 \rightarrow HONO + O_2 \qquad (55)$$

Recently, however, Niki and coworkers[83] have studied the reaction and could not detect any HONO. They concluded that the predominant reaction is:

$$HO_2 + NO_2 \overset{M}{\rightleftarrows} HOONO_2 \qquad (56)$$

This conclusion is also supported by some of Heicklen's data,[84] but the reaction was not considered explicitly, and k_{13} was not determined. Both Heicklen[85] and Cox[86] found that the loss rate due to $HO_2 + NO_2$ is about 2-10 x 10^7 M^{-1} s^{-1}. This value is uncertain, however, because they did not consider the effect of $HOONO_2$. Calvert and coworkers [87] have also observed HO_2NO_2 and have attempted to obtain some kinetic information from the chemical system, but the system is too complicated to allow unambiguous interpretation. Both Niki and Calvert observed the lifetime of HO_2NO_2 to be ~ 6-8 minutes and both ascribed the loss mechanism to wall reactions. Thus, quantitative kinetic information on the homogeneous reaction is virtually nonexistent.

Because HO_2NO_2 can act as a radical reservoir or sink, the kinetics of HO_2NO_2 can have far-reaching effects in photochemical smog and in stratospheric chemistry. According to this scheme, HO_2 and NO_2 react to form HO_2NO_2, which can "store" the reactive species until it homogeneously decomposes at its natural unimolecular decomposition rate. At that time, it releases the HO_2 and NO_2 back into the reaction mixture to react further with the other species present. Thus, it is important to estimate the rate constants for association and decomposition.

As a starting point for estimating the rate constants, we can use the rates determined by Hendry[88] for the reaction of peroxyacetylnitrate (PAN):

$$CH_3\overset{O}{\overset{\|}{C}}OONO_2 \rightarrow CH_3COO + NO_2 \qquad \log k/s^{-1} = 16.2 - 26.8/\theta \qquad (57)$$

This reaction is analogous to that for HO_2NO_2 and its Arrhenius parameters provide a good starting point. The major uncertainty is whether the $[OO\text{-}NO_2]$ bond dissociation energy in PAN is equal to that in HO_2NO_2. For most radical association reactions there is no activation energy. Thus the A-factor for the association reaction can be derived from that of the decomposition step and ΔS_R^0 for the reaction. In the case of PAN decomposition, ΔS_R^0 for the reaction is estimated to be 42 Gibbs/mole, giving $\log A_{-57} = 8.8$ for the association. This value is not unreasonable for radical association reactions, but may be a little low.

A detailed estimate for the entropy of HO_2NO_2 was made based on the value of 72.2 e.u. for $MeONO_2$[89] by adjusting for the change of internal rotor from a methyl to an OH and including the corresponding rotational barrier change due to the loss of two hydrogen atoms, and correcting for spin gives $S_f^0(HO_2NO_2) = 71.6$ e.u. The frequency assignment for the molecule is given in Table XXI. The first five frequencies listed are those actually observed by Niki, et al.[83]; the remaining frequencies are based on those for FNO_3, H_2O_2, and HNO_3, with the low frequency torsions adjusted to give $S_f^0(HO_2NO_2) = 71.6$ e.u. The values used are compatible with the known torsion barriers for O-OH and O-NO_2. In the transition state, the N-O stretch is assumed to become the reaction coordinate, and the NO_2 group is assumed to be free rotor. Other vibrational frequencies were lowered as in Table XXI to give an entropy for the transition state that yields the desired high pressure A-factor. If $E_{56} = 0$ and $\log_{10} A_{56} = 9.0$ (similar to PAN), then $\log A_{-56} = 15.9$. The results of the calculations are given in Table XXII

Table XXI

FREQUENCY ASSIGNMENT FOR HO_2NO_2

Frequency in Molecules (cm^{-1})	Frequency in Transition State (cm^{-1})	Type
3540[a]	3540	OH stretch
1728[a]	1728	NO_3
1304[a]	1304	NO_3
803[a]	803	NO_3
1396[a]	1396	OH bend
633	Reaction coordinate	NO stretch
500	200	NO_2 rock
735	435	NO_2 wag
125	Free rotor	O-NO_2 torsion
400	100	OOH bend
880	580	OO stretch
200	150	HO-O torsion

[a]From reference 83.

Table XXII

RRKM CALCULATED k/k_∞ FOR HO_2NO_2 DECOMPOSITION

	Collision Efficiency		
	0.4	0.5	0.6
E = 23.1 kcal/mole log A/s^{-1} = 15.9	0.46	0.50	0.53
E = 25.1 kcal/mole log A/s^{-1} = 15.9	0.56	0.60	0.63
E = 27.1 kcal/mole log A/s^{-1} = 15.9	0.65	0.68	0.71

for three high-pressure activation energies and three values of γ, the collision efficiency. The values of k/k_∞ are near unity at 1 atm and 300 K and are presented as a function of E_{-56} in Figure 16 for two values of the collision efficiency that are expected to bracket that of N_2 or O_2. These results show that reactions (56) and (-56) may be very important in controlling the concentration of NO_2 in smog chamber experiments. In the following section, the effects of this reaction will be illustrated by computer simulations.

The major question here is whether HO_2NO_2 and PAN are expected to have the same activation energy for decomposition. Since this question cannot be answered with any confidence, the activation energy E_{-56} may be used as an adjustable parameter in simulating smog chamber data. Although this procedure is not very satisfactory, it does illustrate the necessity for accurate rate data if this issue is to be resolved.

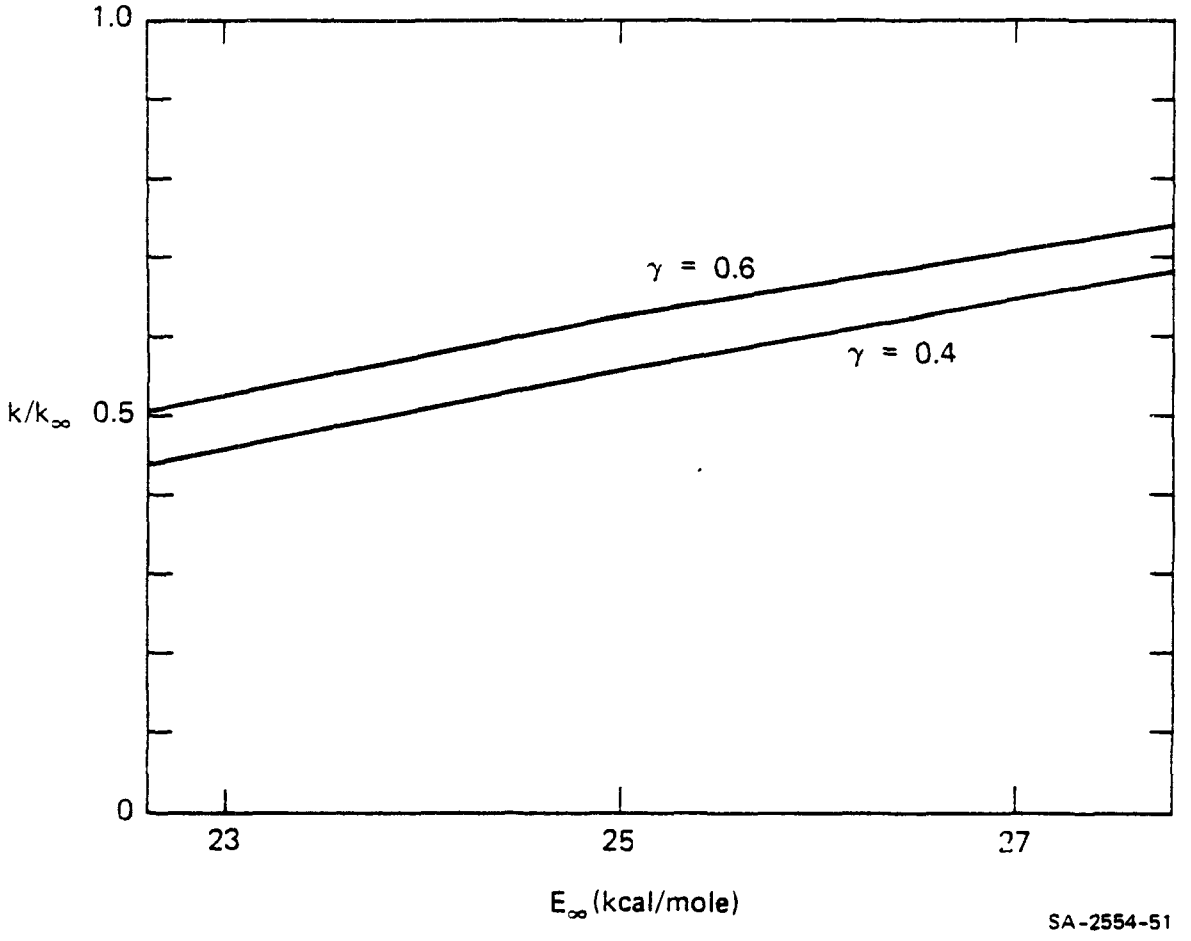

FIGURE 16 Falloff Calculated by RRKM Theory as a Function of Activation Energy for the Reaction $HO_2NO_2 \rightarrow HO_2 + NO_2$

Simulations of Smog Chamber Experiments

A major use for an explicit photochemical smog mechanism is to establish U.S. Environmental Protection Agency regulations for controlling pollutant emissions into the troposphere. While it is important to validate a proposed mechanism, it is difficult to use real atmospheric data for this purpose because of the wide variety of organic reactants, the complexity of products, and the presence of capricious transport phenomena. Smog chambers are often employed for carrying out experiments on relatively simple reaction mixtures thought to represent pollutants in the real urban atmosphere; the results obtained are useful in testing assumed mechanisms because the effects of transport phenomena are minimized while temperature and light intensity can be controlled.

Associated with smog chambers, however, are several troublesome problems. The most obvious problem is that the pollutant concentrations are generally higher in a smog chamber than in the real atmosphere; thus when a reaction mechanism is applied to real atmospheric problems, there is an extrapolation into regimes where the mechanism has not been validated. This extrapolation could tend to magnify errors in the chemical mechanism and thus it is important to devise a mechanism which is as accurate as possible in relation to the smog chamber data. A second and most troublesome problem is that of "chamber effects" in which chemical species interact with the walls of the chamber or even appear to desorb from the walls. This manifests itself in a poor mass balance between reactants and products, and in the sometimes observed necessity for postulating a radical source associated with the chamber. Although every attempt must be made to understand the sources of such problems, there is always the possibility that an effect ascribed to "chamber effects" is really

due to a deficiency in the postulated reaction mechanism; conversely, an error in the reaction mechanism might conceal effects better ascribed to the smog chamber.

Since the postulated reaction mechanism must be tested against smog chamber data, it is important that the data be of high quality and that care be taken to minimize "chamber effects." We have been using data reported by Pitts and coworkers[90] at the Statewide Air pollution Research Center located at the University of California, Riverside, who have taken great care in an effort to minimize chamber effects and to characterize their experimental conditions.

The reaction mechanism is complex and partly speculative, and therefore not all elementary reaction steps have been individually measured, yet many important reaction rates are now well known.[91] One may hope that the effects of the unknown rate constants will not predominate in the reaction mechanism. Calvert and coworkers,[1] Pitts et al.,[21] Niki et al.,[92] and Hecht et al.,[93] have made major strides in elucidating the mechanisms of photochemical smog. Our efforts are built upon their work, with the emphasis placed upon systematically estimating and evaluating families of reactions, as described in the preceding sections. Our guiding philosophy has been to start with a "first guess" mechanism, consisting of well-known reactions and our own best estimates for other reactions, and then to make any refinements necessary, within the uncertainties of the experimental data and estimated rate constants.

Our work thus far has been primarily concerned with the photooxidation of propene, butane, and propene/butane mixtures. Although we are continuing

to work on the reaction mechanisms for these species, we feel that the postulated mechanisms are substantially complete, and that it is possible to point out the areas of greatest uncertainty.

Reactions of n-Butane

Since n-butane is thought to be representative of the straight chain alkanes present as pollutants in the urban atmosphere, it is used as a model compound in smog chamber experiments. The experiments are performed on air mixtures containing a few ppm of n-butane and somewhat less NO and NO_2; CO is often present as well. The initial concentrations and relative ratios of RH to NO_x and NO to NO_2 have been varied somewhat in different experiments to provide data over a range of initial conditions.[90]

The major reaction pathways for carbon-containing species in the n-butane system are depicted in Figure 17. The rate constants shown correspond to 300 K and one atmosphere of air and are expressed in units of min^{-1} and ppm^{-1} min^{-1}. For bimolecular reactions involving O_2, the concentration of O_2 (2.1×10^5 ppm) has been multiplied by the appropriate bimolecular rate constant (units of ppm^{-1} min^{-1}) to give an effective first-order rate constant (units of min^{-1}). The rate constants shown represent our best estimates or the best experimental data available.

The initial attack of OH radical on n-butane is known to give ~ 86% sec-butyl radical and ~ 14% n-butyl radical.[91] These radicals combine very rapidly with O_2 to give the corresponding peroxyl radicals. As long as NO is present, the peroxyl radicals oxidize NO to form NO_2 and alkoxyl radicals, which can go on to react as described in the preceding sections.

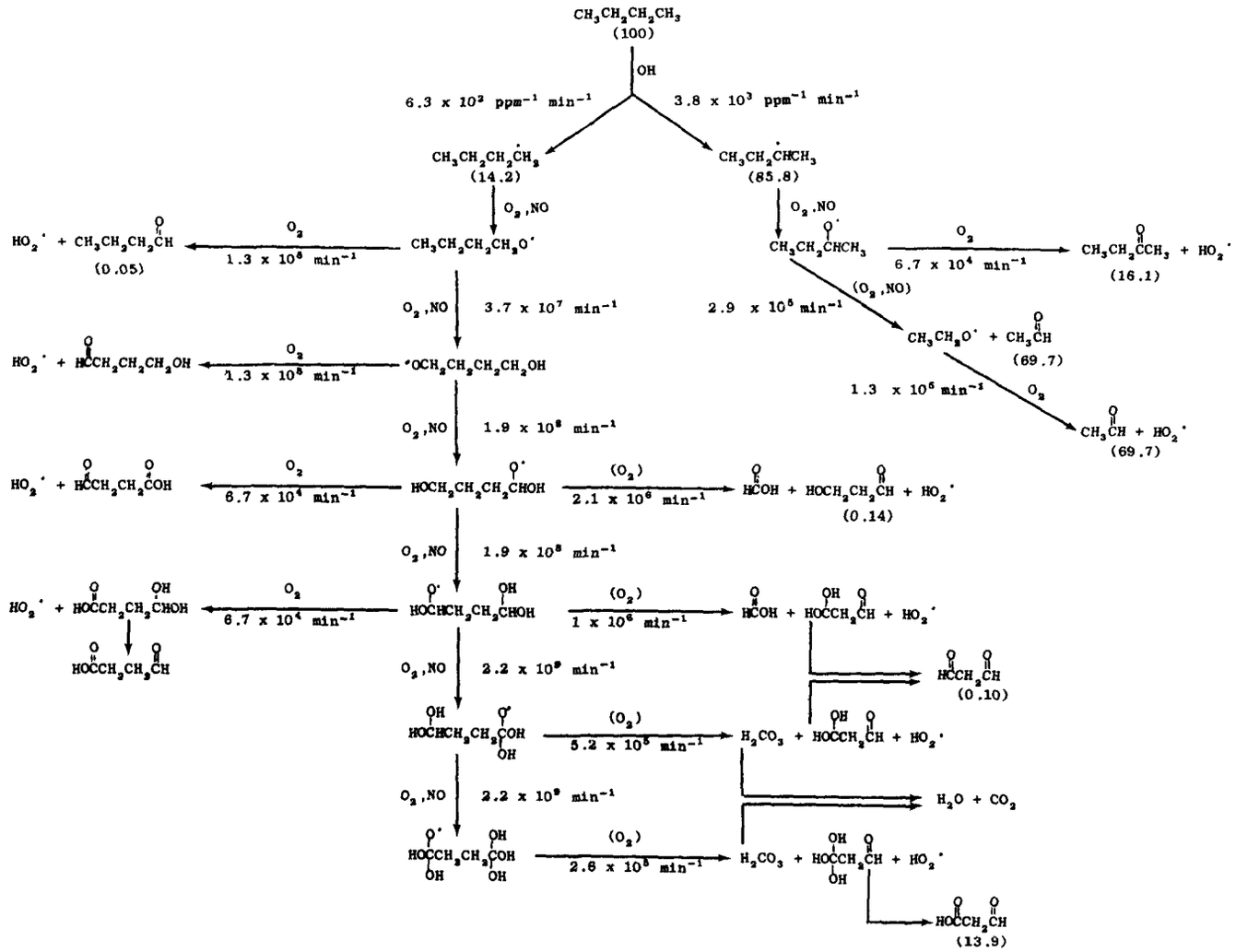

FIGURE 17 Reactions of n-Butane

s-Butoxyl radicals can either react with oxygen to give 2-butanone and HO_2, or they can decompose to give acetaldehyde and ethoxyl radical; the major fate of ethoxyl is to react with oxygen to give acetaldehyde. Although acetaldehyde and 2-butanone react with OH and photolyze, they disappear only slowly, and the ratio of their yields gives a sensitive measure of the relative rates for loss of s-butoxyl: decomposition versus reaction with O_2. Since the s-butoxyl decomposition rate is known fairly accurately, and its reaction with O_2 is rather uncertain, the rate constant for the latter reaction can be adjusted to give the proper relative value.

n-Butoxyl radical also can react with O_2 or slowly decompose, but it has the additional reaction channel of isomerization. In fact, the estimated isomerization rates are so fast that the other possible reactions hardly compete. Examination of Figure 17 shows that about 98% of the original n-butoxyl radical formed ends up as the polyhydroxylated aldehyde $(HO)_3CCH_2CHO$ and only a small amount appears as butanal and other products. The fate of $(HO)_3CCH_2CHO$ is not known, but if it dehydrates, the product $HO(CO)CH_2CHO$ might photolyze quickly to give free radicals that can continue the chain mechanism. Although only 14% of the butane reacts by the n-butoxyl reaction pathways, n-butoxyl accounts for about 36% of the NO oxidized directly by alkoxyl radicals. This is directly attributable to the isomerization reactions.

A reaction not included in our mechanism which might dramatically alter the course of reactions is:

$$R_1\underset{\underset{O}{|}}{\dot{C}}R_2 + O_2 \rightarrow R_1\underset{\underset{O}{\|}}{C}R_2 + HO_2 \qquad (58)$$

If this reaction is fast compared to simple addition of O_2 to form peroxyl radical, the isomerization steps would not have an opportunity to take place, and the character of the n-butane reaction would be quite different from that described above. Reliable experimental data are needed in order to assess the importance of reaction (58), but we would not expect it to compete effectively with addition of O_2, which has the same A-factor and no activation energy.

Another area of uncertainty in the mechanism that deserves mention is the photolysis reactions of aldehydes and ketones. Photolysis rate constants and products for many of the carbonyl compounds are not known and must be estimated. Radical photolysis products serve to accelerate the overall reaction and so are very important. In the absence of good data, many of the rates have simply been estimated by analogy with those rates that are known. In the butane simulations presented below, a radical influx from the chamber walls must also be assumed in order to reproduce the observed rate of butane consumption. It is quite possible that the assumed radical influx is merely compensating for an underestimate of the photolysis rates of carbonyl reaction products, or some other reaction sequence that has been overlooked so far. Further experiments are necessary to clear up this point.

Two computer simulations of the smog-chamber experiment on the n-butane system are presented in Figures 18 and 19. The first simulation (Figure 18) represents our "first guess" mechanism, consisting of experimental rate constants, where available, and our best estimates for unknown rate constants. The activation energy for HO_2NO_2 decomposition was assumed to equal that of PAN (26.8 kcal/mole). Using these rates, an influx of $\sim 10^{-3}$ ppm min^{-1} of HO_2 radicals is necessary to approximate the correct conversion rate of n-butane. It is noteworthy that HO_2NO_2 acts as a radical reservoir--storing HO_2 radicals from the early period of the reaction and slowly releasing them in the later stages.

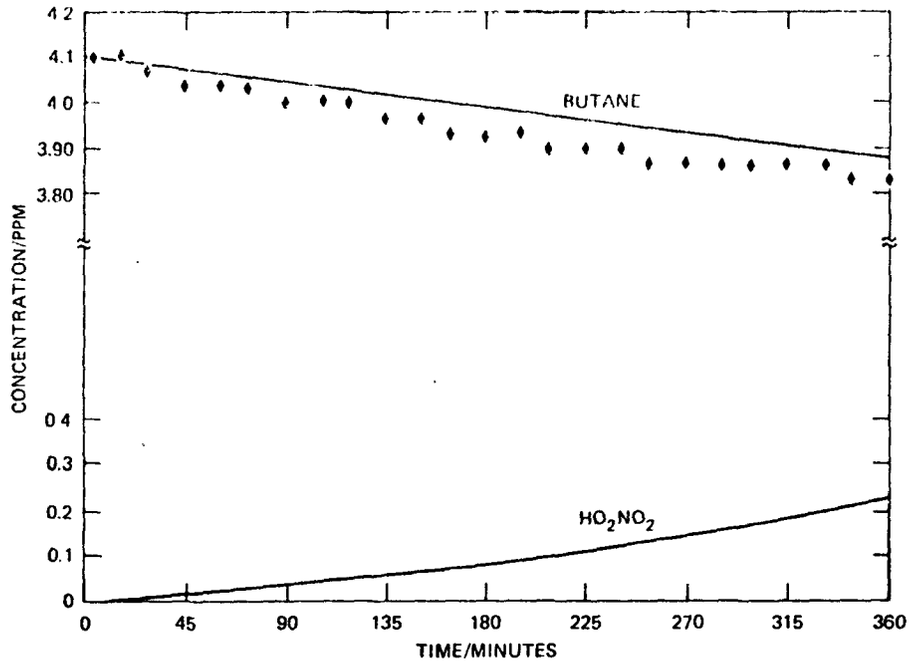

(a) Simulation of Run EC-41 in Reference 90. Initial Concentrations: Butane, 4.03 ppm; NO_2, 0.068 ppm; NO, 0.524 ppm.

The points are experimental results; the lines represent the computed concentration profiles for butane and peroxynitric acid. Radical input is 1×10^{-3} ppm min^{-1} of HO_2. The rate of decomposition of HO_2NO_2 has an assumed activation energy of 26.8 kcal/mole.

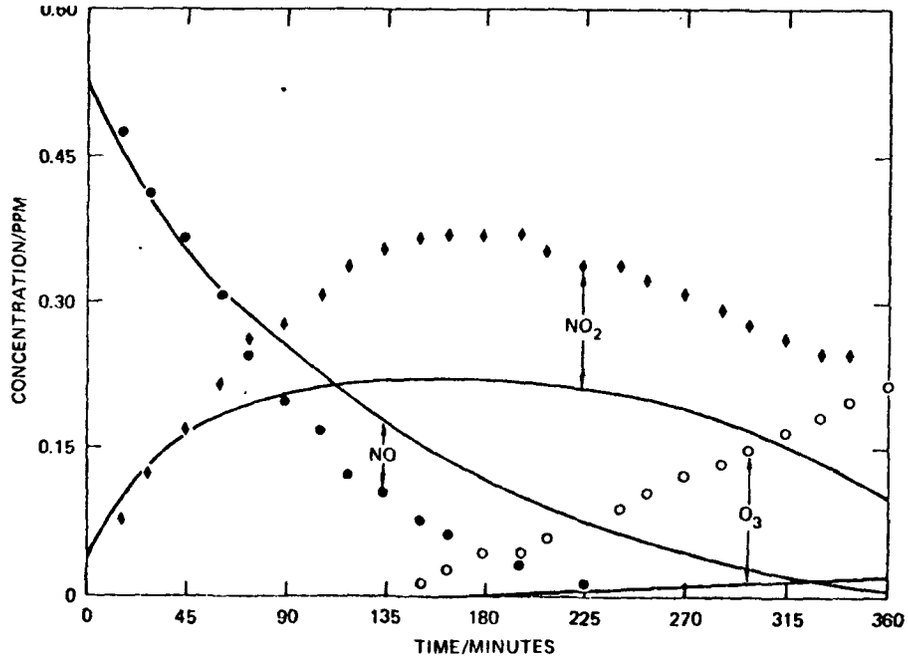

(b) Simulation of run EC-41, as in 7(a), showing the Concentrations of NO_2, NO, and ozone.

FIGURE 18

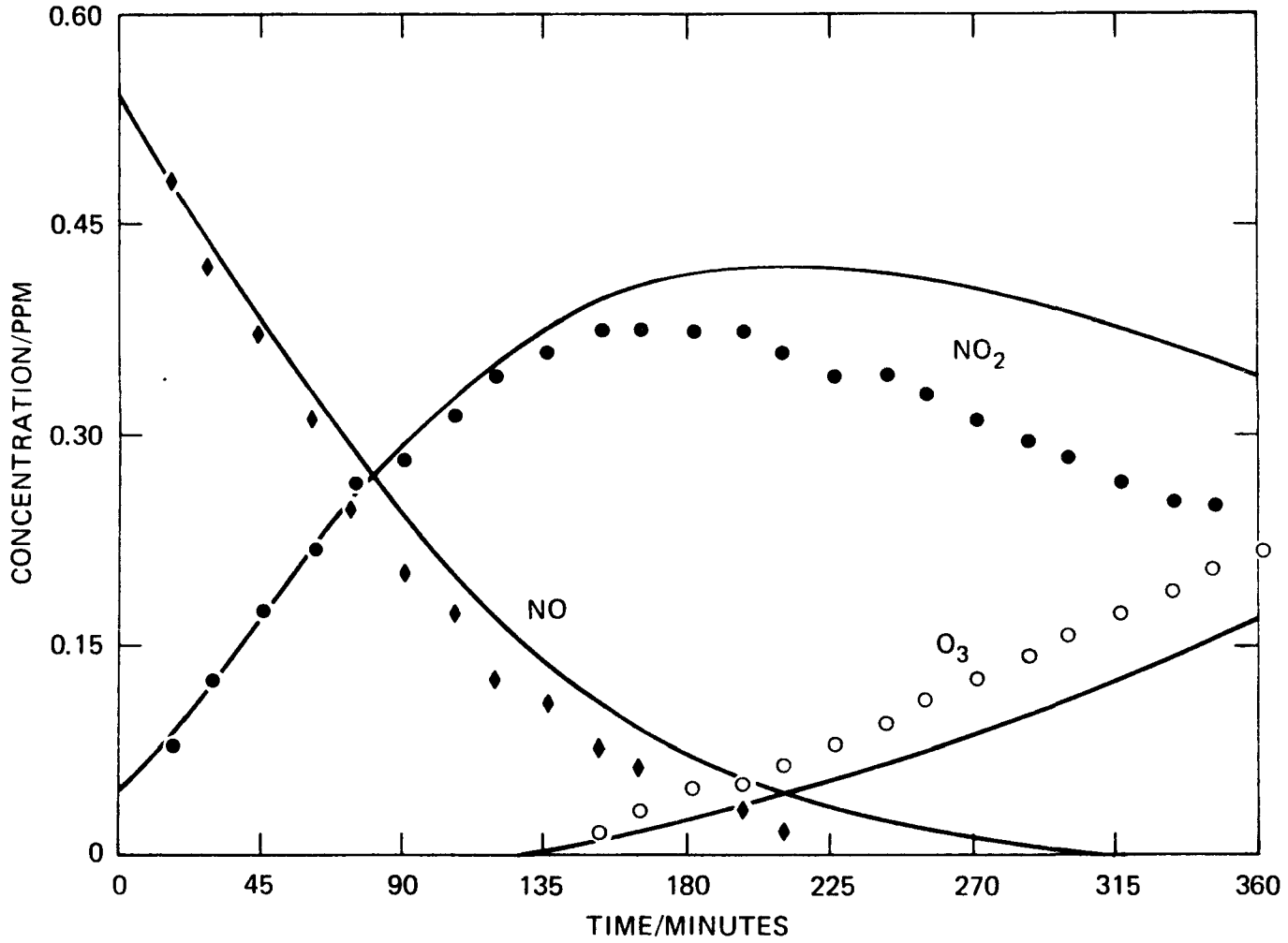

FIGURE 19 Simulation of Run EC-41 in Reference 90. Radical input is 2×10^{-4} ppm min^{-1} of HO_2. The rate of decomposition of HO_2NO_2 has an assumed activation energy of 23 kcal/mole.

Much of the nitrogen is tied up as HO_2NO_2, and relatively less is present as NO_2, affecting both the PAN yield and O_3 production. It may be argued that HO_2NO_2 is expected to contribute to the experimental NO_2 measurement (as does PAN), and thus the NO_2 data may represent the sum of contributions from HO_2NO_2 and NO_2. This question about the correct interpretation of the experimental NO_2 concentration adds an extra element of uncertainty in comparing the simulation to the experiment and must be resolved by laboratory experiments. Another feature of this first simulation is that ozone and PAN production are greatly underestimated as is the consumption of butane. This is due to the quenching effect HO_2NO_2 formation has on the reaction mechanism.

If the HO_2NO_2 decomposition activation energy is less than 26.8 kcal/mole, the influence of HO_2NO_2 formation becomes less important. If the activation energy for decomposition of HO_2NO_2 is assumed to be $\sim$ 23 kcal/mole, HO_2NO_2 has little effect, and the simulation is in much better agreement with experiment (see Figure 19). Moreover, an influx of 2×10^{-4} ppm min^{-1} of radicals must be assumed to match the observed conclusion rate of n-butane. Note that PAN and ozone formation are near the experimental values and HO_2NO_2 concentrations are too low to be shown in the figure. Our experience with simulations of this nature is that the activation energy for HO_2NO_2 decomposition probably falls somewhere between 23 kcal/mole and 25 kcal/mole, but this number is highly tentative, and we must await an experimental determination before this major uncertainty can be resolved.

Once the overall mechanism has been brought into good agreement with experiment, various rate constants can be adjusted within their uncertainties to bring the various product yields into agreement. For example, our first-guess mechanism predicts .018 ppm of 2-butanone and .17 ppm of acetaldehyde

after 360 minutes, but .125 ppm and .082 ppm, respectively, are observed in the experiment. As mentioned earlier, these product yields depend mainly on the following reactions:

$$CH_3CH_2\overset{O^{\bullet}}{\overset{|}{C}}HCH_3 \xrightarrow{M} HC\overset{O}{\overset{\|}{C}}H_3 + CH_3\dot{C}H_2 \qquad (59)$$

$$\xrightarrow[O_2]{} CH_3\overset{O}{\overset{\|}{C}}CH_2CH_3 + HO_2 \qquad (60)$$

Since the rate of reaction (59) is fairly well known, and the rate of reaction (60) is quite uncertain, the latter can be changed to 8.8×10^5 min^{-1}, in order to produce the correct product yields. Unfortunately, not many different product species were measured in the experiments, making it impossible to assess the estimated rate parameters for many of the reactions.

Reactions of Propene

The reactions of alkenes in photochemical smog are quite different from those of alkanes. Not only is hydroxyl radical attack important, but the reactions of oxygen atoms and of ozone must also be considered (see Figure 20). Generally, the reactions which involve addition of these species to the double bond are very fast and result in alkenes reacting substantially more quickly than alkanes in the smog environment.

Although the total rate constants for the reactions of O, O_3, and OH with propene are well known,[91] neither the products of the reaction, nor specific branching ratios into the various product channels are known with certainty for environmental conditions. Thus, the propene mechanism relies considerably on the products observed in the smog chamber data to define specific reaction channels.

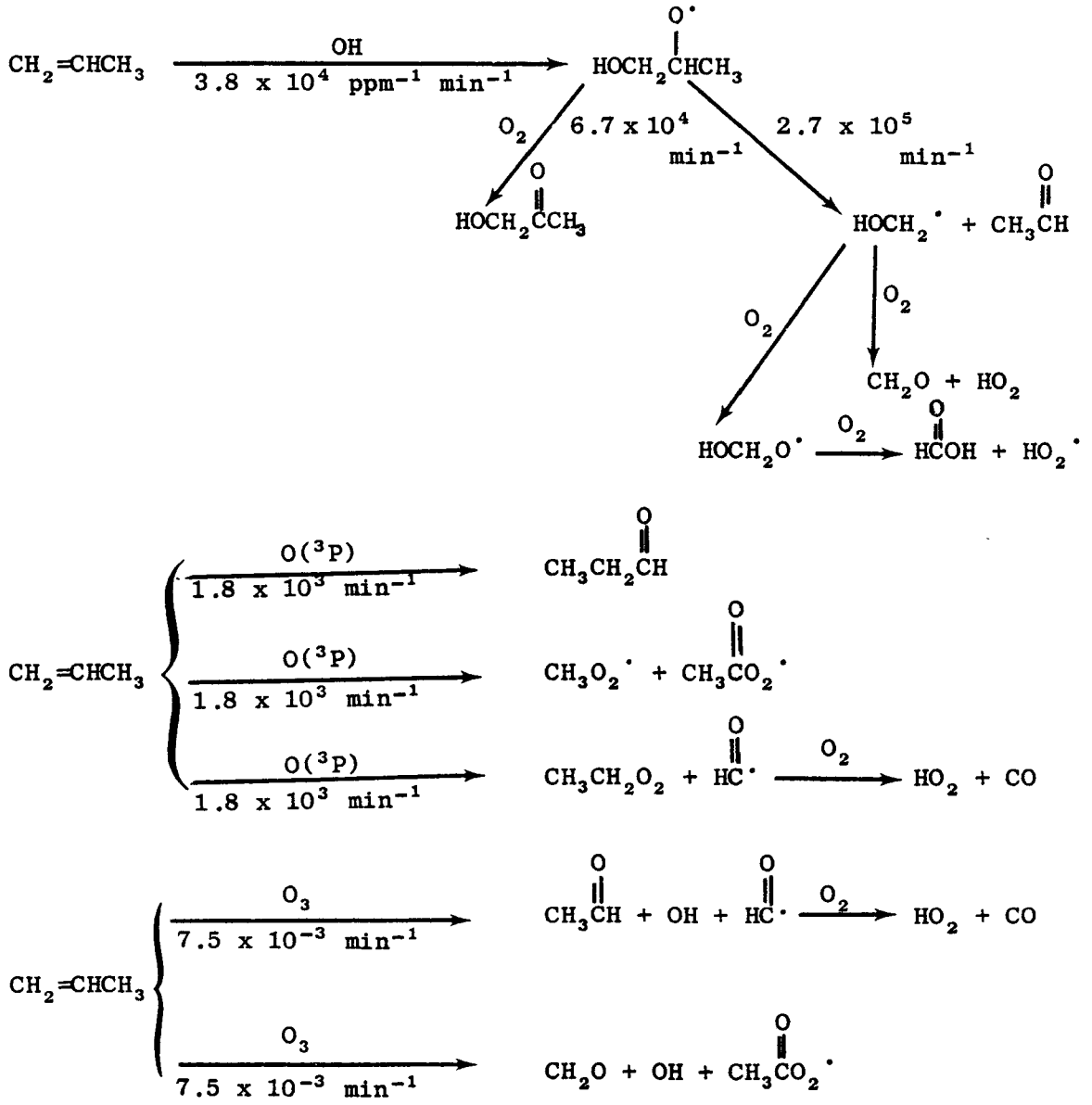

FIGURE 20 Reactions of Propene

Unlike the butane system, it has been found that propene reacts quickly enough so that it is not necessary to assume a constant influx of radicals due to chamber effects. Rather, one can postulate that HONO is present initially (due to $H_2O + NO + NO_2 \rightleftarrows 2\ HONO$) and provides a radical source when photolyzed. Once the reaction has been initiated, further chamber sources of radicals need not be postulated. On the other hand, if a chamber source of radicals is assumed, as in the butane system, good results are still obtained.

The most important reactions of propene are shown in Figure 20. As noted above, the overall rate constants for the reaction of OH, O, and O_3 are known, but the branching ratios were obtained by computer simulations of the smog chamber data. The aldehydes produced in the initial reactions can be photolyzed to give shorter carbon skeletons and free radicals; peroxyacetyl radicals formed in the initial steps can react with NO_2 to give PAN or can oxidize NO to NO_2.

A typical simulation of the smog chamber data is presented in Figure 21. Inspection of the figure shows that product yields are well represented by the assumed mechanism; while better agreement certainly would be desirable, variation between smog chamber runs suggests that there are also some uncertainties in the reported data which contribute to lack of precision in the fit.

Conclusions

There are many uncertainties associated with the complex mechanism for degradation of hydrocarbons in photochemical smog. In several cases, we have used estimation techniques to exploit the limited experimental data for reactions important in these mechanisms. However, experimental information

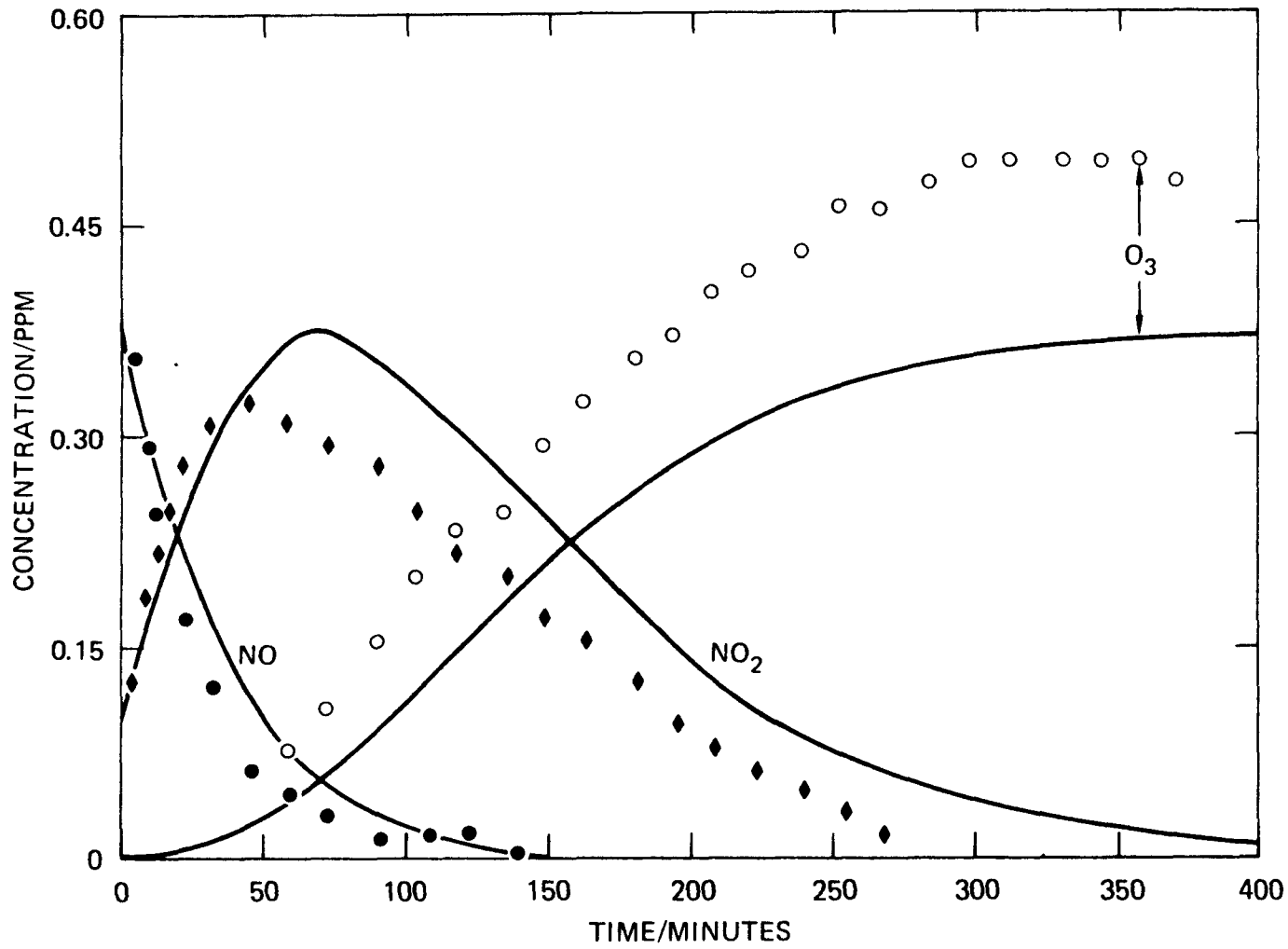

FIGURE 21 Simulation of Run EC-121 in Reference 90. Initial Concentrations: Propene, 0.483 ppm; NO_2, 0.101 ppm; NO, 0.410 ppm; HONO, .04 ppm. The rate of decomposition of HO_2NO_2 calculated using an activation energy of 23 kcal/mole.

on branching ratios, chamber effects, identities and concentrations of minor products, and laboratory data on critical reaction rate constants are necessary to reduce the remaining uncertainties present in our updated model mechanisms for butane and propene. Available experimental data can be simulated fairly well, but there is still considerable latitude in adjusting many individual rate constants. Although these uncertainties do not seem severe in simulating the available data, it is currently difficult to predict the reliability of the mechanisms when applying them to atmospheric concentrations.

REFERENCES AND FOOTNOTES

1. K. L. Demerjian, J. A. Kerr, and J. G. Calvert, Adv. Environ. Sci. Technology, 4, 1 (1974).

2. (a) P. Gray, R. Shaw, and J.C.J. Thynne, Progress in Reaction Kinetics, 4, 63 (1967);

   (b) S. W. Benson and H. E. O'Neal, Kinetics Data on Gas-Phase Unimolecular Reactions, NSRDS-NBS 21, U.S. Government Printing Office, Washington, D.C. (1970).

3. L. Batt, R. D. McCulloch, and R. T. Milne, Int. J. Chem. Kinetics, Symposium 1, 441 (1975); L. Batt and R. T. Milne, Int. J. Chem. Kinetics, 6, 945 (1974).

4. M. Delepine, Bull. Soc., Chim. Fr., (3) 13, 1044 (1895); Beilstein I, p. 284. The compound is reported to detonate by shock.

5. P. L. Hanst and J. G. Calvert, J. Phys. Chem., 63, 104 (1959).

6. Procedure from J. A. Gray and D.W.G. Style, Trans. Faraday Soc., 48, 1137 (1952).

7. D. M. Golden, R. Walsh, and S. W. Benson, J. Amer. Chem. Soc., 87, 4053 (1965).

8. S. W. Benson and G. N. Spokes, J. Amer. Chem. Soc., 89, 2525 (1967); D. M. Golden, G. N. Spokes, and S. W. Benson, Angw. Chemie (Int'l Ed.), 12, 534 (1973).

9. G. Emanuel, Int. J. Chem. Kinetics, 4, 591 (1972).

10. H. E. O'Neal and S. W. Benson in Free Radicals, Vol. II, Chapter 17, 275 (1973), edited by Jay K. Kochi, John Wiley and Sons, Inc., New York.

11. L. Phillips and R. Shaw, Tenth Symposium (International) on Combustion, 453 (1968), Williams and Williams, Baltimore, Md.

12. G. Baker and R. Shaw, J. Chem. Soc., 6965 (1965).

13. G. N. Spokes and S. W. Benson, J. Amer. Chem. Soc., 89, 6030 (1967).

14. S. W. Benson, et al., Chem. Rev., 69, 279 (1969).

15. D. R. Stull, E. F. Westrum, Jr., and G. C. Sinke, The Chemical Thermodynamics of Organic Compounds, John Wiley and Sons, Inc., New York, 1969.

16. R. Silverwood and J. H. Thomas, Trans. Faraday Soc., 63, 2476 (1967).

17. L. Batt and S. W. Benson, J. Chem. Phys., 36, 895 (1962).

18. G. Baker, et al., J. Chem. Soc., 1286 (1965).

19. (a) W. E. Vaughn, Disc. Faraday Soc., 10, 330 (1951).

(b) A. C. Egerton, W. Emele, and G. S. Minkoff, ibid., 278 (1951).

20. H. A. Wiebe, A. Villa, T. M. Hellman, and J. Heicklen, J. Amer. Chem. Soc., 95, 7 (1973).

21. J. N. Pitts, Jr. and B. J. Finlayson, Angew. Chem. (Int. Ed.), 14, 1 (1975) and references cited therein.

22. L. Batt and R. D. McCulloch, Int. J. Chem. Kinetics, 8, 491 (1976).

23. Y. Takezaki and C. Takeuchi, J. Chem. Phys., 22, 1527 (1954).

24. D. M. Golden, R. Walsh, and S. W. Benson, J. Amer. Chem. Soc., 87, 4053 (1965).

25. Y. Takezaki, and T. Miyazaki, and N. Nakahara, J. Chem. Phys., 25, 536 (1956).

26. C. W. Gear, The Numerical Solution of Initial Value Problems, Prentice-Hall, Englwood Cliffs, New Jersey, 1971.

27. H. E. O'Neal and W. H. Richardson, Comprehensive Chemical Kinetics, Vol. 5 (C. H. Bamford and C.F.H. Tippler, Ed., Elsevier, Amsterdam, 1972).

28. D. Gray, E. Lissi, and J. Heicklen, J. Phys. Chem., 76, 1919 (1972).

29. H. A. Wiebe and J. Heicklen, J. Amer. Chem. Soc., 95, 1 (1973).

30. Pollard and Wyatt, Trans. Faraday Soc., 45, 760 (1949).

31. S. W. Benson, Foundations of Chemical Kinetics, McGraw-Hill Book Co., New York, 1960.

32. K. J. Reed and J. I. Brauman, J. Amer. Chem. Soc., 97, 1625 (1975).

33. G. D. Mendenhall, D. M. Golden, and S. W. Benson, Int. J. Chem. Kinetics, 7, 725 (1975), see Section

34. J. Heicklen and H. S. Johnston, J. Amer. Chem. Soc., 84, 4030 (1962).

35. R. Shortridge and J. Heicklen, Can. J. Chem., 51, 2251 (1973).

36. J. Heicklen, Advances in Chemistry Series, No. 76, Vol. II, 23 (1968).

37. W. G. Alcock and B. Mile, Combustion and Flame, 24, 125 (1975).

38. K. D. Bayes and N. Washida, 12th ternational Symposium on Free Radicals (January 4-9, 1976), Laguna Beach, California.

39. S. W. Benson, Thermochemical Kinetics, John Wiley and Sons, Inc., New York, 1968.

40. J. Weaver, R. Shortridge, J. F. Meagher, and J. Heicklen, J. Photochem., 4, 109 (1975).

41. Note that only for unimolecular reactions is $\Delta S^{\ddagger}$ independent of the choice of standard states. For bimolecular reactions with standard states in units of concentration, the Arrhenius rate constants are related by $k_c = (RT)k_p$; for termolecular reactions, $k_c = (RT)^2 k_p$. Since thermochemical quantities for gases are tabulated in terms of atmosphere as standard state, this requires considerable care in relating forward and reverse reactions (see Ref. 42).

42. D. M. Golden, J. Chem. Educ., 48, 235 (1971).

43. S. W. Benson and D. M. Golden, "Reactions in Condensed Phases," Chapter II, Vol. 7, in Advanced Physical Chemistry, edited by H. Eyring and D. Henderson, John Wiley and Sons, Inc., New York (1975).

44. H. E. O'Neal and S. W. Benson, J. Chem. and Eng. Data, 15, 266 (1970).

45. A. F. Trotman-Dickenson and G. S. Milne, Tables of Bimolecular Gas Reactions, NSRDS-NBS9, U.S. Government Printing Office, Washington, D.C., 1967.

46. E. Ratajczak and A. F. Trotman-Dickenson, Supplementary Tables of Bimolecular Gas Reactions, OSTI, Publishing Department, UWIST, Cardiff, Wales (1969.

47. J. A. Kerr and E. Ratajczak, Second Supplementary Tables of Bimolecular Gas Reactions, The University, Birmingham (1972).

48. G. S. Hammond, J. Amer. Chem. Soc., 77, 334 (1955).

49. J. L. Franklin et al., Ionization Potentials, Appearance, Potentials, and Heats of Formation of Gaseous Positive Ions, NSRDS-NBS 26, U.S. Government Printing Office, Washington, D.C. (1968).

50. The potential energy, V_{ion}, of the ion pair (separation = r Å) relative to the separated neutral species of infinity is given by:

$$V_{ion} = -\frac{14.4}{r} + \text{(ionization potential-electron affinity)}$$

All energies in electron volts, $V_{ion} = 0$ when $r = \frac{14.4}{(\text{I.P.} - \text{E.A.})}$ (Å).

51. Reference 39, p. 110.

52. S. C. Chan. J. T. Bryant, L. D. Spicer, and B. S. Rabinovitch, J. Phys. Chem., 74, 2058 (1970).

53. Thermodynamically, $RT\ln K_{eq} = -\Delta G^0 = -\Delta H^0 + T\Delta S^0$. For an adiabatic reaction with standard state in atmosphere, $\Delta H^0 = -RT$, and the energy of AB^* is just the sum of the energies of the reactants A + B.

54. D. Garvin and R. F. Hampson, editors of Chemical Kinetics Data Survey VII, NBS IR74-430, Washington, D.C. (1974).

55. J. Troe, Ber. Buns. Physiki. Chem., 73, 144 (1964); 73, 906 (1969); H. Gaedtke, H. Hippler, and J. Troe, Chem. Phys. Letters, 16, 177 (1972).

56. J. N. Pitts, Jr., J. H. Sharp, and S. I. Chan, J. Chem. Phys., 40, 3655 (1964).

57. S. Jaffe and F. S. Klein, Trans. Faraday Soc., 62, 3135 (1966).

58. F. Kaufman in Chemiluminescence and Bioluminescence, edited by M. J. Cormier, D. M. Hercules, and J. Lee, Plenum Publ. Co., New York, 1973, p. 83.

59. J. T. Herron and F. S. Klein, J. Chem. Phys., 40, 2731 (1964).

60. H. Hippler, C. Schippert, and J. Troe, Int. J. Chem. Kinetics, Symposium 1, 27 (1975).

61. H. J. Johnston and C. Parr, J. Amer. Chem. Soc., 85, 2544 (1963).

62. A. A. Zavitsas, Ibid., 94, 2779 (1972).

63. Z. B. Alfassi and S. W. Benson, Int. J. Chem. Kinetics, 5, 879 (1973).

64. ΔH_f^0(·CO-OO·) is obtained by starting with ΔH_f^0(HCOOOH) = − 65 kcal/mole. Assuming the H-C and O-H bonds are the same as in formic acid (93 kcal/mole) and H_2O_2 (90 kcal/mole), respectively, we find ΔH_f^0(·CO-OO·) = 14 kcal/mole and ΔH_r = 40 kcal/mole, endothermic.

In similar fashion we estimate ΔH_f^0(ON-O-NO) = 22 kcal/mole; ΔH_f^0(H-CO-ONO) = − 44 kcal/mole, and ΔH_f^0(·CO-ONO) = − 3 kcal/mole. This yields for the reaction NO_2 + CO → ·CO-ONO, ΔH_r = 15 kcal/mole.

65. (a) L. Batt, R. D. McCulloch, and R. T. Milne, Int. J. Chem. Kinetics, 6, 945 (1974).

(b) L. Batt, R. D. McCulloch, and R. T. Milne, Int. J. Chem. Kinetics, Symposium No. 1, 441 (1975).

(c) L. Batt and R. T. Milne, Int. J. Chem. Kinetics, 8, 59 (1976).

(d) L. Batt and R. D. McCulloch, Int. J. Chem. Kinetics, 8, 911 (1976).

66. T. Berces and A. F. Trotman-Dickenson, J. Chem. Soc., 348 (1961).

67. C. Leggett and J.C.J. Thynne, J. Chem. Soc., (A), 1188 (1970).

68. J. M. Ferguson and L. Phillips, J. Chem. Soc., 4416 (1965).

69. D. L. Cox, R. A. Livermore, and L. Phillips, J. Chem. Soc., (B), 245 (1966).

70. R. L. East and L. Phillips, J. Chem. Soc., (A), 1939 (1967).

71. P. Cadman, A. F. Trotman-Dickenson, and A. J. White, J. Chem. Soc., (A), 2296 (1971).

72. F. W. Bires, C. J. Danby, and C. M. Hinshelwood, Proc. Roy. Soc. (London), A239, 154 (1957).

73. N. J. Quee and J.C.J. Thynne, Trans. Faraday Soc., 63, 2970 (1967).

74. G. R. McMillan, J. Amer. Chem. Soc., 82, 2422 (1960).

75. J. A. Kerr and M. J. Parsonage, Evaluated Kinetic Data on Gas-Phase Addition Reactions, CRC Press, Cleveland, Ohio (1972).

76. G. Emanuel, Aerospace Report No. TR-0200(4240-20)-5.

77. D. M. Golden, R. K. Solly, and S. W. Benson, J. Phys. Chem., 75, 1333 (1971).

78. J. R. Barker, S. W. Benson, and D. M. Golden, Int. J. Chem. Kinetics, 9, 31 (1977). See Section 4, A.

79. "Semonov Rule," see K. J. Laidler, Chemical Kinetics, McGraw-Hill, Inc., New York, 1965, p. 132.

80. W.P.L. Carter, K. R. Darnall, A. C. Lloyd, A. M. Winer, and J. N. Pitts, Jr., Chem. Phys. Letters, 42, 22 (1976).

81. G. Z. Whitten and H. H. Hugo, SAI Report EF76-126, Draft Final Report (1976).

82. S. W. Benson, Thermochemical Kinetics, 2nd Ed., John Wiley and Sons, Inc., New York, 1976.

83. H. Niki, P. D. Maker, C. M. Savage, and L. P. Breitenbach, Chem. Phys. Letters, to be published.

84. D. Gray, E. Lissi, and J. Heicklen, J. Phys. Chem., 76, 1919 (1972).

85. R. Simonaitis and J. Heicklen, J. Phys. Chem., 78, 653 (1974).

86. R. A. Cox, Int. J. Chem. Kinetics, Symposium No. 1, 379 (1975); R. A. Cox and R. G. Derwent, J. Photochem., 4, 137 (1975).

87. S. Z. Levine, W. M. Uselman, W. H. Chan, J. G. Calvert, and J. H. Shaw, Chem. Phys. Letters, to be published.

88. D. G. Hendry and R. A. Kenley, J. Amer. Chem. Soc., 99, 0000 (1977).

89. Reference 15; J. D. Cox and G. Pilcher, Thermochemistry of Organic and Organometallic Compounds, Academic Press, Inc., 1970.

90. J. N. Pitts, Jr., K. R. Darnall, A. M. Winer, and J. M. McAfee, Mechanisms of Photchemical Reactions in Urban Air, Vol. II, Chamber Studies, U.S. Environmental Protection Agency, 600/3-77-014b, February 1977.

91. For a recent review, see NBS Technical Note 866 (1975).

92. See, for example, H. Niki, E. E. Daby, and W. Weinstock, Advan. Chem. Series, 113, 16 (1972).

93. T. A. Hecht and J. H. Seinfeld, Environ. Sci. Technol., 6, 47 (1972); T. A. Hecht, J. H. Seinfeld, and M. C. Dodge, Environ. Sci. Technol., 8, 327 (1974).

APPENDIX A

INTERNATIONAL JOURNAL OF CHEMICAL KINETICS, VOL. VII, 943–949 (1975)

VLPP Unimolecular Rate Theory

JOHN R. BARKER

Department of Thermochemistry and Chemical Kinetics, Stanford Research Institute, Menlo Park, California 94025

Abstract

The exact theory is derived for the thermal unimolecular decomposition of gas-phase molecules activated and deactivated exclusively through heterogeneous collisions with the walls of a spherical vessel. This theory is appropriate for the treatment of very-low-pressure pyrolysis (VLPP) experiments and other experiments carried out at very low pressures. It is shown, however, that the exact theory is closely approximated by ordinary gas-phase unimolecular rate theory and that for practical application to experiments the results of both theories are indistinguishable.

Introduction

In most gas-phase thermal unimolecular reaction studies, heterogeneous de(activation) is a complication arising at low pressures and which is best avoided. Maloney and Rabinovitch [1] considered such heterogeneous effects for the case of a spherical reactor. They derived expressions for the heterogeneous contribution by writing down the diffusion equation and solving it subject to the proper boundary conditions. Implicit in their treatment are the usual assumptions of unimolecular rate theory [2, chap. 8], (1) the lifetimes of activated molecules are random, and (2) the time intervals between colisions are random. These assumptions lead to time-independent rate constants for decomposition and deactivation [2, chap. 8].

In very-low-pressure pyrolysis (VLPP) experiments [3] the pressure is deliberately maintained so low that heterogeneous (de)activation predominates, and gas–gas collisions are a complication to be avoided. This corresponds to the low pressure limit of the analysis by Maloney and Rabinovitch [1]. Under these conditions, when an activated molecule leaves the wall, it has a good chance of drifting through a collision-free region for a relatively long period of time, a circumstance not matched in the gas–gas collision case. Consequently, the distribution of time intervals between collisions (flight times) is not random, and the gas-phase formulation of thermal unimolecular rate theory is not exactly correct for these conditions.

In the following analysis, the exact expression for the flight time distribution (in a spherical reactor) is derived and compared to the random distribution. The

differences between the two distributions are relatively small, leading to only small errors ($\leq 5\%$) if the usual gas–gas unimolecular theory is employed instead of the exact theory.

General Expression for k_{uni}

If a particle is activated to the energy range E to $E + dE$, the "random lifetime assumption" [2, p. 9] states that in the absence of collisions the probability of not decomposing during the time interval $(0,t)$ is

$$P_d(t) = \exp\{-k(E)t\} \tag{1}$$

where $k(E)$ is the rate constant for decomposition of particles excited to energy E; $k(E)$ can be calculated by statistical theory [2, chap. 4–7].

Presumably the probability of surviving decomposition in the absence of collisions is not correlated with $P_c(t)$, the probability of not experienceing a collision during the same time interval. Thus the joint probability of surviving the time interval $(0,t)$ is $P_c(t)P_d(t) = P_c(t)\exp\{-k(E)t\}$. The probability of decomposing during any given increment of time (t to $t + dt$) is just $k(E)dt$. Thus the probability of an activated particle decomposing in the next time increment after having survived the interval $(0,t)$ is

$$P_d(t)P_c(t)k(E)dt = P_c(t)k(E)\exp\{-k(E)t\}dt \tag{2}$$

This probability must be integrated over all lifetimes possible during a given experiment in order to get the total probability of decomposition during the course of the experiment [2, p. 10].

$$P_{tot}\ k(E) = \int_0^\tau P_d(t)P_c(t)k(E)dt \tag{3}$$

The upper limit τ is the maximum lifetime possible in the experiment, that is, the duration of the experiment. Since τ is usually many times longer than the average flight time or lifetime with respect to decomposition, little error is introduced by assuming $\tau \approx \infty$.

If the particles are activated at the rate R_c, the steady-state rate of decomposition is R_cP_{tot}, which may be written [2, chap. 8]

$$-\frac{d[A^*]}{dt} = R_c\int_0^\infty P_c(t)k(E)\exp\{-k(E)t\}dt \tag{4}$$

where $[A^*]$ is the concentration of active particles of energy E.

For collisional activation (strong collision assumption), in the absence of any other process, the collisional rate of activation equals the rate of collisional deactivation:

$$A + M \underset{-1}{\overset{1}{\rightleftharpoons}} A^* + M$$

$$R_c = k_1[M][A] = k_{-1}[M][A^*] = \omega[A^*] \tag{5}$$

where [A] is the total concentration of species A. Under these conditions [A*] is the equilibrium concentration: $[A^*] = [A]P_e(E)dE$ for energy range E to $E + dE$, where $P_e(E)$ is the equilibrium distribution function. It follows that the rate of activation is given by $R_c = \omega[A]P_e(E)dE$, and this expression holds (for activation), regardless of whether other channels are open for depletion of [A*]. It should be pointed out that R_c is the average rate of activation, regardless of whether it takes place due to gas–gas collisions or due to gas–wall collisions. The collision rate ω is calculated differently depending on the mode of activation, but this fact makes no difference. The difference between VLPP unimolecular rate theory and gas–gas unimolecular rate theory is due to the distribution of "flight times" at the same average collision rate.

Under steady-state conditions the expression for the rate of decomposition is

$$\frac{-d[A]}{dt} = \int_0^\infty -\frac{d[A^*]}{dt}\,dE = k_{uni}[A] \tag{6}$$

where the unimolecular rate constant is

$$k_{uni} = \omega \int_0^\infty \int_0^\infty P_e(E)k(E)\exp\{-k(E)t\}P_c(t)dtdE \tag{7}$$

In the next section an expression for $P_c(t)$ will be derived for a spherical reactor and VLPP conditions. It is informative, though, to derive k_{uni} for gas–gas collisions. In this case the random flight time assumption [2, chap. 8] applies and

$$P_c^{gas}(t) = \exp(-\omega t) \tag{8}$$

Thus for gas–gas collisions,

$$k_{uni}^{gas} = \int_0^\infty P_e(E)\frac{\omega k(E)}{\omega + k(E)}dE \tag{9}$$

which is the usual expression for a unimolecular rate constant. It will be shown below that the final rate constant for heterogeneous (de)activation can be expressed in similar form with a multiplicative factor $B(E)$, which is always close to unity for a spherical reactor:

$$k_{uni}^{VLPP} = \int_0^\infty B(E)P_e(E)\frac{\omega k(E)}{\omega + k(E)}dE \tag{10}$$

k_{uni} for Spherical VLPP Reactor

A direct way of calculating $P_c(t)$, the probability that the flight time equals or exceeds t, is to first calculate the path-length distribution and then fold in the Maxwell–Boltzman velocity distribution.

The probability that a particle will leave the inner surface of a sphere and have its velocity vector directed in the range of solid angle w to $w + dw$ is assumed to be random:

$$p(w)dw = \frac{dw}{2\pi} \tag{11}$$

If θ is the angle between the velocity vector and the normal to the surface (that is, the radius vector), eq. (11) can be written

$$p(\theta)d\theta = \frac{2\pi \sin\theta\, d\theta}{2\pi} = \sin\theta\, d\theta \tag{12}$$

If the sphere is of radius r, the length of the path within the sphere at angle θ is $s' = 2r\cos\theta$, giving the probability for a path length s' to $s' + ds'$:

$$p(s')ds' = \frac{ds'}{2r} \tag{13}$$

The probability that the path length is greater than or equal to s is

$$P(s) = \int_s^{2r} p(s')ds' = 1 - \frac{s}{2r} \tag{14}$$

If a particle is moving along a path with speed v to $v + dv$, the probability that the flight time is greater than or equal to t is the joint probability that $2r \geq s \geq vt$ and that the speed is in the range v to $v + dv$:

$$\begin{aligned} p(v,t)dv &= P(v)dv \cdot \left[1 - \frac{vt}{2r}\right], \qquad vt < 2r \\ &= 0, \qquad vt > 2r \end{aligned} \tag{15}$$

The total probability (for all speeds) that the flight time is greater than t is the integral over speed from 0 to ∞. The conditions on $p(v,t)$ can be incorporated into the integration limits, and the result is

$$P_c(t) = \int_0^{2r/t} P(v)\left[1 - \frac{vt}{2r}\right]dv \tag{16}$$

where $P(v)dv$ is the Maxwell–Boltzman speed distribution,

$$P(v)dv = 4\pi\left(\frac{m}{2\pi kT}\right)^{3/2} v^2 \exp\left(-\frac{mv^2}{2kT}\right)dv \tag{17}$$

and the symbols have their usual meanings.

Equation (16) can be integrated exactly [4] to give

$$P_c(t) = 4\pi\left(\frac{m}{2\pi kT}\right)^{3/2}\frac{8r^3}{t^3}\cdot\left\{\frac{1}{3}\,{}_1F_1\left(\frac{3}{2},\frac{5}{2},-\frac{2r^2m}{kTt^2}\right) - \frac{1}{8}\,{}_1F_1\left(2,3,-\frac{2r^2m}{kTt^2}\right)\right\} \tag{18}$$

where ${}_1F_1(p,q,x,)$ is the confluent hypergeometric function [5].

The collision frequency ω for particles with the walls of a sphere is [3]

$$\omega = \frac{3}{r}\sqrt{\frac{kT}{2\pi m}} \tag{19}$$

Using this identity and the known transformations of the hypergeometric function [5], the expression for $P_c(t)$ can be put in more familiar terms:

$$P_c(t) = P_c(a) = \mathrm{erf}(a^{1/2}) - \frac{2}{\sqrt{\pi a}}\left\{1 - \exp(-a)\right\} \tag{20}$$

where $a = 9/\pi(\omega t)^2$. A semilog plot of this function versus ωt is presented in Figure 1 along with $P_c^{\mathrm{gas}}(t)$ for comparison. It may be observed that the pure exponential function $P_c^{\mathrm{gas}}(t)$ is a good approximation to the overall behavior of $P_c(t)$, but with slight deviations due to three factors: (1) the fixed geometry of the reactor allows a considerable collision-free region not found in a homogeneous gas ($\omega t \lesssim 1$); (2) the boundaries of the reactor limit the flight times of particles moving at average speeds ($1 \lesssim \omega t \lesssim 5$); (3) the broad velocity distribution causes a deviation from the pure exponential after long times ($\omega t \gtrsim 5$). It is qualitatively clear, however, that $k_{\mathrm{uni}}^{\mathrm{VLPP}}$ is closely approximated by $k_{\mathrm{uni}}^{\mathrm{gas}}$.

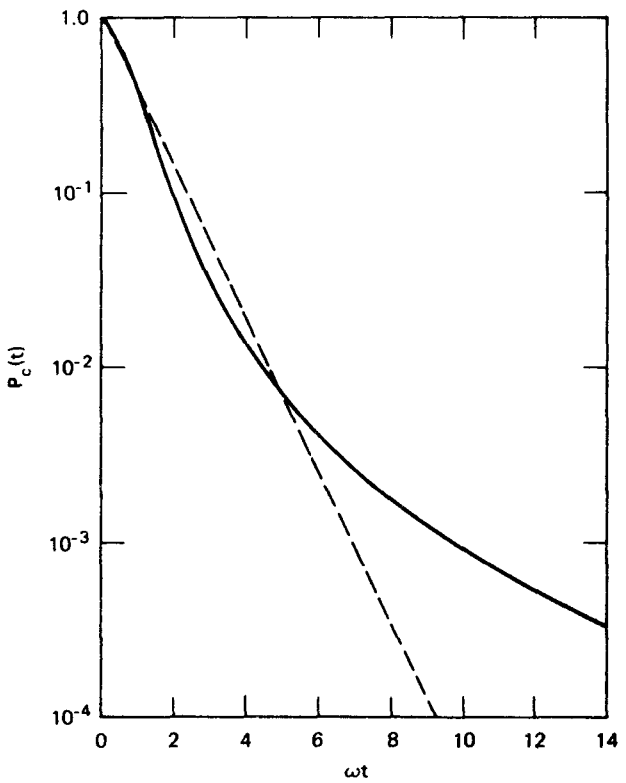

Figure 1. Flight-time probability distribution functions. Solid line—exact probability for a spherical vassel; dashed line—pure exponential behavior appropriate to gas–gas collisions.

For the quantitative assessment of $k_{\text{uni}}^{\text{VLPP}}$ it is necessary to integrate eq. (7) with eq. (20) substituted for $P_c(t)$. Before carrying out the integration, however, it is convenient to scale the integral by transforming to a new variable $x = [\omega + k(E)]t$. This substitution gives

$$k_{\text{uni}}^{\text{VLPP}} = \int_0^\infty \frac{\omega k(E) P_e(E) dE}{\omega + k(E)} \int_0^\infty P_c(x,z) e^{-x(1-z)}\, dx \tag{21}$$

where $P_c(x,z)$ is just $P_c(t)$ expressed in terms of the new variable x and the parameter $z = \omega/[k(E) + \omega]$, a function of energy E. From this it is clear that the factor $B(E)$ in eq. (10) is just

$$B(z) = \int_0^\infty P_c(x,z) e^{-x(1-z)}\, dx \tag{22}$$

Results and Conclusions

Equation (21) was evaluated numerically by a fifteen-term Gauss–Laguerre integration [5, chap. 25], and the B factor is presented in Figure 2 as a function of $\omega/k(E)$. From inspection of this figure it is clear that B never differs from unity by more than $\pm$ 5%. Under the usual VLPP conditions, $\omega \ll k(E)$, and B is very close to unity. Even in the worst of cases, gas-phase unimolecular rate theory eq. (9) should be quite adequate since VLPP experimental errors are generally expected to exceed $\pm$ 5%.

The interesting behavior of $B(E)$ is a direct consequence of the positive and negative deviation of the flight time distribution relative to the random collision-time distribution. When $k(E) \gg \omega$, the distribution is hardly sampled at all and

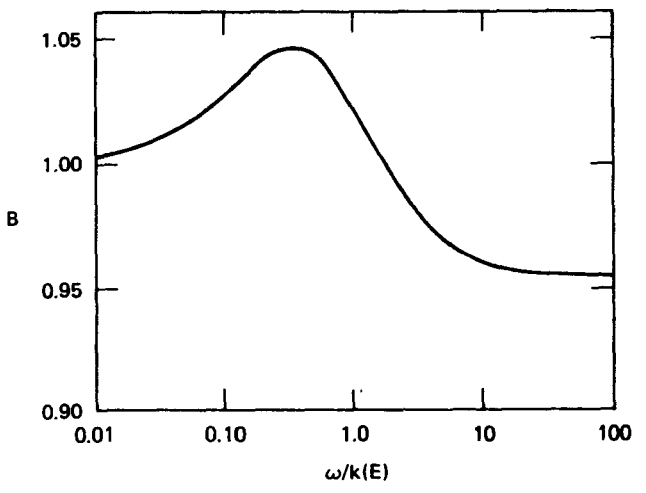

Figure 2. B factor dependence on $\omega/k(E)$.

$B(E) \gtrsim 1$. When $k(E) \approx \omega$, the collision-free drift region of the spherical reactor is important, and more decomposition takes place than in the random collision time distribution, leading to $B(E) > 1$. When $k(E) < \omega$, the finite boundaries of the reactor become important, effectively limiting the flight times of active molecules moving at average speeds, leading to $B(E) < 1$. The deviation of the flight-time distribution from the random collision-time distribution, evident at very long times ($\omega t > 5$ in Figure 1), has a slight effect on $B(E)$, but is far less important than the other two effects mentioned.

In principle, an expression for $P_c(t)$ can be derived for any geometrical configuration; most VLPP reactors are approximately cylindrical. The factor $B(E)$ for other reactor geometries will probably be of magnitude similar to that calculated here for the sphere, since the major feature of VLPP appears to be the existence of a collision-free region not present in a homogeneous gas.

In conclusion, it was found that the exact theory for a spherical VLPP reactor differed only slightly from the usual gas-phase unimolecular rate theory.

Acknowledgment

Useful discussions with Sidney W. Benson and David M. Golden are gratefully acknowledged, as are some helpful suggestions from the referees.

This work was supported by the U. S. Environmental Protection Agency under grant R802288.

Bibliography

[1] K. M. Maloney and B. S. Rabinovitch, *J. Phys. Chem.*, **72**, 4483 (1962).

[2] W. Forst, "Theory of Unimolecular Reactions," Academic Press, New York, 1973.

[3] For a review, see D. M. Golden, G. N. Spokes, and S. W. Benson, *Angew. Chem., Int. Eng. Ed.*, **12**, 534 (1973).

[4] I. S. Gradshteyn and I. M. Ryzhik, "Table of Integrals, Series, and Products," Academic Press, New York, 1965.

[5] M. Abramowitz and I. A. Stegun, "Handbook of Mathematical Functions," Dover, New York, 1968, chap. 13.

Received April 8, 1975
Revised June 11, 1975

TECHNICAL REPORT DATA
(Please read Instructions on the reverse before completing)

1. REPORT NO. EPA-600/3-77-110	2.	3. RECIPIENT'S ACCESSION NO.
4. TITLE AND SUBTITLE MEASUREMENT OF RATE CONSTANTS OF IMPORTANCE IN SMOG		5. REPORT DATE October 1977
		6. PERFORMING ORGANIZATION CODE
7. AUTHOR(S) John R. Barker, Sidney W. Benson, and David M. Golden		8. PERFORMING ORGANIZATION REPORT NO.
9. PERFORMING ORGANIZATION NAME AND ADDRESS SRI International 333 Ravenswood Avenue Menlo Park, California 94025		10. PROGRAM ELEMENT NO. 1AA603 AF-03 (FY-77)
		11. CONTRACT/GRANT NO. R 802288
12. SPONSORING AGENCY NAME AND ADDRESS Environmental Sciences Research Laboratory - RTP, NC Office of Research and Development U. S. Environmental Protection Agency Research Triangle Park, North Carolina 27711		13. TYPE OF REPORT AND PERIOD COVERED Final 4/73 - 7/77
		14. SPONSORING AGENCY CODE EPA/600/09
15. SUPPLEMENTARY NOTES		

16. ABSTRACT

To provide understanding of elementary reactions of importance in smog, a three-part investigation has been carried out: (1) experimental determinations of certain elementary reaction rate constants, (2) development of general techniques for estimating elementary reaction rate constants, and (3) estimation of many reactions important in smog.

Specific estimated rate constants included the following reactions:

(1) Decomposition of alkoxy radicals
(2) Isomerization of alkoxy radicals
(3) Reactions of alkoxy radicals with oxygen
(4) The reaction $HO_2 + NO_2 \overset{(M)}{\rightleftharpoons} HO_2NO_2$

In addition, a limited number of computer simulations were carried out for the photo-oxidation of n-butane and propene.

17. KEY WORDS AND DOCUMENT ANALYSIS

a. DESCRIPTORS	b. IDENTIFIERS/OPEN ENDED TERMS	c. COSATI Field/Group
* Air Pollution		13B
* Smog		04B
* Reaction kinetics		07D
* Photochemical reactions		07E
Ozone		07B
Hydrocarbons		07C

18. DISTRIBUTION STATEMENT RELEASE TO PUBLIC	19. SECURITY CLASS (This Report) UNCLASSIFIED	21. NO. OF PAGES 144
	20. SECURITY CLASS (This page) UNCLASSIFIED	22. PRICE

EPA Form 2220-1 (9-73)